THE UNIVERSITY OF CALGARY

Determinants of cat medial gastrocnemius muscle force during simulated locomotion

by

Jan L.F. Weytjens

A THESIS

SUBMITTED TO THE FACULTY OF GRADUATE STUDIES

IN PARTIAL FULFILLMENT OF THE REQUIREMENTS FOR THE

DEGREE OF DOCTOR OF PHILOSOPHY

DEPARTMENT OF MEDICAL SCIENCE

CALGARY, ALBERTA

MARCH, 1992

© Jan L.F. Weytjens 1992

National Library of Canada
Bibliothèque nationale du Canada

Canadian Theses Service
Service des thèses canadiennes

Ottawa, Canada
K1A 0N4

The author has granted an irrevocable non-exclusive licence allowing the National Library of Canada to reproduce, loan, distribute or sell copies of his/her thesis by any means and in any form or format, making this thesis available to interested persons.

The author retains ownership of the copyright in his/her thesis. Neither the thesis nor substantial extracts from it may be printed or otherwise reproduced without his/her permission.

L'auteur a accordé une licence irrévocable et non exclusive permettant à la Bibliothèque nationale du Canada de reproduire, prêter, distribuer ou vendre des copies de sa thèse de quelque manière et sous quelque forme que ce soit pour mettre des exemplaires de cette thèse à la disposition des personnes intéressées.

L'auteur conserve la propriété du droit d'auteur qui protège sa thèse. Ni la thèse ni des extraits substantiels de celle-ci ne doivent être imprimés ou autrement reproduits sans son autorisation.

ISBN 0-315-75254-8

Canada

THE UNIVERSITY OF CALGARY

FACULTY OF GRADUATE STUDIES

The undersigned certify that they have read, and recommend to the Faculty of Graduate Studies for acceptance, a thesis entitled, "Determinants of cat medial gastrocnemius muscle force during simulated locomotion" submitted by Jan L.F. Weytjens in partial fulfillment of the requirements for the degree of Doctor of Philosophy.

Supervisor, J.A. Hoffer,
Dept. of Clinical Neurosciences

M. Hulliger, Dept. of Clinical Neurosciences

H.E.D.J. ter Keurs, Dept. of Medical Physiology

W. Herzog, Dept. of Physical Education

External Examiner, R.B. Stein
University of Alberta

March 27, 1992

Abstract

In order to study the central nervous system's control of posture and movement muscle models are required that perform well under normal conditions (non-constant activation at non-tetanic rates, non-constant muscle lengths). Such muscle models should be based on relevant experimental data, and should be testable and tested experimentally. Relevant experimental data are scarce at present, if not non-existent. It was the purpose of this work to study the dependence of the forces developed by motor units of the medial gastrocnemius muscle of the cat on muscle fibre length during normal locomotion.

In conscious, chronically implanted cats recordings were made of muscle force, origin-to-insertion muscle length, muscle fibre length, the length of a section of the aponeurotic sheet, and electrical activity during locomotion on a treadmill. In the same animals under deep anaesthesia the muscle was thoroughly fatigued (in order to partially restore recruitment order of motor units), and locomotion was reproduced by means of a muscle puller controlled by the chronically measured muscle length signal and distributed stimulation of five ventral root filaments, using the chronically measured muscle force and fibre length signals as the target signals to be matched. Reproduction was done with and without distributed stimulation, and with and without stimulation of additional small filaments containing only a small number of α-motoneuron axons. From the

resulting measurements estimates of both the changes in tendon length and the forces developed by motor units during locomotion were derived.

The relation between muscle force and tendon length was complex: lengthening occurred with decreasing force, and shortening occurred in the absence of measurable tendon force. The observed relation between muscle force and tendon length could be explained if it was assumed that muscle is thixotropic. As it happened, this hypothesis provided a unifying explanatory basis for a number of other hitherto unexplained muscle phenomena. Estimates of motor unit forces obtained during simulation of locomotion without distributed stimulation were quite reproducible from filament to filament. On the other hand, estimates obtained during simulations with distributed stimulation were quite variable. This variability could not be explained on the basis of known characteristics of force-length or force-velocity dependence. Its cause could not be identified, although the data suggest that it might be due to differences in the interactions between different motor units.

In conclusion, while not yet providing an experimental basis for model construction, the results do show clearly that it is incorrect to make inferences about the forces produced by motor units in the normal animal from forces measured in passive muscles, and that "classical muscle mechanics," as summarized by the force-length and force-velocity curves, is unsuitable for realistic muscle model building. As such, the results also show the need for much more experimentation.

Acknowledgements

Thanks go to Andy Hoffer, Manuel Hulliger, Henk ter Keurs, John Remmers, Dick Stein, Walter Herzog, Uwe Windhorst, Teresa Razniewska and Dave Viberg. Andy Hoffer was my supervisor, and provided laboratory space and financial support. Manuel Hulliger and Henk ter Keurs provided additional supervision as members of my Supervisory Committee. John Remmers served as an additional examiner on my Candidacy Oral Examination Committee. Dick Stein was the external examiner of my Thesis Examination Committee. Walter Herzog served as an additional member on both my Candidacy Oral Examination and my Thesis Examination Committee. Uwe Windhorst provided office space after Andy Hoffer took up a position at Simon Fraser University. Manuel Hulliger and Uwe Windhorst gave helpful comments on the first draft. Teresa Razniewska and Dave Viberg provided technical assistance.

Special thanks go to my father and my mother, and to Barbara, for unrelenting support.

Jan Weytjens

Calgary, Alberta
March 1992

To Barbara

Jouer juste est considérablement moins difficile que de trouver l'idée juste.

Augustin Dumay, 1985

Table of Contents

List of Tables

List of Figures

Chapter 1.

INTRODUCTION

In the analysis of any control system, especially one as complex as that governing movement, it is essential to have a clear understanding of the physical nature of the actuators and also tractable mathematical representations of their dynamics.

In order to insure that future muscle modeling efforts do not stray too far from reality, there will be a need for many more experimental data than are currently available on the behavior of various muscles under histories of activation, force, and motion that are more complex than in the standard isometric and isotonic experiments.
George I. Zahalak, 1990

1.1 Introduction

In order to study the central nervous system's control of posture and movement under normal conditions, muscle models are required that perform well under those conditions. Such muscle models should be based on relevant experimental data, and should also be tested experimentally. This was the basic premise from which I started. Zahalak eloquently expressed the same view; his quotations thus made for a perfect introduction.

Mathematical models allow inferences to be made far beyond what can be extracted from empirical data with descriptive methods, and are thus essential for analysis. What constitutes a good model depends on the specific purpose of the model (and the bias of the investigator), and may be a matter of debate. Muscle

models for use in the analysis of biological motor control should, I think, at least meet the requirement that they can reproduce muscle force with acceptable accuracy. Additional—and stronger—requirements could be imposed; e.g., that they also reproduce internal muscle movement with acceptable accuracy. In the end, it is how good the models are that determines whether or not inferences made from them puts us on a path that converges the truth.

In previous work (Weytjens and Loeb, 1987) I tested the predictions of an interference EMG based Hill-type muscle model against actual measurements of the forces generated by the medial gastrocnemius muscle of chronically instrumented cats walking on a treadmill. Anatomically and functionally, this model was reasonably "realistic": it consisted of a muscle fibre in series with a compliant tendon; it took into account pinnation; and it incorporated what is discussed in classical muscle mechanics: "the length-tension curve" and "the force-velocity curve" (Woledge et al., 1985; Pollack, 1990). It also included viscosity—of which much more will be said in this thesis. However, on average, the model's performance was rather mediocre, the main problem being the use of interference EMG as the input. While excellent correspondence between predictions and measurements could be obtained in some instances, the model's predictive power lacked generality, and there was, in the absence of knowledge of the desired output, no *a priori* way of knowing whether or not the predictions would be acceptable. This experience convinced me that the proper type of muscle model for addressing problems of neural control of movement, are distributed models

that use action potential trains (point processes) as inputs. Justification for this view comes from (1) biological realism—the motor units of real muscle (the final common pathways) are indeed controlled by trains of action potentials—and (2) the fact that distributed, point process based models possess a number of desirable properties that lumped models do not: (a) as opposed to interference EMG, which represents the true input to muscle in a rather indirect and complex way, trains of action potentials are unambiguous as inputs, (b) since trains of stimuli can be easily generated electronically, all predictions can, in principle, be rigorously and independently tested experimentally, and (c) on the premise that they are tested carefully, distributed point-process based models are well suited for *analytical* purposes. On the other hand, such models will not lend themselves easily to *estimation* of forces, since with current technology it is impossible to simultaneously measure the action potential trains of all the motor units of a given muscle active at a given time (experimental measurement of muscle activation under normal conditions thus almost always defaults to measurement of interference EMG); but then, this would not be their purpose.

There is more to muscle mechanics than just the classical length-tension and force-velocity curves. These curves describe only *steady-state* conditions (isometric and isotonic, respectively) of *tetanically activated* whole muscles or single isolated muscle fibres, and are very likely insufficient to adequately characterise the complex behaviour of muscle or motor units activated at intermediate, non-constant rates, at continually varying muscle lengths; i.e., under

conditions such as typically prevail during normal behaviour. In this area the fields of muscle mechanics and motor control are characterised by a dearth of data. As a matter of fact, until very recently, there even seemed to be little interest in the mechanics of motor units or the mechanics of naturally activated muscle: a survey of the literature at the time the experiments were conceived revealed only one publication in which either length or velocity dependence of motor units was studied (Stephens et al., 1975). Lately, however, many authors have expressed the need for experimental data under conditions other than the standard isometric or isotonic and maximal activation (see, e.g., the chapters by Zahalak; Winters; and Loeb and Levine in Winters and Woo, 1990). The reasons were variously phrased: (for Zahalak, see above); "we want to utilize a muscle model [with] negligible capacity for providing misinformation of significance" (Winters), but carried the same message: the study of multiple muscle systems under normal conditions requires "good" muscle models; i.e., muscle models that are good in the sense made precise above.

Force generation by muscle is a parallel distributed process that depends in complex ways not only on muscle length/muscle fibre length and muscle velocity/muscle fibre velocity, but also on short-term and long-term activation history, and kinematic history. In addition, motor units interact with each other. The rationale behind the experimental approach then was as follows: (1) first obtain estimates of the forces generated by motor units under natural conditions (*in casu* cat locomotion), and "separate out" the effects of the various force-

determining factors in order to assess their importance, and (2) systematically study those factors that are found to contribute importantly to force generation and quantify/model their effects.

1.2 The Original Purpose of the research

The original purpose of the research was:

1. To simulate normal locomotion—i.e., muscle length, muscle force, and muscle fibre length—in deeply anaesthetized cats, and obtain reproducible measurements of forces generated by single motor units activated "naturally" under those conditions.

2. To separate out the effects of muscle length/muscle fibre length, and to quantify those effects in order to establish a basis on which the first version of a general point-process based muscle model could be designed.

1.3 Unexpected difficulties and unexpected results

Experiments (fortunately?) do not always turn out the way one expects them to. Simulating locomotion in anaesthetized cats was relatively straightforward.[1] However, these simulations brought to light a rather unexpected relationship between tendon force and tendon length. This relationship was most easily explained if it was assumed that the viscosity of the muscle decreases with

[1] Simulation of locomotion in anaesthetized cats has been done before (e.g., Elek et al., 1990). What was new in my experiments was that (1) the simulations were done in the same cats as those from which chronic measurements were obtained, and (2) not only muscle length and muscle force were simulated, but also muscle fibre length.

movement (shear); i.e., that muscle is thixotropic.[2] As it happened, two hitherto unexplained muscle phenomena could be explained on the same basis: (1) mechanical history dependent potentiation of single motor unit forces, and (2) the peculiar shape of single motor unit force-velocity curves (Heckman et al.; see Discussion). In addition, simulations with simple mathematical models of thixotropy (the "thixotropic Kelvin model" and the "distributed thixotropic Kelvin model") showed that both the time course of the force responses of passive muscle to ramp-and-hold stretches and the fast rise time of the forces generated by the medial gastrocnemius muscle during locomotion could be easily reproduced on this basis (the first one of these results suggests that besides short-range elasticity other mechanisms might co-determine the observed passive force responses). The experiments and simulations seemingly had revealed yet another factor on which muscle force depends.

Measuring *single* motor unit forces during the simulations turned out to be technically unfeasible. The main reason for this was considerable variability in the "background" force due to potentiation and fatigue, which made it impossible to resolve small forces, even with averaging. Consequently, only *multi*-unit filaments

---

[2] "Thixotropy" is a technical term used in colloid chemistry (see, e.g., Jirgensons and Straumanis, 1962; Hiemenz, 1986) and in rheology (the physics of deformation and flow; see, e.g., Billington and Tate), and in its current use refers to a shear dependent decrease in viscosity, as mentioned in the text. Originally, the term had the more restricted meaning of reversible gel-sol/sol-gel transformation in response to the application and removal of shear stress (Jirgensons and Straumanis, 1962). Synonymous with thixotropy is "shear thinning." Since for a thixotropic material *the* viscosity does not exist and what is measured depends on the history of shear stress, the viscosity is usually referred to as apparent viscosity.

were studied, and even here problems were encountered. The decomposition technique devised for separating out the effects of muscle length/muscle fibre length required muscle fibre-isometric motor unit force measurements at muscle fibre lengths spanning the muscle fibre length range during simulated locomotion. Muscle fibre length was held *quasi*-isometric by using constant background stimulation. Yet, again due to variability in the background force, muscle fibre-isometric data were difficult to obtain: the background forces measured with and without stimulation of the multi-unit filament under study would not always match. In addition, those filaments for which seemingly reliable data were obtained, exhibited unexpected variability in their responses. The sources of this variability could not be identified on the basis of the current data; in particular, it was not clear whether or not the fibre-isometric force were co-determined by the background force, and, if so, to what extent. It was considered pointless then at this stage to decompose the measured forces: decompositional analysis cannot be done without careful control of the different force-determining factors at work; this in turn presupposes that it is known what those factors are.

In summary, the data did not form (the beginning of) a database for studying the characteristics of well-known functional dependencies under normal conditions. Instead, they revealed unanticipated complexity—complexity inviting further study.

Chapter 2.

HISTORICAL BACKGROUND

[W]e present the subject in the traditional "battles and kings" style of history.... "Battles and kings" is all very well, but which battles and which kings?
Paul R. Halmos, 1985

2.1 Introduction

Halmos's question is a pertinent one: exactly which battles and which kings should be discussed here?

This chapter should be the place for a critical review of previous, related research, out of which the current hypotheses and research grew. For the tendon-force/tendon-length data the story is simple and is given in section 2.2, together with background information on muscle thixotropy. But what about my Original Purpose? The ideas grew out of dissatisfaction with the performance of interference EMG based muscle models and a perceived need for mechanically realistic, distributed, stochastic muscle models. The experiments, moreover, were not designed to cast new light on old problems, test hypotheses, or falsify theories, but simply and plainly to gather empirical data relevant for subsequent model construction. To the best of my knowledge, the questions asked and the methods devised for answering them—in particular, the decomposition

method—were new; in addition, as of yet no one seems to have studied muscle mechanics under mechanical and activation conditions similar to those in the conscious, normally behaving animal. Thus there was, and still is, no direct and strong connection with previous work.

What background material then is relevant here? A critical account of the whole field of muscle mechanics? An exhaustive discussion of muscle models? Critically reviewing previous work in muscle mechanics would have been a monumental task and have involved a great deal of repetition of material available elsewhere (e.g., Hill, 1970; A.F. Huxley, 1980; McMahon, 1984; Woledge et al., 1985; Pollack, 1990). Also, a great part of the review would not have been directly relevant. The same would have been true for a comprehensive critical survey of muscle models (for a brief recent review, see Winters and Woo, 1990). Thus, the account of muscle mechanics was restricted to the mechanics of single motor units. Because of the scarcity of publications, it is rather brief. Muscle models are not discussed, since the work reported here did not include any (serious) muscle modelling.

2.2 The Great Tendon Compliance Controversy

Hoffer et al. (1989), using a method for measuring muscle fibre length *in situ* (Griffiths, 1987), recently found that the length of the cat medial gastrocnemius muscle (origin-to-insertion) and the length of its muscle fibres do not vary in unison during treadmill locomotion. In the early stance phase, when the limb is loaded, the muscle fibres shorten, although the muscle yields; in the early swing

phase, by contrast, the muscle fibres lengthen, although the muscle shortens. The observed differences between muscle length and muscle fibre length were large: approximately 2.3 mm in the early stance, and 5 mm in the early swing phase (see their Fig. 2). Initially, these differences were attributed solely to stretch of compliant "tendinous elements in series with the [muscle fibres]," but later (Caputi et al., 1989; see also the introduction of Elek et al., 1990), variations in the angle of pinnation, deformation of the aponeurotic sheets, and shortening of the muscle below slack length were also held responsible. These results led Hoffer et al. (1989) to conclude that muscle spindles do not signal muscle length.

Hoffer et al.'s report prompted Elek et al. (1990) to simulate locomotion in anaesthetized cats, and estimate total extramysial displacement[1] by means of Rack and Westbury's spindle null method (Rack and Westbury, 1984). In this method muscle fibre length is indirectly controlled by matching actual group Ia or group II spindle afferent firing to desired target firing patterns, the basic assumption being that spindle afferent firing accurately reflects muscle fibre length. Matching is done either by stimulation of the parent muscle (Rack and Westbury, 1984) or modification of the length changes imposed to the muscle (Elek et al., 1990). The extramysial displacement was estimated at various operating lengths with forces ranging from 10 to 30 N. The estimates ranged from

[1] The expression "extramysial displacement" was used by Elek et al. (1990) as a convenient abbreviation for all possible sources of discrepancy between muscle length and muscle fibre length.

0.3 to 0.7 mm (early stance phase), values much smaller than Hoffer et al.'s 2.3 mm.

Muscle length measurements made with saline-filled length gauges are notoriously hard, if not impossible, to calibrate accurately (see Methods). In the step cycle reproduced in Hoffer et al.'s Fig. 2 the total change in muscle length was about 11 mm. In the experiments reported here the typical length range was about 8 mm, which is somewhat smaller. The latter figure may be more reliable, since it was obtained from muscle length measurements made with piezoelectric length gauges, which, in contrast with saline-filled length gauges, do allow for accurate calibration (see Methods). The differences between muscle length and muscle fibre length derived from Hoffer et al.'s Fig. 2 may thus have been overestimates of the actual discrepancies. It seems unlikely, however, that errors in muscle length calibration alone can account for the discrepancy between Hoffer et al.'s and Elek et al.'s results.

As in Elek et al. (1990), the simulations reported here were done with and without stimulation of the muscle. Matching of muscle fibre length, however, was done using direct measurements rather than via the spindle null method. Also measured, besides muscle fibre length, were the length of a part of the aponeurotic sheet and the length of the third side of the triangle whose other two sides were the muscle fibre and aponeurotic sheet lengths (see Fig. 3.4 in Methods). From the latter, "transverse" measurement and the fibre and aponeurotic sheet length measurements the angle of pinnation was computed by

triangulation. With origin-to-insertion muscle length, muscle fibre length, and angle of pinnation available under both active and passive conditions, extramysial displacement during locomotion could be studied directly.

The results were rather surprising. Muscle force and tendon length did not change in phase, as would be expected for a structure that is predominantly elastic. Rather, the relation between muscle force and tendon length was complex, and, as indicated in the Introduction, suggested the presence of substantial, shear-dependent viscosity in the muscle.

Muscle thixotropy

Thixotropic behaviour of muscle has been reported before (Lakie et al., 1984; Hagbarth et al., 1985). Lakie et al. (1984) found that the amplitude of the displacement of the wrist in response to sinusoidal torques increased and the phase lead of the velocity on the applied torque decreased after the application of large "stirring torques." Voluntary flexion and extension movements had the same result. The effect persisted as long as the wrist was kept in motion and disappeared within 1 to 2 s after the motion had ceased. It was attributed to a transformation of the "system" from a gel to a sol state due to agitation. This transformation was implied to occur in the myofilaments since the observed changes in stiffness were believed to be due to the breakage of attached crossbridges, following D.K. Hill's interpretation of short-range elasticity (D.K. Hill, 1968). Similar results were obtained for the finger flexors by Hagbarth et al. (1985) using rectangular extension torques. The observed decrease in the stiffness

of the finger flexor muscles, however, persisted for many minutes. As in Lakie et al., the decrease in stiffness was attributed to attachment of crossbridges in passive muscle and breakage of these bridges with stretch. In the same study Hagbarth et al. observed that flexor torques had a stiffening effect. This stiffening effect did occur within seconds (see their Figs. 3 and 4). It was explained by the same mechanism. Both Lakie et al. and Hagbarth et al. excluded joint thixotropy as a possible explanation for the data: Lakie et al. observed thixotropic effects in biceps femoris while the knee was stationary, and Hagbarth et al. observed thixotropic effects in response to strong isometric contractions.

The effect observed in both studies, an increase in angular displacement of the joint studied in response to torques of constant amplitude after application of a perturbation, was considered indicative of a decrease in stiffness of the system studied and was explained as such. Explanation in terms of a decrease in stiffness is undeniably straightforward, but is not necessarily correct. The dependence of the frequency response (i.e., Bode gain and phase) of a system on its parameters can be very complex and is not always monotonic for all parameters. No extraordinary degree of complexity is required for this to be true. E.g., the Bode gain of a system consisting of a Kelvin element[2] and a mass (a crude model of bone attached to biological tissue) may, depending on the values of the mass and

[2] The Kelvin element consists of a spring in parallel with a series arrangement of another spring and a dashpot. It is one of a number of mechanical models used in the study of viscoelastic materials (see, e.g., Fung, 1981). Its initial "short-range" elastic response to a unit force step input is determined by $\mu_p+\mu_s$, where μ_p and μ_s are the stiffness of the parallel and series spring, respectively. The Kelvin model is further discussed in Results and Discussion.

the viscosity, go through multiple maxima with decreasing "short-range" stiffness $\mu_p+\mu_s$. In other words, a decrease in stiffness does not necessarily result in an increase in displacement. Similarly, a decrease in apparent viscosity may, depending on the mass and the stiffness of the parallel and series springs, result in a significant increase in displacement. In general, changes in the parameters of a system do not only affect the gain but also the phase angle. It surprising then that Lakie et al. observed only a small decrease in the phase lead of velocity on torque.

Lakie et al. did not have direct evidence for a decrease in stiffness nor, for that matter, for a decrease in apparent viscosity. Neither is it possible on theoretical or other grounds to favour one mechanism over the other. Both possibly contributed. As such, Lakie et al.'s data, while not providing direct support for shear thinning of muscle, are certainly not inconsistent with it.

The remarks made above do not directly apply to Hagbarth et al.'s data, since rectangular torques (1-2 s duration) were used as inputs rather than sinusoidal ones, and the steady state solution of a viscoelastic system to a step increase in force (if it has one) does not depend on the viscosity. The viscosity does, however, affect the time required to reach the steady-state, i.e., the time constants of the system: the smaller it is the faster the system responds to changes in the input. An increase in angular displacement in response to step torques as a result of a decrease in apparent viscosity then may result if the time constants of the system are initially large in comparison with the duration of the steps and

decrease significantly after application of the perturbation. This is not a far-fetched possibility. The time constants of the Kelvin element, for instance, are directly proportional to the viscosity (see Results). Consequently, if the viscosity decreases 10 to 100-fold, the time constants would also do so. As in Lakie et al.'s data, there is neither evidence for nor against this explanation, nor for or against a decrease in stiffness (note that a decrease in stiffness also affects response time: it increases with decreasing stiffness). Hagbarth et al.'s data are thus not at variance with muscle thixotropy, although it is not clear why the apparent viscosity (or stiffness) of the finger extensors would take much longer to "set" than the apparent viscosity (or stiffness) of the flexors.

2.3 Motor unit mechanics

Length dependence

Lewis and co-workers (Lewis et al., 1972; Bagust et al., 1973) found that the optimum length for fused tetani of cat flexor digitorum longus motor units is shorter than the optimum length for twitch contractions. The same result was obtained for cat medial gastrocnemius motor units by Stephens et al. (1975), who also found that the contraction speed and twitch/tetanus ratios vary with muscle length. With increasing length force development becomes slower: both the twitch contraction time and the twitch half-relaxation time increase (at long lengths both measures of contraction speed decrease slightly). The twitch/tetanus ratio first increases then decreases with increasing length; it is maximal at a length slightly

longer than the optimum length for tetanic contractions. The data obtained by Heckman et al., who also studied cat medial gastrocnemius, further corroborate these results.

The mechanism(s) underlying these length dependencies remain to be elucidated. Stephens et al. (1975) speculated that muscle fibre shortening during tetanic contractions might in part explain the difference in optimum length for tetani and twitches. This explanation, however, is unlikely to be correct since muscle fibre shortening, for constant muscle length, would cause the tetani to occur at sarcomere lengths that are systematically shorter than those at which the twitch contractions are elicited. Hence, it would result in the opposite effect: the optimum length for tetani would be longer than that for twitches.

Velocity dependence

Devasahayam (1989) found V_{max}, the maximum velocity of shortening, for tetanically stimulated motor units of the rat soleus muscle, to be on average 8.7 muscle lengths per second, or 20.6 μm per second per sarcomere. The force-velocity curves, from which the individual values for V_{max} were obtained by extrapolation, were constructed using force data acquired during constant velocity shortening ramps (3 mm at velocities ranging from 3 to 140 mm/s); i.e., velocity was the independent variable. This isovelocity release method was first used by A.V. Hill (discussed in Hill, 1970). Hill, however, first computed the isometric forces corresponding to particular release velocities from the force-velocity curve, then released the muscle at those velocities when the forces generated by the

muscle reached the computed values. When the forces so *computed* were estimated correctly, then the *measured* forces would be constant. Otherwise, the forces would first increase or decrease before reaching a constant value. In Devasahayam's work, the various constant velocity ramps were always initiated during the plateau phase of the motor unit tetani. As his figures indicate, there may not always have been enough time for the motor unit forces to reach a steady value. Consequently, the V_{max}s may have been overestimated. V_{max} did seem to vary with the inverse of twitch contraction time, but the correlation was found not to be significant.

Petit et al. (1990), studying the stiffness of cat peroneus longus muscle motor units of different type activated tetanically, found that the force responses to slow ramp-and-hold stretches (0.5 mm at 2.4, 3.5 and 5.3 mm/s) of type S units are larger than those of type FR and FF units (i.e., they found type S units to be stiffer than type FR and FF units). This difference was attributed to different rates of cross-bridge cycling in the muscle fibres of the three types of motor unit.

Heckman et al. studied the velocity-dependence of motor units of the cat medial gastrocnemius muscle activated at various non-tetanic rates during both lengthening and shortening isovelocity ramps (4, 8, 12, 20, 40 and 60 mm/s). Under those conditions, the motor unit forces are not only determined by the effects of velocity, but also by those of length. Heckman et al. did correct for the effects of length dependence, and found that for shortening the normalized force-velocity curves of type S units are steeper than those of type FR and FF motor

units, and that the steepness of this part of the force-velocity curves increases with increasing stimulation rate. It was also observed that the single motor unit force-velocity curves are peculiar in the sense that the isometric forces are often smaller than the forces measured during both lengthening and shortening. This unusual shape apparently results from potentiation of the non-isometric forces due to movement (see also the next section).

Aftereffects of changes in length

Powers and Binder (1991) found that small trapezoidal movements in both the shortening and lengthening directions (1 mm at 2 mm/s; the duration of the isometric phase was 0.5 s) imposed during stimulation of cat tibialis posterior motor units at 50 pulses/s, alters the force after the end of the movement. Stretch-first movements cause a lasting post-movement decrease in force; release-first movements, on the other hand, cause a post-movement increase in force. No explanations were given. It is well known in muscle mechanics that active shortening of muscle leads to a lasting decrease in force, and vice versa, active lengthening (beyond the optimum length) leads to a lasting increase (see, e.g., Woledge et al. 1985). What is unusual in the results of Powers and Binder is that, for reasons that are unclear, this decrease or increase in force did not occur until after the second ramp movement—the forces measured during the isometric phase of the trapezoidal movement were found not to be statistically significantly different. Powers and Binder also studied the effect of movement amplitude in one pair of motor units (0.02, 0.05, 0.1, 0.25 and 1 mm; see also the next section).

Except for the 1 mm movement all forces measured during release-first *increased* after movement initiation and thereafter remained *greater* than the isometric control. The opposite effect was seen for the 0.05 and 0.1 mm stretch-first movements (0.02 mm amplitude stretch-first movements were not used). These findings are at variance with previous observations on muscle force during active shortening and lengthening (see, e.g., Woledge et al., 1985). Whether or not they are isolated results is not clear, however, since only one pair of motor units was studied.

Heckman et al. found that the 2 mm isovelocity (10 mm/s) length changes used to move the muscle to different lengths when studying force-length effects, had a strong potentiating effect on the motor unit forces. The amount of potentiation varied inversely with the amplitude of the twitch forces: it was largest for the smallest motor units and was absent for twitch contractions greater than about 200 mN. This potentiation was also seen with shortening movements of the same amplitude and velocity (Heckman et al., unpublished observations). In two units the time course of potentiation was studied: after the end of the movement, the effect first decayed rapidly, then more slowly; it disappeared after about 10 seconds. This movement-dependent potentiation was tentatively explained (following Emonet-Dénand et al., 1990) in terms of frictional interactions between muscle fibres.

Non-linear summation of motor unit forces

A number of authors have reported supralinear summation of motor unit forces in a number of different cat hind leg muscles (Emonet-Dénand et al., 1987; Clamann and Schelhorn, 1988; Emonet-Dénand et al., 1990; Powers and Binder, 1991). In all cases this more than linear summation was attributed to the presence of opposing frictional forces between active and passive muscle fibres when motor units were stimulated in isolation. Frictional forces, however, have opposite direction but equal magnitude. Thus, when an active muscle fibre experiences frictional resistance from neighbouring passive fibres, the opposing frictional force exerted by the passive fibres is equal in magnitude to the force "lost" by the active fibre, but is directed in the opposite direction, and, consequently, pulls on the tendon. The net effect is cancellation: the force measured at the tendon is equal to the force generated by the active fibre (ignoring pinnation angle), although some of this force is transmitted through neighbouring fibres. Both this "friction hypothesis" (Emonet-Dénand et al., 1990) and the criticism hinge on the assumption that muscle fibres can transmit force laterally to other muscle fibres. Evidence for lateral force transmission has been presented by Trotter (1990) for series-fibred muscles of the cat hind leg (biceps femoris and tenuissimus). Whether or not it also occurs in continuous-fibred muscles remains to be established.

Powers and Binder (1991) found that the trapezoidal movements imposed during tetanic stimulation of pairs or triples of motor units (see above), reduce the

non-linearity of the summation. The threshold movement amplitude for this reduction was found to be 20 μm for release-first and 50 μm for stretch-first movements. It was believed to be due to a decrease in the "frictional drag" between active and passive muscle fibres as a result of a reduction in the viscosity of the "viscous substance linking adjacent muscle fibres," i.e., the endomysium, caused by the movement. In this formulation Powers and Binder's hypothesis is essentially identical to the hypothesis proposed and discussed in detail in this thesis to explain the time course of change in tendon length during locomotion.

During tetanic stimulation of even single motor units the muscle fibres very likely shorten (much) more than 20 μm, Powers and Binder's release-first threshold value for a reduction in the viscosity of the endomysium. Consequently, a decrease in viscosity would also be expected to occur at the onset of an isometric tetanus. Thus, If the explanation is correct, Powers and Binder's result indicates that the viscosity of the endomysium does not change in an all-or-none manner, but, instead, may change incrementally.

Chapter 3.

METHODS

I took typing seriously. I bought a teach-yourself-the-touch-system pamphlet at Woolworth's (for 10 cents) and practiced half an hour after lunch everyday for several months. I became a good touch typist—not super, but good. I made mistakes, but I could copy fast, and for the next 25 years or so I did all my own typing—correspondence, class notes, exams, papers, and books. When a prospective Ph.D. student approached me, in later years, I asked him, first thing, whether he could type, and told him to learn if he couldn't. That was regarded as eccentric for a while, and then as passé, but now, with computers on the desk of many executives, it might become a sensible notion again. I read once that the true mark of a pro—at anything—is that he understands, loves, and is good at even the drudgery of his profession. The apothegm impressed me, and I patted myself on the back; I was sure that my attitude to typing helped to prove that I was a real pro.
Paul R. Halmos, 1985

3.1 The experimental animal

The experiments were performed on cats, which for two reasons were the animal of choice: (1) cats can be easily trained to walk on a treadmill for many minutes, and (2) since Sherrington (1857-1952) the cat has been the motor control neurophysiologist's "classical" preparation. A great part of our current knowledge of motor control derives from work done in cats. Friendly, cooperative cats were purchased from Laka Inc. in Quebec through the Animal Resources Centre of the University. Useful data were acquired in eight animals.

3.2 Training of the cats

The cats were trained to walk on a treadmill using food rewards and affection. The training typically lasted three to six weeks, during which period they were trained daily (i.e., five days per week). On the first few days of the training period they were not made to walk, but simply put into the plexiglass case enclosing the treadmill, and allowed to explore this new environment. At the same time the treadmill motor was turned on and off a number of times to allow them to become accustomed to the noise of the motor. Once they got to know the treadmill, they were encouraged to walk on it. To provide an incentive to walk, the cats were deprived of food before they were put onto the treadmill (in the morning), and food was presented visually from behind the plexiglass door at the front of the treadmill. It was given to them as a reward at the end of the training session. Fully trained cats would walk on the treadmill for periods up to thirty minutes.

3.3 Chronic surgery

After the training period the medial gastrocnemius muscle of either the left or right hind leg was instrumented with various transducers: (1) three pairs of cylindrical piezoelectric crystals (for measuring muscle fibre length and other "local" dimensions; see below), (2) three or four pairs of bipolar EMG electrodes, (3) a tendon force buckle, (4) two or three muscle length gauges, and (5) a thermistor. An "active" and "dummy" conventional saline-filled muscle length gauge (see below) was implanted in all cats. In six cats these conventional length

gauges were supplemented by a piezoelectric length gauge, either of the "prototype" type (two cats) or of the "hybrid" type (four cats) (see below).

Each operation was done aseptically under deep anaesthesia induced and maintained with halothane (Fluothane, Ayerst) in an oxygen/nitrous oxide mixture. The typical procedure was as follows. The night before the surgery a broad-spectrum antibiotic was injected subcutaneously in the neck (1 ml of Derapen-C, Ayerst (100,000 IU penicillin G procain, 100,000 IU penicillin G benzathine and 0.25 g dihydrostreptomycin sulphate)). The next morning acepromazine maleate (Atravet, Ayerst) was injected subcutaneously as a pre-anaesthetic tranquillizer (0.5 mg/Kg). Half an hour later general anaesthesia was induced by circulating the halothane/oxygen/nitrous oxide gas mixture (1 to 2.5 % halothane, in 60/40% oxygen/nitrous oxide) through the closed plexiglass box in which the cat was put. After anaesthesia had been induced, the cat was taken out of the box, put on the preheated surgical table (heating pad: Aquamatic K Module model K-20-C, Hamilton), and intubated with a 4 mm inner diameter tracheal tube (Lo-Pro, Mallinckrodt Critical Care) after spraying a local anaesthetic (Xylocaine Endotracheal Aerosol) onto the glottis. The plastic tubes of the inhalation anaesthesia unit (Fluotec 3, Cyprane) were detached from the plexiglass box and plugged into a cylindrical CO_2 sensor that was attached to the tracheal tube, and the level of halothane was reduced to 0.5 to 1 %. The CO_2 sensor was used to monitor expiratory CO_2 level continuously throughout the operation (Datex CO_2 monitor, Puritan-Bennett Corporation). The cat was shaved: the throat,

the distal two thirds of the back, the proximal third of the tail, the hind leg, and the proximal third of the foot. These areas were sterilized by rubbing them with gauze dipped in povidone/iodine (Triadine, Triad Medical Products, H&P Industries). From this point on all further manipulations were done under aseptic conditions. Sutures for the backpack connector (see below) were inserted at the level of T13 and L4 with a large curved needle (conventional cutting, 1/2 circle, 4 cm diameter). Each suture consisted of two 30 cm long strands of Mersilene size 2 (Ethicon). These sutures were passed not just through the skin but through the muscles of the back (multifidus and interspinal), the critical test for proper insertion being the ability to lift the cat off the surgical table by pulling the sutures upwards (not just the skin off the deep tissues). The cat was turned onto its back and covered with a surgical drape, leaving the neck exposed. A 3 to 4 cm long rostrocaudal incision was made along the medial side of the left or right external jugular vein, and the vein was dissected free from the underlying tissue. A cylindrical stainless steel probe (5 mm diameter) with a removable bullethead was passed subcutaneously to the back. A catheter was passed through this probe, which then was pulled all the way through. A 10 ml syringe filled with 5% dextrose in 0.9% sodium chloride solution (Travenol Canada) was inserted into the distal end of the catheter, and the catheter was flushed. The vein was ligated rostrally, and the catheter was inserted into the vein through a small incision made distal to the ligation. It was tied to the vein with silk sutures (Ethicon), and the skin was then closed. The cat was then turned on its belly again. The distal

three fourths of the foot were wrapped into a sterile cloth and slipped through the hole in a second surgical drape with which the hindquarters of the cat were covered. An 8 to 10 cm long dorsomedial incision was made from the distal end of the popliteal fossa (the distal edge of the fatpad) down to the heel. The skin on both sides of the incision was separated from the underlying tissues by blunt dissection. The crural fascia was cut over the medial gastrocnemius muscle from the heel up to the distal edge of the popliteal fatpad so as to expose not only the distal part of the muscle but also the part proximal to the semitendinosus muscle. Beginning at the medial edge, the deep (ventral) side of the medial gastrocnemius muscle was separated from the underlying muscle (plantaris). Distally, the medial gastrocnemius muscle was separated from the lateral gastrocnemius muscle, to which it is attached, by blunt dissection. The gap between the two muscles was extended caudally beyond the muscle bellies to isolate the tendon of the medial gastrocnemius. A pair of cylindrical piezoelectric crystals (see below for details) was sutured to the ventral (deep) aponeurotic sheet with size 5-0 sutures (5-0 TI•CRON, Atraumatic), about 25 mm proximal to the caudal belly-tendon junction. The muscle fibres underneath this crystal pair were stimulated with a bipolar concentric needle electrode (a blunt gauge 21 needle, bent slightly, into which a multistranded Teflon-coated stainless steel wire was glued (Biomed AS632, Cooner Wire); 100 μs, 0.1-1 mA biphasic pulses delivered every 0.5 s) to locate their opposite ends on the dorsal (superficial) surface of the muscle. This location was identified as the site at which a tiny dimple appeared in response

to stimulation, due to local shortening. This dimple was marked with methylene blue and another pair of piezoelectric crystals was sutured to the aponeurotic sheet at this location. The distance of this pair of crystals from the distal end of the aponeurotic sheet on the dorsal side of the muscle was 25.9 ± 7.9 mm (mean and standard deviation; range: 13.7-33 mm). The third pair was sutured to the deep side of the muscle, approximately 10 mm proximal to the first pair. The arrangement of the three pairs of crystals is illustrated in Fig 3.1. The EMG electrodes were inserted transversally into the muscle by pulling the silk suture at their ends (see below) through the muscle belly with a medium-sized curved needle (conventional cutting, 3/8 circle, 3 cm diameter). The silk suture was tied to the aponeurotic sheet to secure the electrodes in place. The locations of the different pairs of electrodes relative to the distal end of the aponeurotic sheet on the dorsal side of the muscle were as follows (means and standard deviations): (1) distal pair (DI): 4.0 ± 3.8 mm (0.0-10.0 mm), (2) distal intermediate pair (DIN): 21.2 ± 6.1 mm (15.7-33 mm), (3) proximal intermediate pair (PIN): 37.2 ± 5.2 mm (30.0-43.0 mm), and (4) proximal pair (PR; six cats): 45.7 ± 8.6 mm (37.7-62.0 mm) (see Fig. 3.1). The tendon was inserted into the force transducer. It was tied to the transducer with two loose sutures, one through each hole in the transducer, to prevent the tendon from slipping out of place. In addition, the leads of the transducer were loosely sutured to the crural fascia approximately 10 mm rostral to its proximal end. The leads of the devices were passed in two bundles, one medial and one lateral, through two small holes in the crural fascia, and the fascia

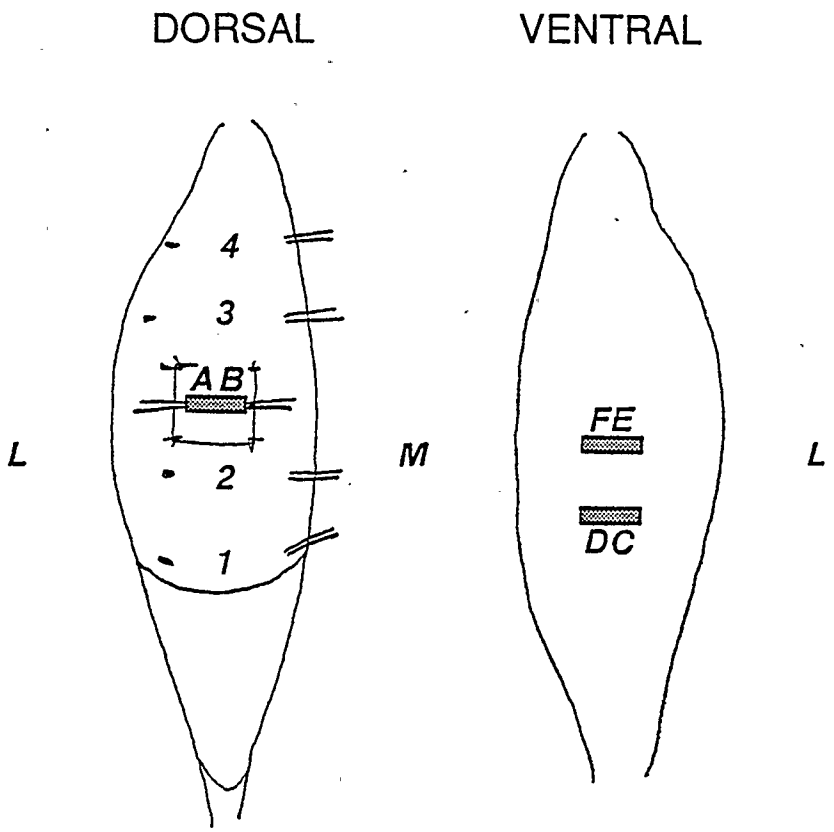

Fig. 3.1. Semi-realistic diagram of the left medial gastrocnemius muscle and the position of the piezoelectric crystals and EMG electrodes. L, lateral, M, medial. The piezoelectric crystals were assembled and used in pairs, labelled AB, CD, and EF. Measurements were typically made as follows: muscle fibre length: A-C; aponeurotic sheet length: D-F; S3: E-B. Bipolar intramuscular EMG electrodes were used (labelled 1 through 4). Only the knots with which they were tied to the aponeurotic sheet, and the leads are shown.

was closed with size 3-0 sutures (Ethibond, Ethicon). A large curved needle (conventional cutting, 1/2 circle, 4 cm diameter) was manually driven through the calcaneus to make a hole for suturing the length gauges to. Access to the origin of the medial gastrocnemius muscle, in particular to the sesamoid bone in the tendon of origin, was gained through a 4 cm long rostrocaudal incision at the knee on the medial side of the leg. The sartorius muscle was split along the direction of its fibres by blunt dissection, and the cranial and caudal parts of the semimembranosus muscle, which overlie the medial epicondyle and the tendon of origin of medial gastrocnemius, were separated. One suture of the length gauges was passed through the sesamoid bone with a large needle (conventional cutting, 3/8 circle, 6 cm diameter) and tied to the other suture with two square knots. The area was flushed with saline and closed in layers with size 3-0 sutures: cranial and caudal parts of semimembranosus, sartorius, fascia, and skin. The distal sutures of the length gauge(s) were tied to the calcaneus. This was done while monitoring the impedance of the active saline-filled gauge, in order to insure that it was greater than the impedance of the dummy gauge (see below). The thermistor was inserted into the hole in the fascia with the medial bundle of leads, and sutured into place. A ground wire was sutured to the skin. The two bundles of leads were passed to the back with the 5 mm diameter probe. For strain relief, small loops were made with each bundle, which were tucked away in skin pockets. The skin was closed with size 3-0 sutures. From this point on further manipulations were no longer done under strictly aseptic conditions. The

backpack connector was put into place. The jugular catheter was connected to the curved shaft of an gauge 18 blunt needle built into the backpack (covered with a small cap of silicone tubing filled with silicone adhesive). The leads were soldered to the backpack. The backpack sutures were tied, and the knots covered with silicone adhesive. An hour before turning off the gas anaesthesia acepromazine maleate (0.5 mg/Kg) was injected subcutaneously (to prevent morphine mania), as well as 1 ml of the antibiotic Derapen-C. Half an hour later, morphine sulphate (0.2 mg/Kg, Abbott Laboratories) was injected subcutaneously to help the cats through the night.

3.4 Implanted hardware

Except for the piezoelectric muscle length gauges (Weytjens et al., submitted), variations of all the transducers mentioned above have been described and used before (for reviews, see Prochazka 1984; Loeb and Gans, 1986; Hoffer, 1990). Thus, only the muscle length gauges are discussed in detail.

Jugular catheter

The jugular catheter consisted of a 50 cm long silicone tube (Dow Corning 602-205; i.d. 1.02 mm, o.d. 2.16 mm), one end of which—the end to be inserted into the external jugular vein—was folded back over a few cm, and attached, in parallel, to the remaining part of the tube with a 1 cm long piece of large silicone tubing (Dow Corning 602-335) that was filled with silicone adhesive. The tip of

the short end was cut at an angle of approximately 60 degrees to make insertion into the vein easy.

Transducers for measuring local muscular dimensions

Three local muscular measurements were made in each cat: fibre length, a length of approximately 10 mm of aponeurotic sheet, and a "transverse" measurement: from the ventral to the dorsal side of the muscle, but not along the direction of the muscle fibres (see Figs. 3.1 and 3.4). The second measurement is referred to in the remainder of the text as aponeurotic sheet length, the third as S3 (the 3rd Side of the triangle formed by the three local measurements). As indicated above, these measurements were made with cylindrical piezoelectric crystals (1.3 mm diameter; CY5-2, Triton Technology) used in pairs. The principle of these measurements is discussed below (see Muscle length transducers).

An area of approximately 1 mm^2 on the outer surface of the crystals was gently roughened by scratching it with a scalpel blade, and a 50 cm long Teflon-coated multistranded stainless steel wire (Biomed AS634, Cooner Wire) was soldered to this area. Scratching of the surface was required for good adhesion of the solder. A second wire was glued to the inside of the cylinders with conductive epoxy resin (Conductive system KS-0002, Hysol). Pairs of crystals with leads so attached were glued together longitudinally with a water-resistant epoxy (aquatapoxy, American Chemical Corporation), the leads extending outwards. Once the junction was solid, the pairs were coated with aquatapoxy, and at the ends, where the leads protruded, also with a relatively soft epoxy (Barrier D, BLH

Electronics). The pairs were attached by the leads to a 1 cm^2 piece of Dacron (Dow Corning) with silicone adhesive, the back side of which had been previously covered with a thin layer of silicone. This layer of silicone served to avoid adhesion to the connective tissue that grew locally at the site of the transducers.

EMG electrodes

Bipolar EMG electrodes were used. They consisted of two Teflon-coated multi-stranded stainless steel wires (Biomed AS632, Cooner Wire) with 3 mm bare ends. These bare ends were folded back over 5 mm, and tied in sequence (inter-electrode distance 6-7 mm) to a 10 cm long size 3-0 silk suture (Ethicon). The knots were covered with 3 mm long pieces of silicone tube (Dow Corning 602-135) that were filled with silicone adhesive.

Force transducer

The force transducers were of the "E" type, as described by Walmsley et al. (1978) (see also Loeb and Gans, 1986). The substrate "E" was hand-crafted out of 1 mm thick spring-type stainless steel. A 2 mm long U-shaped semiconductor strain gauge (ESU-060-350, Entran Devices) and two small soldering pads were glued to either side of the "E" with epoxy glue (Ciba-Geigy AV 138M resin and HV 998 hardener). The strain gauges were positioned on the vertical stroke of the "E" between two transverse strokes, opposite each other. The soldering pads were positioned in the middle of the vertical stroke. The 25 μm gold leads of the strain

gauge elements, as well as two Teflon-coated multi-stranded stainless steel wires (Biomed AS631, Cooner Wire), were soldered to the soldering pads. The soldering pads and gold leads, but not the strain gauge elements, were covered with aquatapoxy[1] for protection. The strain gauges, aquatapoxy, and leads were covered with Barrier D. For strain relief, the leads were covered with silicone adhesive over 2 mm beyond the "E."

Muscle length transducers

The conventional implantable muscle length gauge consists of a thin, 4 to 10 cm long compliant silicone rubber tube, filled with either mercury or hypertonic saline (45 g of NaCl per litre), with either platinum or stainless steel electrodes in contact with the fluid column at each end (Prochazka et al., 1974; Loeb et al., 1980; see also the reviews mentioned above; the details of the gauges described in these papers and reviews vary considerably). The measurement rests on the principle of a change in electrical resistance of the gauge with stretch. These gauges enable measurements to be made that reflect the time course of muscle length change with acceptable error (see Loeb et al., 1980, for an error analysis), yet they have two major drawbacks: (1) the measurements are sensitive to

[1] Most epoxy resins absorb water. They become rubbery and loose their adhesive properties when in a wet environment (e.g., saline) for several weeks. Among a dozen different epoxy resins from different companies aquatapoxy turned out to be the only epoxy resin impervious to such treatment. As a consequence, it is an excellent epoxy resin to provide *protection* and *strain relief* for various implantable devices—as is clear from the description of the devices. However, it is not suitable for *bonding* strain gauges to a substrate, since it is a filled epoxy (the particles deform the gauges too much), nor for *coating* them, since, in general, gauges tend to stick better to the aquatapoxy than to the epoxy with which they are glued to the substrate.

changes in resistance that are not related to changes in length, and (2) there is no direct and accurate way to calibrate the measurements. The device is also non-linear. However, as shown below, errors due to non-linear behaviour are small.

Changes in resistance not related to changes in length may be produced by a variety of mechanisms, such as changes in temperature (approximately 2% change in conductance per °C for ionic solutions; Fried et al., 1977) and diffusion of interstitial fluid into the length gauge tubing. Whatever the mechanism, the result is drift. Slow changes probably underlie the poor day-to-day reproducibility of the measurements, and are difficult to eliminate or circumvent. Drift due to temperature sensitivity, however, can be minimised by implanting a second, "dummy" length gauge, left slack, for use as a second external arm in the AC-bridge.

Calibration of muscle length measurements is usually done by comparison with muscle lengths computed from joint angles measured on single video frames and measurements of bone lengths. This "videotape method" is tedious and is known to be prone to substantial errors (Loeb et al., 1980). Drift in the measurements makes the process of calibration only more difficult.

Since the volume of the fluid column in the tubing is constant, its cross-sectional area decreases with stretch. As a result, its resistance varies quadratically with length, rather than linearly. Prochazka (1984) found the maximum deviation from linearity (MDFL), i.e., the maximum deviation from a straight line fit, for a 20 mm length range to be less than 2% for mercury-filled gauges and

approximately 10% for saline-filled ones (the latter figure was computed from data in Loeb et al., 1980). There is no theoretical reason why both types would differ in this respect. Calculations for a 50 mm long saline-filled length gauge of the type used in the experiments reported here (see below; i.d. 1.09 mm, o.d. 1.6 mm, specific conductance 0.065705 $Ohm^{-1}cm^{-1}$) yielded an MDFL of 2.23% for a 20 mm length range (55-75 mm; 40% fractional length change). For a 10 mm length range (55-65 mm; 20% fractional length change), the MDFL was only 0.57%. Measurements on a 49 mm long length gauge of otherwise identical dimensions yielded values of 2.32% (53-73 mm) and 0.59% (53-63 mm), respectively.[2] These theoretical and experimental values agree rather well. Also, the values for the 20 mm length range correspond well with Prochazka's value for mercury-filled gauges. In conclusion, except when the fractional length change is large, errors due to non-linearity are rather small.

The lack of an accurate calibration procedure is the most serious weakness of conventional muscle length gauges. The new type of length gauge described below obviated the problems mentioned above by operating on the principle of sonomicrometry, i.e., the measurement of lengths with piezoelectric crystals.

In sonomicrometry lengths are measured by conversion of the time it takes for brief bursts of ultrasound emitted by one piezoelectric crystal of a pair to

---

[2] The length gauge, immersed in water at room temperature, was connected in series with a 10.079 KΩ resistor and driven by a 25 KHz sine wave generated by a function generator. The voltage across the resistor, V_R, was measured on an oscilloscope. The resistance of the gauge was computed from Ohm's law as $R_L = R(V - V_R)/V_R$, where R is the resistance of the series resistor, and V the driving voltage.

travel to the other, to length through multiplication by the velocity of sound transmission in the medium in which the measurements are made. A continuous output is obtained by making measurements repeatedly and low-pass filtering of the resulting signal. This technique was developed by Rushmer et al. (1956) to measure cardiac dimensions, but has since also been applied to skeletal muscle. In hind leg muscles, in particular, it has been used for measuring fibre lengths (Griffiths, 1987; Hoffer et al., 1989; Griffiths, 1991), and, indirectly, angles of pinnation (Caputi et al., 1989; Hoffer et al., in press). Equipment to make these sonomicrometric measurements is commercially available. The measurements described here were made with a Sonomicrometer 120 (Triton Technology). With this machine, calibration of the measurements is straightforward: in "calibration mode" its output consists of 1-mm voltage steps over the working range.

The bursts of ultrasound generated by the emitter-crystal cause the receiver-crystal to vibrate. These vibrations, in turn, induce measurable oscillations in voltage that vary with time at the same frequency. The amplitudes of the different component waves of these brief electrical oscillations decrease with the distance between emitter and receiver, but so long as the first wave, which indicates arrival of the burst of ultrasound, can be reliably detected over the entire length range of interest by appropriately setting a trigger level, a smoothly varying output is obtained.

Initially I simply replaced the electrodes at the ends of the conventional design by piezoelectric crystals. I quickly discovered, however, that the silicone

tubing altered the way the amplitude of the received signal decreased with distance. Specifically, upon stretching the gauge, the first wave would quickly attenuate and vanish, then the amplitudes of the second, third, and subsequent waves would decrease, and vanish in succession. Triggering on successive waves resulted in discrete jumps in the output signal. The tubing thus restricted the length range over which reliable measurements could be made. The fact that the gauges worked much better when suspended in air than when immersed in water suggested that this behaviour was due to loss of energy into the medium surrounding the tube through refraction. This phenomenon was inversely related to the stiffness of the tubing—the attenuation was less when stiffer tubing was used. The first workable design ("prototype gauges") was based on i.d. 1.57 mm, o.d. 2.41 mm silicone tubing (Dow Corning 602-265). Its working range, however, was restricted to approximately 10 mm. The "hybrid" piezoelectric length gauge described below extended this range by omitting the tubing and using a conventional length gauge as an external guide for the crystals (Fig. 3.2). Specifically, it consisted of a 55 mm long conventional saline-filled length gauge and two 30 mm lengths of i.d. 1.57 mm, o.d. 2.41 mm silicone tubing (Dow Corning 602-265), each of which contained a disk-shaped piezoelectric crystal. These two tubes were aligned with the conventional gauge, and thus, upon stretch, measured the same change in length.

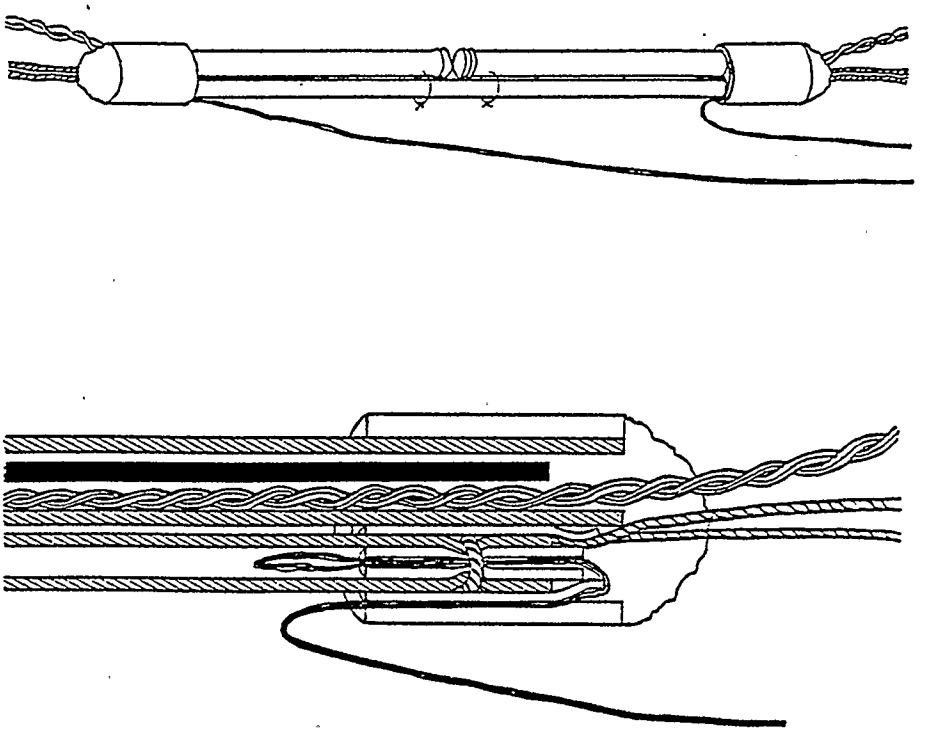

Fig. 3.2. Schematic illustration of the hybrid length transducers. The two silicone tubes with the piezoelectric crystals were attached to a conventional length gauge, which acted as a mechanical guide. The darkly shaded part in the longitudinal cross-section of the length gauge (bottom panel) is the 0.5 mm diameter stainless steel rod used to reinforce the tubes with the crystals. Further details and dimensions are given in the text.

The construction procedure was as follows:

1. The ends of two 50 cm long Teflon-coated multi-stranded stainless steel wires (Biomed AS632, Cooner Wire) were stripped over 1 cm and made into loops by inserting them into small 6 mm long silicone tubes (Dow Corning 602-135; i.d. 0.51 mm, o.d. 0.94 mm) that were expanded in toluene and filled with silicone adhesive while still expanded.

2. A 55 mm long piece of i.d. 1.09 mm, o.d. 1.6 mm silicone tubing (Sil-Med) was filled with hypertonic saline (45 g NaCl/l) coloured with a green food dye, and the loops were inserted into the ends and tied to the tube with size 2 Mersilene sutures.

3. A 7 mm long piece of i.d. 1.47 mm, o.d. 1.96 mm silicone tubing (Dow Corning 602-235) was expanded in toluene, slid over the Mersilene knots and filled with silicone adhesive.

4. Disk-shaped piezoelectric crystals of 2.5 mm diameter were cut out of 5.8 mm square pieces (purchased from Triton Technology). A patch of about 1 mm^2 on both surfaces was slightly scratched with a scalpel blade, and a Teflon-coated multi-stranded stainless steel wire (Biomed AS634, Cooner Wire) was soldered to these scratched surfaces. The solder joints were reinforced with aquatapoxy. Both leads were twisted and the whole assembly was coated with Barrier D to avoid electrical leaks and to completely cover the aquatapoxy, which easily dissolves in toluene. In order to minimise loss of signal strength due to

slight misalignments that may occur during movement, care was taken to fashion the epoxy over each crystal into convex lenses. The crystals were inserted into the 3 cm long silicone tubes, expanded in toluene, by pulling the leads through, and the tubes were filled with silicone adhesive. After the adhesive had set, the tubes were stiffened by inserting 2.5 cm long, 0.5 mm diameter stainless steel rods (Fig. 3.2).

5. The tubes with the crystals were attached to the conventional gauge by 7 mm long pieces of i.d. 3.35 mm, o.d. 4.65 mm tubing (Dow Corning 601-335) that were expanded in toluene, slid over both ends of the conventional gauge and the tubes with the crystals, and filled with silicone adhesive. To keep the crystals aligned with the conventional gauge, they were, in addition, tied to the conventional gauge with two relatively loose (to still permit sliding) size 5-0 sutures (TI•CRON, Atraumatic).

Length gauges, when implanted, must not be allowed to become slack at the shortest physiological muscle lengths. Thus, in order to maximise signal strength, the gauges were always assembled such that at slack length the crystals would just touch. During implantation, the stainless steel rods were often bent slightly to fit the shape of the muscle.

Length gauges should also add as little stiffness as possible in parallel to the muscle of which they measure the length. Since the volume V of the tubing

wall was constant, its cross-sectional area A, and thus also its stiffness, decreased with length. Specifically, the force F exerted by the tubing was

$$\begin{aligned} F &= cA(L - L_0) \\ &= cV(1 - \frac{L_0}{L}), \end{aligned} \tag{3.1}$$

where L_0 denotes slack length, and c is a constant. The constant c was estimated for a number of length gauges by fitting (3.1) to actual measurements of stiffness, which were made by fixing one end of the length gauges and hanging various weights to the other. Results for two gauges are shown in Fig. 3.3. A numerical measure of stiffness with the dimensions N/mm was obtained by multiplying c by A (for convenience at L_0). At L_0 = 50 mm the prototype gauges had a stiffness of 0.092 N/mm, the hybrid gauges a stiffness of 0.050 N/mm (values computed from straight line fits to stiffness data from 3 gauges of slightly different lengths). I.e., the prototype length gauges were approximately twice as stiff as the hybrid length gauges.

In contrast with conventional muscle length gauges, the piezoelectric length gauges described here were (1) linear devices that enabled accurate relative measurements of muscle length to be made that (2) did not drift, and (3) were quite easy to calibrate. Disadvantageous in comparison with conventional gauges was that (1) the new transducers were bigger in size, and (2) their construction was more involved. However, compared with what was gained, these weaknesses reduced to mere inconveniences.

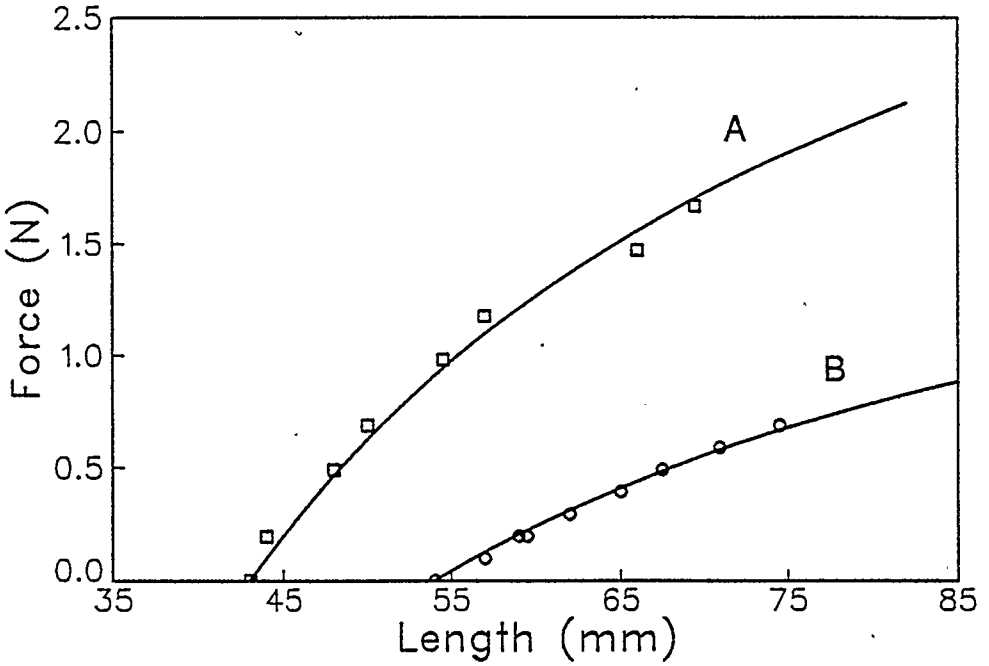

Fig. 3.3. Measurements of the stiffness of the piezoelectric length transducers, and corresponding curve fits. The x-axis is gauge length, the y-axis the force exerted by the weights used to make the measurements. □, prototype length gauge; O, hybrid length gauge. Stiffness at L_0 (cA; see text) was 0.104 N/mm (curve A) and 0.045 N/mm (curve B), respectively.

None of the hybrid gauges was implanted for more than 13 days. *Postmortem* dissections did not show evidence of proliferation of connective tissue that might interfere with the movements of the piezoelectric crystals.[3]

The principle underlying the measurements, as explained above, was discrete: emission of single bursts of ultrasound. The Sonomicrometer 120, in particular, made this elemental measurement 1543 times per second. Muscle length changes during locomotion are slow in comparison. The repeat frequency of the Sonomicrometer 120 was thus well above the Nyquist frequency of the measured muscle length signals, which, consequently, were not distorted by inaccurate sampling.

Sonomicrometric muscle length measurements—as all measurements—are subject to error. Four different sources could be identified:

1. The Sonomicrometer assumed a fixed velocity of sound of 1580 m/s, i.e., always multiplied measured transit times (in μs) by 1.58 mm/μs to compute distance. Actual velocities different from this value would thus introduce systematic errors. In the case of the hybrid length gauges, the ultrasound travelled through muscle and interstitial tissue. Published values for the velocity of sound in muscle vary from 1540 m/s (Ludwig, 1950; living human tissue, mostly

[3] This was also true for a hybrid length gauge that was implanted for 91 days in a cat used in unrelated experiments. The gauge had failed, but not because of connective tissue: one of the 5-0 sutures used to keep the tubes with the crystals aligned with the conventional gauge had come loose. The tube it had held in place was stuck out of alignment. The other tube could still move freely.

muscle) to 1603 m/s (Goldman and Richards, 1954; rabbit muscle at 26°C, parallel to fibres). Using a value of 2.4 m/s°C to compensate for the effect of temperature (see below), these values would yield an error range of -3.0 to 2.6 % (100 x (1580 - v_a)/v_a, where v_a is the actual velocity of sound in m/s). However, for the cat medial gastrocnemius muscle, the Sonomicrometer's 1580 m/s was found to be accurate within 0.2% (Caputi, et al., in press). For the prototype length gauges, using 1531 m/s for the velocity of sound (the velocity of sound in sea water at 25°C; see below), and 2.4 m/s°C for temperature compensation, the error was computed to be 1.3%.

2. As the amplitude of the first wave of the received ultrasound burst decreased with length, the relative position of the trigger level set to detect it changed. This resulted in an overestimation error that grew with increasing length. Numerically this error was maximally 1.58 mm/μs times the duration of one quarter of a period (which for the 3 MHz piezoelectric crystals used in both designs was 0.083 μs), or 0.13 mm, or, for an 8 mm change in length—a typical range for the medial gastrocnemius muscle of the cat during treadmill locomotion—1.63% (the worst case: amplitude of the first wave much larger than the trigger level at the shortest length and comparable at the longest length).

3. The piezoelectric crystals were coated with epoxy resin (Barrier D) which transmits sound faster than 1580 m/s. The thickness of the coating was approximately 0.5 mm. The velocity of sound in Barrier D was found to be 2146 m/s at 37°C (Sonomicrometer 120 measurement made with piezoelectric crystals

glued to both ends of a 10.3 mm long cylinder made out of Barrier D; the transmission time was measured on an oscilloscope from the raw signals). With this value, the error—an underestimation—was computed to be 0.264 mm for all distances. However, since the length gauges did not yield absolute muscle length measurements, this source of error was irrelevant.

4. As the velocity of sound in liquids varies with temperature, the length measurements were temperature dependent. The variation with temperature for both distilled and sea water (which contains approximately 19 g Cl^- and 10.5 g Na^+ per Kg) is 2.4 m/s°C (Becker, 1990). Systematic data for the velocity of ultrasound in skeletal muscle or hypertonic saline as a function of temperature do not seem to exist. It seemed safe, however, given the above data, to assume that the variation with temperature in those media was not very different from 2.4 m/s°C. Thus, with the velocity of sound at 37°C assumed to be 1580 m/s (the value assumed by the Sonomicrometer), temperature dependence resulted in an error of 0.15% per °C.

What then was the accuracy of the piezoelectric length gauges? Combining the different sources of error, and assuming a maximum change in temperature of ±1°C, the following (conservative) error bounds were obtained: -1.0 to 2.5% (-0.27 to 1.98%) and 0.5 to 3.5% (1.15 to 3.08%) for the hybrid type and prototype length gauges, respectively.

Thermistor

The thermistor (YSI 44004, Yellow Springs Instrument) consisted of a 2.4 mm diameter spherical body (the *therm*ally sensitive res*istor* coated with epoxy resin) and two 7.5 cm long tinned copper wires. These copper wires were trimmed to about 1 cm, and two 50 cm long Teflon-coated multi-stranded stainless wires (Biomed AS632, Cooner Wire) were microwelded to them. The welds were covered with Barrier D, and the assembly was put into a 2 cm long toluene-expanded silicone tube (Dow Corning 602-305) that was filled with silicone adhesive.

Ground wire

The ground wire consisted of a 50 cm long Teflon-coated multi-stranded stainless wire (Biomed AS632, Cooner Wire) one end of which was stripped over 20 mm and made into a loop in the same way as the electrodes of the conventional part of the length gauges.

3.5 Backpack connector

The connector was of the "backpack" or "saddle" type (Loeb and Gans, 1986). It consisted of a 40-pin IDC (Insulation Displacement Connector) header (3M 3432) mounted on a printed circuit board (PCB) with 40 connections. The PCB in turn was mounted on a 5.5 cm by 10 cm sheet of Dacron-reinforced silicone rubber with silicone adhesive.

3.6 Chronic recording

Two days after the chronic surgery the cats were put on the treadmill again for daily training. Chronic signals for use in the acute experiments were not acquired until the animals had fully recovered and walked without visible limping. At recording time, the cats were connected to the recording equipment by means of a ribbon cable with a 40-pin IDC socket at each end, and made to walk at a speed of 0.5 m/s (1.8 Km/h). The fibre length, aponeurotic sheet length, S3, tendon force, and muscle length signals were appropriately adjusted (the gains and offsets of the two muscle length measurements were adjusted such that the two signals would superimpose), and, together with the EMGs, recorded onto FM tape (Honeywell model 96; 15 inches per second, bandwidth DC-10 KHz), while the cat's movements were recorded onto videotape. For later synchronisation, a time code signal (IRIG B, generated by a Datum 9300 Time Code Generator/Translator) was recorded onto both the videotape and the FM tape. The gain of the EMG amplifiers (AC Differential Amplifier MDA-2, Bak Electronics) was always 1000, and their bandwidth 50-5000 Hz. The bandwidths of the DC-bridge (tendon force; custom-built low-noise, low-drift DC-bridge) and AC-bridge (conventional muscle length measurement; AC Bridge Integrator ABI-1, Bak Electronics) were DC-5 KHz and DC-1 KHz, respectively. After a few minutes of walking, the cats were disconnected, and 1-mm voltage calibration steps were recorded onto tape for all four Sonomicrometer signals.

3.7 Software

Four programs were used for data acquisition and analysis: ATOD1 (Analog TO Digital 1), SMUF1 (Single Motor Unit Forces 1), ATOD2, and SMUF2. ATOD1 and SMUF1 ran on a PDP-11/23+ minicomputer (Digital Equipment Corporation) under RT-11, ATOD2 and SMUF2 on PCs under DOS. ATOD1 (Pascal and MACRO-11) was used to digitize chronic data on FM tape, condition the signals, and make "acute" files for use by SMUF1 in the acute experiments. SMUF1 (FORTRAN and MACRO-11) was used to run the acute experiments: it simultaneously controlled the muscle puller, output stimuli for distributed stimulation and stimulation of the multi-unit filament under study (see below), and sampled the acute signals of interest. ATOD2 (C; written by Morten Haugland) was used in the last two experiments to digitize twitch contractions and corresponding EMGs in between series of runs (see below). SMUF2 (C) was the data analysis program. The accuracy of the A/D conversion (both A/D conversion programs) was checked with sine waves of known frequency and amplitude. The timing of the stimuli was checked on an oscilloscope. The calibration of the control signal for the muscle puller was checked by moving the puller to various target positions (in "ruler" cm; see The muscle puller) under program control, and comparing target and actual positions. Further details of the programs are given in the sections below.

3.8 "Acute" data files

The videotapes were scanned for periods of steady walking in the middle of the treadmill. The corresponding data on FM tape were digitized in segments of five seconds using the 1 KHz time code signal on the tape as an external clocking pulse. Analog-to-digital conversion was done with ATOD1 using the Data Translation DT3382 A/D board. Prior to digitization, the EMGs were rectified and bin-integrated (Pulsed Sample/Hold Integrator PSI-1, Bak Electronics; Bak and Loeb, 1979). A binwidth of 10 ms was used. From the digitized data an approximately 2 s long segment spanning two step cycles was chosen for use in the acute experiments. The main selection criterion was the presence of clear maxima in the passive force at the end of the swing phase. The reason for this was that these passive maxima simplified the matching of acute and chronic signals (see below). The conventional muscle length measurement was used to determine the endpoints of the segment, which were chosen to be on the shortening movement in the early swing phase such that the length at the end of the segment was greater than the length at the beginning by one sample. In this way, the muscle puller, for which the conventional length measurement was used as the control signal, did not have to be moved between runs (paradigms 1 through 4; see below). Data conditioning included digital low-pass filtering (FIR filter computed with the Blackman window) of the conventional length signal (cut-off frequency 40 Hz) and of the rectified and bin-integrated EMGs (cut-off frequency 10 Hz). Calibration factors (A/D integers to mm) were computed for

all the piezoelectric length measurements from straight line fits to the 1-mm voltage steps output by the Sonomicrometer (Volts to mm) and the voltage range and resolution used for the data acquisition (± 2.5 Volts and 12 bits, respectively). The lengths measured by the piezoelectric length gauge were used to calibrate the conventional measurement. Tendon force could not be calibrated until the end of the acute experiments, whence a low-noise, low-drift DC-bridge was used, to ensure that the gain would not change from the time of the chronic recording till the end of the acute experiment. All relevant signals—conventional muscle length, piezoelectric muscle length, muscle fibre length, aponeurotic sheet length, S3, rectified/bin-integrated/filtered EMGs, and tendon force—were stored in "acute" data files for use by SMUF1. Only odd-numbered samples were stored because of a speed constraint imposed by the PDP-11/23+ (see below); i.e., the sampling frequency was reduced from 1 KHz to 500 Hz. Also stored in these files were the different calibration factors and a stimulus train (stored as a sequence of zeros and ones) for the ventral root multi-unit filaments to be studied (see below). This stimulus train consisted of two identical sequences of six stimuli loosely synchronized to the periods of active force generation in the chronic measurements. The interpulse intervals were 24, 30, 40, 50 and 60 ms. They were chosen such that their instantaneous frequency plot resembled the active force generated.

3.9 Experiments under anaesthesia

The acute experiments were performed two days after the day of the chronic recording. Anaesthesia was induced and maintained with small amounts of sodium pentobarbital (20% Somnotol (65 mg/Kg) in 0.9% sodium chloride solution) administered intravenously through the jugular catheter. The cat was intubated. Expiratory CO_2 level was monitored throughout the experiment as above. The hind leg was extensively denervated. A 5 cm long incision was made in the groin, and the femoral nerve and the two branches of the obturator nerve were cut. A 5 cm long incision was made on the lateral side of the thigh, parallel to the ventral edge of the biceps femoris muscle. The proximal part of the biceps femoris muscle was separated from the surrounding muscles, and the muscular branch of the sciatic nerve innervating the hamstring muscles was cut. An 8 cm long incision was made on the dorsal side of the leg, from halfway the thigh to halfway the calf. The common peroneal nerve was cut. The popliteal fatpad was removed, and the branch of the tibial nerve innervating the lateral gastrocnemius and soleus muscles was cut, as well as the tibial nerve itself, distal to the branch innervating the medial gastrocnemius muscle. Care was taken so as not to pull on or damage any of the leads of the implanted devices. All incisions were closed with size 3-0 sutures to avoid leakage of the paraffin oil in the pool on the back (see below). The foot was amputated. A longitudinal incision was made on the dorsal side. The skin was dissected free and cut radially. All the blood vessels were ligated and cut, and muscles and tendons were cut. The foot was cut

through at the level of the proximal metatarsal joints, and the skin was closed. The amputation served to avoid undesirable changes in muscle length during the experiment due to oscillations of the foot caused by movement of the muscle puller. The backpack was cut loose, moved to the side of the back, and resutured to the skin. A laminectomy was performed from S2 to L4. The cat was mounted in a sturdy metal frame with 3/8" diameter stainless steel pins at the hip and at the distal end of the femur and a clamp on the spinous process of the L3 vertebra. The skin of the back was pulled up and tied to the frame to make a paraffin oil pool. The dura mater was cut open, the L7 and S1 dorsal and ventral roots were separated, and cut close to their points of entry into the spinal cord. The stump of the foot was hooked up to the muscle puller by clamping the dorsal part of the calcaneus into a U-shaped holder attached to the puller's armature with two sharpened size 10-32 bolts, which were locked with wingnuts. The holder was made of stainless steel, and was 6 cm long (to allow enough space for the stump of the foot to flex and extend with movement of the muscle puller), 3.2 cm wide, and 5 mm thick. Body temperature was monitored with a rectal thermometer and kept at 37°C by means of a heating blanket and radiant heat. Leg temperature was monitored with the implanted thermistor and maintained at 36°C with radiant heat.

The muscle puller

The muscle puller was (in a previous life) a large hard disk drive (Telex 8331 Model 2). It was disassembled, except for the head actuator, and modified to suit

the needs of the experiment: (1) an aluminum shaft, onto which the U-shaped holder was mounted, was rigidly attached to the mounting block for the read/write heads (attached to the motor's armature), (2) a linear position transducer (Short Longfellow SLF-S-100-D-1, Waters MFG), used for providing position feedback, was rigidly mounted on top of the motor, and its shaft attached to the mounting block for the heads, (3) a ruler was mounted on top of the linear transducer, and (4) the electronics were replaced by a servo amplifier (Switching Servo Amplifier SSA-75-07-20, PMI Motors). The total range of movement was about 8 cm. The compliance of the motor was 0.268 μm/N.

Calibration of the muscle puller control and position feedback signals was done (or checked) with SMUF1 the day before the experiment. Eleven 1-Volt steps, ranging from -5 to +5 Volts, were fed to the muscle puller's servo-amplifier, and calibration factors (D/A integers to "ruler" cm and A/D integers to "ruler" cm, respectively) were computed from the corresponding eleven positions (spanning the full range of movement) of the end of the shaft of the linear transducer relative to the ruler by fitting straight lines to the D/A integers and ruler cm values and digitized position feedback signals and ruler cm values, respectively. The calibration factors were stored in a file for retrieval by SMUF1 during the acute experiment. The calibration of the muscle puller was found to be extremely stable and had to be redone only when the settings of the servo-amplifier were changed.

Computer control of experiments

The acute experiments were done under control of SMUF1 (see above). Digital-to-analog conversion of the chronic conventional muscle length measurement (the control signal for the muscle puller in paradigms 1-4; see below) was done with the Data Translation DT2751 D/A-DIO board (12-bit resolution). Stimuli were output as 2 ms TTL pulses using two of the DT2751's four digital outputs. A third digital output was used to output a 50 ms pulse at the start of each run. This pulse served to trigger the different oscilloscopes on which the signals were monitored. Analog-to-digital conversion was done, as above, with the Data Translation DT3382 A/D board. The following signals were sampled: (1) position feedback, (2) conventional muscle length, (3) muscle fibre length, (4) aponeurotic sheet length, (5) S3, (6) tendon force, and (7) piezoelectric muscle length. All input/output was done with MACRO-11 interrupt routines. The clocking frequency was 500 Hz rather than 1 KHz because the interrupt routines did not function properly when clocked at a rate higher than 980 Hz. Digitized signals were displayed on a monochrome video monitor (Electrohome; controlled by a QRGB-Graph Colour Graphics Controller, Matrox Electronic Systems) at 480x512 resolution, together, where applicable, with the corresponding chronic target signals. In two experiments twitch contractions and corresponding EMGs were also digitized in between series of runs with an Intel 80386-based IBM-compatible personal computer (Twinhead Superset 500) using the Data Translation DT2821 board (ATOD2; see above). The sampling frequency was 5 KHz.

Stimulation

The TTL pulses for distributed stimulation triggered a multi-function, multi-channel pulse generator (DC-1 Digital Controller, Bak Electronics), which was used to (1) distribute the stimuli (time delay between stimuli distributed to successive channels: 4 ms), and (2) reduce the pulse duration for each channel to 100 μs (the duration of the TTL pulses output by the DT2751 board was determined by the clock frequency). The outputs of the digital controller were fed to five independently adjustable custom-built biphasic constant-current stimulators. The TTL pulses for the filament under study were fed directly to a commercial biphasic constant-current stimulator (Biphasic Stimulus Isolator BSI-2, Bak Electronics).

Stimulus trains for distributed stimulation

The stimulation patterns used to mimic the active force generated during treadmill locomotion (paradigms 3 and 4; see below) were derived from the chronic EMG measurements, the rationale being the finding of Hoffer et al. (1987) that instantaneous frequency plots of motor unit firing during normal activity resemble rectified and smoothed EMGs. The rectified, bin-integrated and low-pass filtered EMG whose time course best resembled the time course of the active force was converted from Volts to pulses/s to turn it into an instantaneous frequency signal. The reason for this choice was that with these EMGs the best simulation results (muscle force) were obtained. The maximum instantaneous frequency, i.e., the maximum of the EMG, was defined to be 60 pulses/s. For both EMG bursts,

beginning with the last one, the last sample equal to or greater than 15 pulses/s plus a random number uniformly distributed between -5 and +5 pulses/s was used as the starting point for the generation of the stimulus trains, which were then derived recursively using

$$n_{i-1} = n_i - \frac{f_s}{c.\mathrm{EMG}(n_i)}, \tag{3.2}$$

where n_i is the time of occurrence (sample number) of the ith stimulus, f_s is the sampling frequency (500 Hz), c is a scale factor with dimensions pulses/s.Volt, and EMG(.) is the sampled, rectified, bin-integrated, and low-pass filtered EMG. For each EMG burst generation of stimulation times stopped when c.EMG(n_i) was equal to or smaller than 1 pulse/s. As above, the stimulation patterns were stored in an array as a sequence of zeros and ones. Addition of a random number allowed different, slightly differing trains to be generated using the same EMG. Generation of the stimulus trains was done with SMUF1, which, in addition, also allowed the stimulation patterns to be edited manually. Manual editing of the stimulation patterns was required in 7 out of the 8 experiments in which useful data were acquired.

Experimental procedure

The backpack was connected to the equipment with a ribbon cable. The acute Sonomicrometer signals were calibrated. For each signal, three different lengths were digitized by SMUF1. The calibration factors (A/D integers to mm) were computed by fitting straight lines to the digitized voltages and the corresponding

numerical values of the lengths (comparison of acute signals and chronic targets was thus done in mm, not in Volts). The Sonomicrometer signals were adjusted (trigger levels only) while replicating the chronic muscle length signal without acquiring data.

Tetanic forces were acquired at different muscle lengths (0.5 mm intervals) to construct force-length curves. The tetani were produced by stimulating the L7 and S1 ventral roots at 100 pulses/s for 1 s (no distributed stimulation).

The muscle was thoroughly fatigued: it was stimulated at 100 pulses/s for 50 minutes, in 10 periods of 5 minutes. The purpose of fatiguing was to (1) knock out the FF units as much as possible in order to partially restore the natural recruitment order of the motor units (S $\rightarrow$ FR $\rightarrow$ FF), which is reversed by electrical stimulation, and (2) reduce variability in the active force generated in the simulated step cycles due to potentiation and fatigue. Recovery from fatigue was not quantified.

The two step cycles of treadmill walking stored in the acute files were simulated, the primary goal being to match chronic and acute fibre length and tendon force. This was done in two steps: (1) the proper location of muscle length in the range of movement of the muscle puller, i.e., the muscle length offset or muscle puller offset, was determined (muscle length measurements were relative to the minimum distance between the piezoelectric crystals of the length gauges), and (2) a proper amount of active force was generated.

The proper muscle length offset was found as follows. The muscle puller was moved to a position at which there was no measurable passive force in the muscle. Muscle length was replicated repeatedly without stimulating the muscle (paradigm 2; see below). The muscle puller offset was adjusted until the passive forces generated in the swing phase of the step cycles matched. The corresponding maxima in muscle fibre length would then match reasonably well, although there were often discrepancies (see Results). If so, then the muscle puller offset was further adjusted until the maxima in the fibre length signals matched.

Active force was required to minimise the large differences that would still remain at this stage between acute and chronic fibre length in the stance phase of the step cycles. It was generated by distributed stimulation of five small L7 and S1 ventral root filaments. Matching was done as follows. The L7 and S1 roots were subdivided into a small number of filaments. Each filament was tested for its ability to generate active force in the medial gastrocnemius muscle upon stimulation with single pulses. From these "active" filaments five were chosen that produced approximately the same force when stimulated in isolation and a force greater than the target force when stimulated with the stimulation pattern derived from the EMG while muscle length was replicated (paradigm 4; see below). The five filaments were further subdivided and tested (separately and using paradigm 4), and this process was repeated until amplitudes of the acute and chronic forces matched well. However, this could not always be achieved at the initial amplitude of movement (the amplitude of the chronic signal; as described above, the

movement was imposed through flexion and extension of the foot, rather then directly to the muscle). As it turned out, the lower end of the range of change of the imposed movement was a critical variable in the simulations. When, for the same muscle puller offset, the amplitude of the movement was too small, then the force required to make the fibre lengths match was too large. If this was the case, then the amplitude of the control signal for the muscle puller was increased until both muscle fibre length and muscle force matched their respective targets. Differences in time course were reduced, when necessary, by manually editing the distributed stimulation pattern, using educated guesses as to the timing of the stimuli, and trial-and-error. Successful stimulation patterns were stored in files and could be easily retrieved when required. When the forces were so matched, the match between the acute and chronic fibre lengths in the stance phase was in general quite good. Remaining discrepancies (usually amplitude) were reduced by either removing a fraction of one of the five filaments or adding a new small filament.

Multi-unit filaments other than those used for distributed stimulation were studied using seven different paradigms, P1, P2,..., P7, grouped into two sets, P1-P4, and P5-P7. In the first set, the chronic muscle length signal was replicated (simulated walking). In the second set, the muscle was kept isometric at various lengths. The different paradigms differed further by the stimulation patterns used (DS, distributed stimulation, and/or FUS, filament under study); see table 3.1. Simulated walking with distributed stimulation of ventral root filaments is

	Simulated walking				Isometric		
	P1	P2	P3	P4	P5	P6	P7
DS	-	-	+	+	-	+	+
FUS	+	-	+	-	+	+	-

Table 3.1. Stimulus patterns used in the seven paradigms P1, P2,..., P7: DS, Distributed Stimulation of five small ventral root filaments; FUS, stimulation of the ventral root Filament Under Study.

referred to as "active walking," simulated walking without distributed stimulation as "passive walking." In P6 and P7 a constant-frequency train (60 pulses/s) was used for distributed stimulation, starting at the beginning of the run. Typically, ten recordings were made for each paradigm in the following sequence: 1) Set 1: P1 P2 P3 P4 P1 P2 P3 P4 P1 ... P4; 2a) Set 2: P5 P6 P7 P5 P6 P7 P5 ... P7; 2b) Set 2: P5 P6 P7 P5 P6 P7 P5 ... P7; .... The time between different runs was approximately 4 s. The measurements of set two were made at a number of different muscle lengths chosen such that the "isometric" fibre lengths measured in P6 would span the range of "simulated walking" fibre movement in P3 during the periods of active force generation.

At the end of the experiment the ankle was disconnected from the muscle puller. The incision on the dorsal side of the stump of the foot was opened and extended rostrally. The tendon of the medial gastrocnemius muscle was dissected free from the surrounding tissues, and checked to see if all of it was still in the buckle. The sutures of the length gauges were checked for good attachment to the calcaneus. All the other tendons were then cut, the calcaneus was cut through and

a string attached to it, and the force transducer was calibrated with various weights.

The animal was sacrificed with an intravenous or intracardiac overdose of pentobarbital.

3.10 Postmortem examination

In all cats the position and condition of the various devices was carefully checked *postmortem*. As discussed above, the position of the buckle and the distal length gauge sutures were checked at the end of the acute experiment. Further verification was done in *postmortem* examinations. Specifically, it was checked if (1) the piezoelectric crystals were still well attached to the muscle, (2) the EMG electrodes were still in the muscle, and (3) the length gauges were still firmly attached to the sesamoid bone. In three cats, the medial gastrocnemius was excised and fixed in formaldehyde for verification of the position of the crystals with which fibre length was measured relative to the muscle fibres. The location of the previously removed crystals was identified by the presence of a trough in the connective tissue that had grown under the Dacron to which they were fixed. Small bundles of muscle fibres were gently torn away starting at one such trough and the locations of the other end of the bundles identified.

3.11 Data analysis

The data files were transferred from the PDP 11/23+ to an Intel 80386-based IBM-compatible personal computer (Dell System 325) with the communication

program Procomm Plus (Datastorm Technologies) using the Kermit file transfer protocol, and the data files were archived on 3.5" 1.44 Mbyte floppy disks. Analysis was done off-line on the PC with SMUF2. Graphical output was produced using the GraphiC 6.0 library (Scientific Endeavors Corporation).

Terminology

The expressions below are used with the indicated meanings.

Muscle length : the length of the muscle, as measured with the piezoelectric length gauges.

Fibre length : the length of the muscle fibres in between the crystal pairs used to measured this length, as given by (3.4) below.

Angle of pinnation : the angle of pinnation, as given by (3.5) below.

Tendon : the entire tendinous component, i.e., external tendon plus aponeurotic sheet.

For the meaning of aponeurotic sheet length and S3, see above.

Symbols

The following symbols are used:

L_M : muscle length,

L_F : fibre length,

L_T : tendon length,

L_A : aponeurotic sheet length,

α : angle of pinnation,

F_a : the force measured in paradigm P4,

F_p : the force measured in paradigm P2.

Paradigms 1 through 7

All signals within the same paradigm except those from the first run were averaged. The measurements from the first run were not included since they were always slightly different (in particular, the passive force in late swing was always larger). Averaging reduced the noise in some of the acute Sonomicrometer signals (very brief and small spikes occurring seemingly randomly) introduced by the very process of saving the data to hard disk, which could not be eliminated completely. Differentiation of length signals was done with a 4-point Lagrangian differentiator.

Fibre length and angle of pinnation

With one qualification, the error analysis presented above (see Muscle length transducers) also applied to the local measurements made with the cylindrical crystals. The qualification was that the measurements were absolute; i.e., errors due to differences in the velocity of sound in the different media in which the ultrasound travelled—specifically, the effect of the aquatapoxy—did matter and could not simply be ignored. In addition, geometrical errors due to the crystals's finite size also had to be taken into account. As already mentioned, Caputi et al. (in press) found the Sonomicrometer's assumed velocity of sound of 1580 m/s to be accurate within ±0.2% for cat medial gastrocnemius. The cylindrical crystals

had a natural frequency of 5 MHz. Consequently, the errors caused by changes in the amplitude of the first wave of the received burst of ultrasound were smaller than 0.079 mm (about 0.4%). Errors due to changes in temperature were minimised by maintaining whole leg temperature at 36°C. Errors due to the aquatapoxy were corrected for. The velocity of ultrasound in aquatapoxy was found to be 2593 m/s at 37°C.[4] The thickness of the aquatapoxy coating was on average 0.17 mm (difference between average diameter of five coated and uncoated crystals divided by two). From these values the underestimation error in the measured distance was computed to be 0.133 mm.

Fig. 3.4A schematically illustrates how the fibre length measurements differed from the actual fibre lengths, and also defines the variables of interest. Fig. 3.4B shows how the distances f, a, s between the centres of the crystals were computed: the measured distances (fibre length, aponeurotic sheet length, and S3) were incremented by 1.433 mm, which is the sum of 1.3 mm, the diameter of the crystals, and 0.133 mm, the correction for the effect of aquatapoxy. Using the cosine law the angle θ (in radians) was computed from

$$\theta = \cos^{-1}\left(\frac{f^2 + a^2 - s^2}{2fa}\right). \qquad (3.3)$$

Using θ, fibre length was computed from

[4] The measurement was made as described on p. 44. The length of the aquatapoxy cylinder was 32.15 mm. (At 20°C, the velocity was 2702 m/s.)

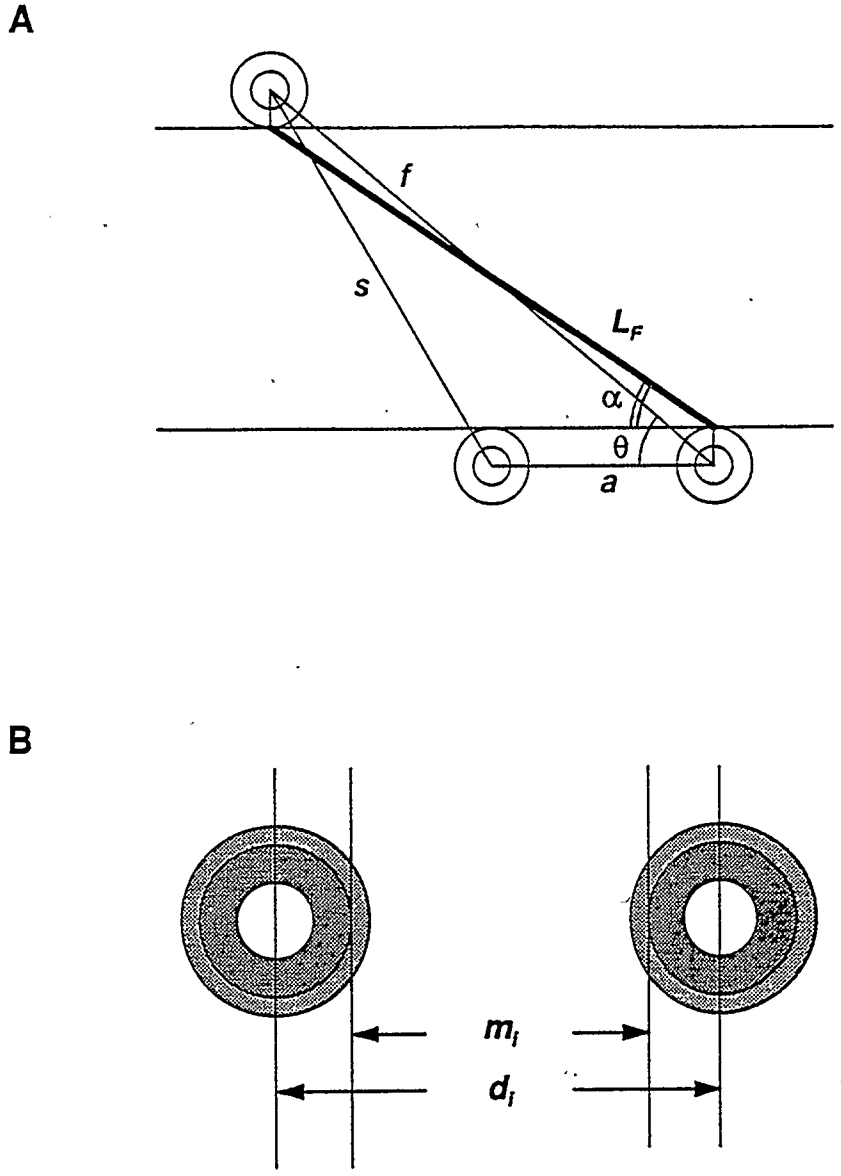

Fig. 3.4. Geometrical arrangement of the piezoelectric crystals in the sagittal plane (A), and the relation of the distances between the centres of the piezoelectric crystals and the actual length measurements (B). Fibre length L_F (thick line) was computed from f, a, s, and θ, and the angle of pinnation α from f, L_F, and θ (following Caputi, Hoffer and Pose, unpublished; see equations (3.4) and (3.5) in the text). The distances between the centres of the crystals d_i (i = f, a, s) were computed from the corresponding measurements m_i by $d_i = m_i + 1.3 + 0.133$ mm, where 1.3 mm is the diameter of the crystals (darkly shaded rings), and 0.133 mm is the correction for the effect of aquatapoxy (the lightly shaded area); see text for further details.

$$L_F = 2\left(\left(\frac{f}{2}\right)^2 + 0.82^2 - 0.82 f \sin\theta\right)^{1/2}, \quad (3.4)$$

which also follows directly from the cosine law. The value 0.82 in this equation was the radius (in mm) of a coated crystal. Using θ and L_F, the angle of pinnation (in degrees) was computed from

$$\alpha = \frac{360}{2\pi} \cos^{-1}\left(\frac{f}{L_F}\cos\theta\right), \quad (3.5)$$

which follows from simple trigonometric considerations. Except for the correction for the effect of aquatapoxy, these equations follow Caputi, Hoffer and Pose (unpublished).

Models of viscoelasticity

In Muscle viscosity (see Results), the experimental data are compared with the outputs of some simple models of viscoelasticity. The differential equations governing these models were solved numerically with a fourth order Adams-Bashforth-Moulton predictor-corrector method (Ralston and Rabinowitz, 1978). Where possible the numerical solutions were checked against analytical solutions.

Chapter 4.

RESULTS

Although theories may be more or less distant from observations, they are interesting only insofar as they can touch, finally, upon observations. Sometimes the route to observations, as in theoretical physics, may be a long one through much theory, but a route there must finally be.
Patricia Smith Churchland, 1986

4.1 Chronic recordings

Fig. 4.1A and B show chronic data from two different cats. In each case the two step cycles that were used in the acute experiments are reproduced. From top to bottom the signals are: (1) muscle force, (2) muscle length (L_M) and muscle fibre length (L_F) (superimposed), (3) aponeurotic sheet length,[1] (4) angle of pinnation, and (5) one of the four EMG measurements. The angle of pinnation was not measured directly, but was derived from the fibre length, aponeurotic sheet length, and S3 measurements (see Methods). The EMG measurements shown are the rectified, bin-integrated and digitally filtered EMGs used for generating stimulation patterns for distributed stimulation.

[1] Only a fraction of the total length of the aponeurotic sheet on the ventral side of the muscle was measured (see Methods). For brevity, however, "aponeurotic sheet length" is used to refer to this measurement rather then the unwieldy "an approximately 10 mm long segment of the ventral aponeurosis."

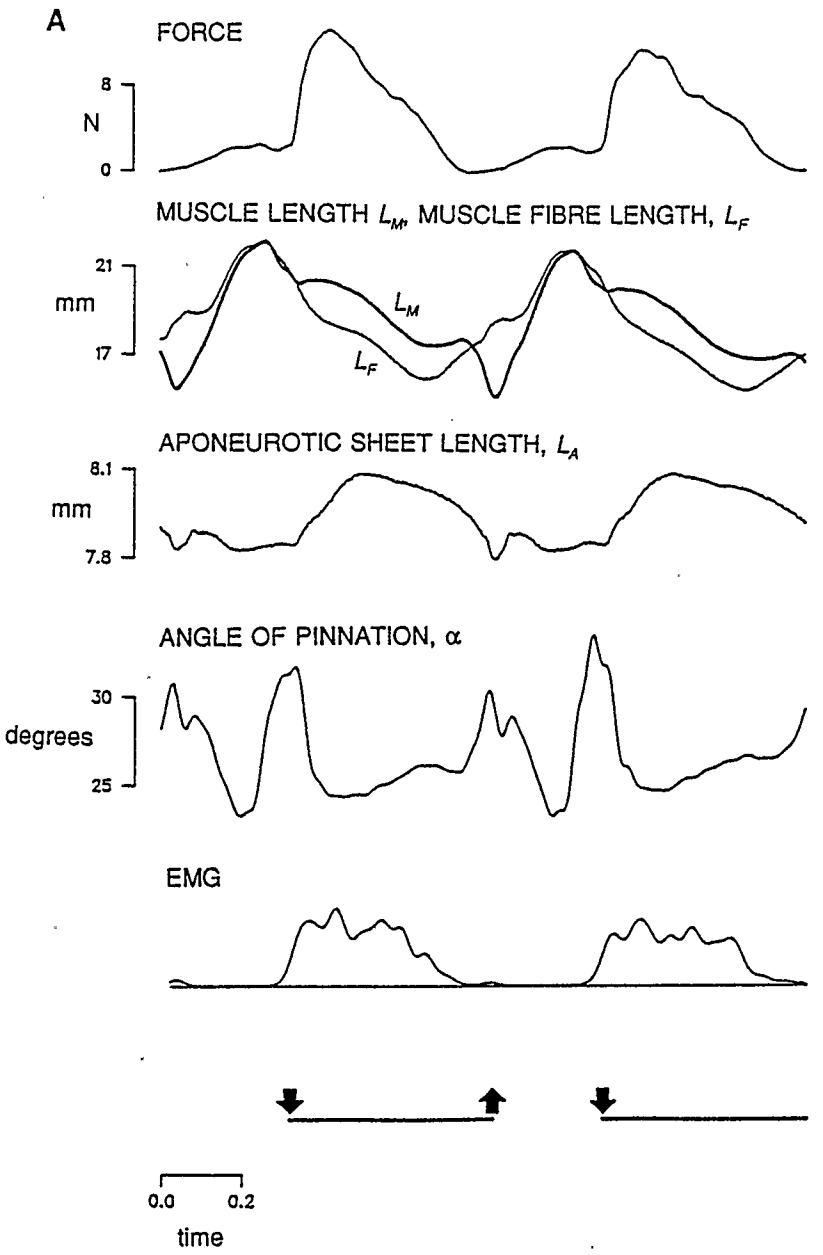

Fig. 4.1. Data obtained in two cats during walking on a treadmill at a speed of 0.5 m/s. From top to bottom: (1) muscle force, (2) muscle length L_M (thick trace) and muscle fibre length L_F (thin trace) (superimposed), (3) aponeurotic sheet length L_A, (4) angle of pinnation α, and (5) one of the four EMG measurements (rectified, bin-integrated, and digitally filtered). Time is in s. The horizontal bars with the down and up arrows denote stance. A constant offset was added to the muscle length signal to match the peak in the muscle fibre length measurement in the swing phase.

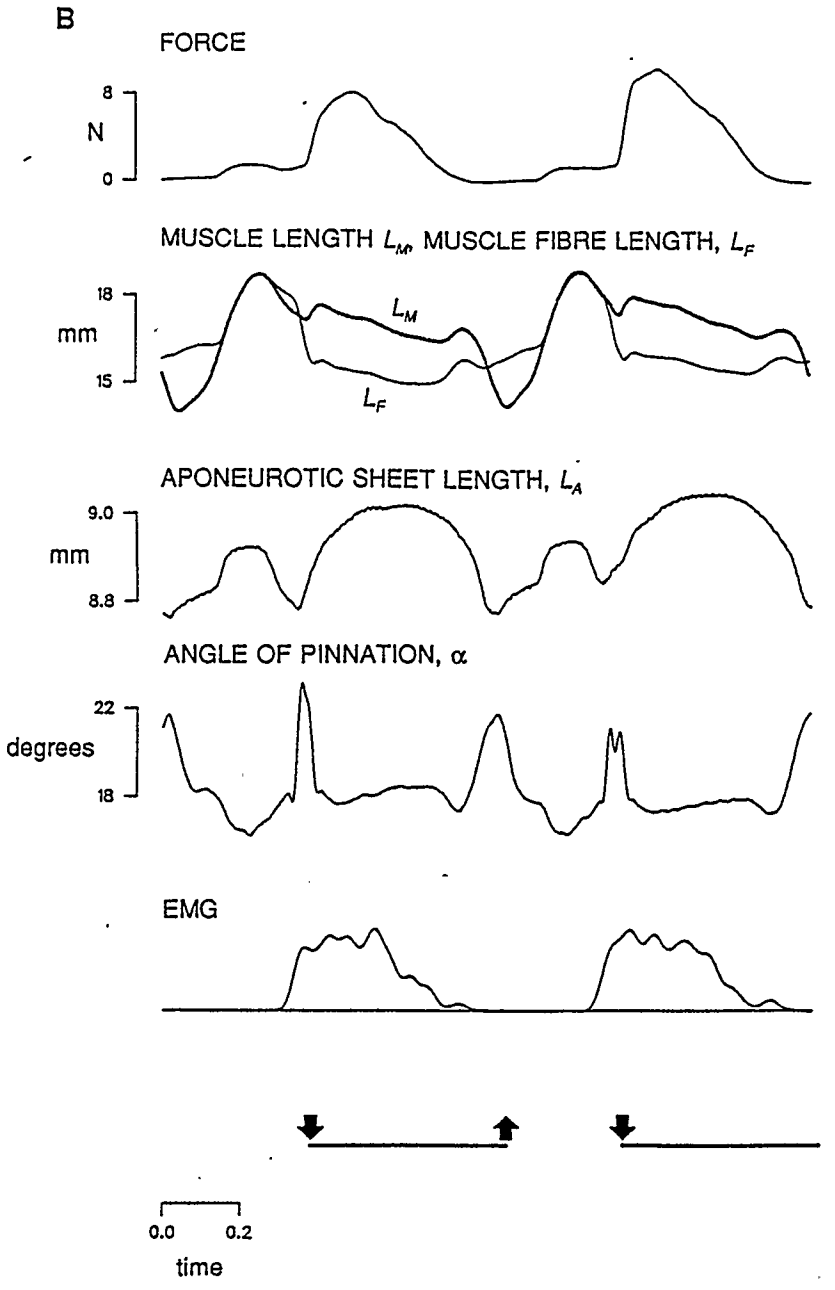

Fig. 4.1. Continued.

At the end of the swing phase the muscles lengthened passively. This passive lengthening gave rise to passive forces with well-defined maxima. In the acute simulations these maxima were used to match acute and chronic signals.

During these passive lengthening movements muscle force and muscle length were slightly out of phase, muscle force being phase-advanced on muscle length. The data files containing the step cycles used in the acute simulations contained a total of 47 step cycles. Of those 47 cycles, 6 had no well-defined passive force maximum. In 3 cycles force lagged length by a few ms. The mean phase advance for the remaining 38 cycles was 21.0 ± 9.3 ms (mean and standard deviation; range: 7.6-47.2 ms). This phase advance was not due to phase-lags introduced by inappropriate low-pass filtering of signals. The DC-bridge's output stage contained a first-order low-pass filter with a cut-off frequency of 5 KHz (see Methods). The phase-lag introduced by this filter was at most 0.8 ms. The Sonomicrometer's output stage contained a fourth-order Bessel low-pass filter with a cut-off frequency of 100 Hz and linear phase up to 80 Hz (-18.34 degrees per 10 Hz). This filter introduced a phase-lag of 5.1 ms. The phase advance of muscle force on muscle length due to low-pass filtering was thus at most 4.3 ms. This phase-advance of muscle force with respect to muscle stretch is just one of a number of phenomena that hints at the presence of viscosity in the muscle (see further below and Discussion).

Following the peak in the passive force, the muscles generated active force. Active force increased gradually at first, then abruptly. Due to synchronous

activation of the motor units, this initially gradual increase in active muscle force could not be simulated in the acute experiments (see Fig. 4.3).

Muscle length and fibre length did not change in unison: (1) during the stance phase the muscle yielded, while the muscle fibres shortened, and (2) during the early swing phase the muscle shortened while the muscle fibres lengthened.

In the stance phase, the length of the aponeurotic sheet first increased, then decreased. In the swing phase, it followed muscle length reasonably closely throughout in Fig. 4.1B. In Fig. 4.1A, on the other hand, it followed muscle length only in early swing; in late swing, during passive lengthening, it shortened rather than lengthened. The pattern illustrated in B was seen in five cats (out of eight), the pattern shown in A in two cats. In one cat the aponeurotic sheet length was inversely related to muscle length throughout the swing phase and not clearly related to either muscle force or muscle length in the stance phase. In the acute simulations only the pattern of Fig. 4.1B was observed; i.e., the three "atypical" patterns switched from "atypical to "typical" (see Fig. 4.3).

The angle of pinnation underwent a complex series of changes during the step cycle. It decreased during the passive lengthening phase at the end of the swing phase, increased rapidly during the phase of gradual build-up of active force, and decreased again during the rapid build-up of force. During the decline of the active force it increased slowly. At the end of the stance phase and during the early swing phase there was a second period in which it increased rapidly.

These patterns were not "typical." In fact, no "typical" pattern was observed; the pattern of change in the angle of pinnation varied from cat to cat, although there did seem to be a general trend: an inverse relationship to muscle length in the swing phase, and approximately constant in the stance phase. In the simulations, the latter pattern was more clearly present (see Fig. 4.3).

In Fig. 4.2A and B muscle force is plotted vs. aponeurotic sheet length (data from Fig. 4.1A and B, respectively). The patterns in A and B appear similar, but this similarity is deceiving, since, as indicated above, the aponeurotic sheet length changed differently in A and B during passive lengthening. During active force generation, the aponeurotic sheet lengthened in both A and B. This lengthening, however, was not in proportion to the force: it continued and reached a maximum during the declining phase, whence the large hysteresis in the plots. The last part of the ensuing shortening occurred at zero or slightly increasing force.

4.2 Acute simulations of locomotion

Fig. 4.3 compares acute simulations and chronic targets (data from same cat as in Fig. 4.1B). The major features of both muscle force and muscle fibre length were reproduced to satisfaction. However, as can be seen, this did not automatically entail that the remaining signals—aponeurotic sheet length, S3, angle of pinnation, and muscle length—were also reproduced well. In fact, there were always discrepancies. Most noticeable were (1) differences in muscle length, and (2) mismatches in passive force. Differences in muscle length were seen in five of the

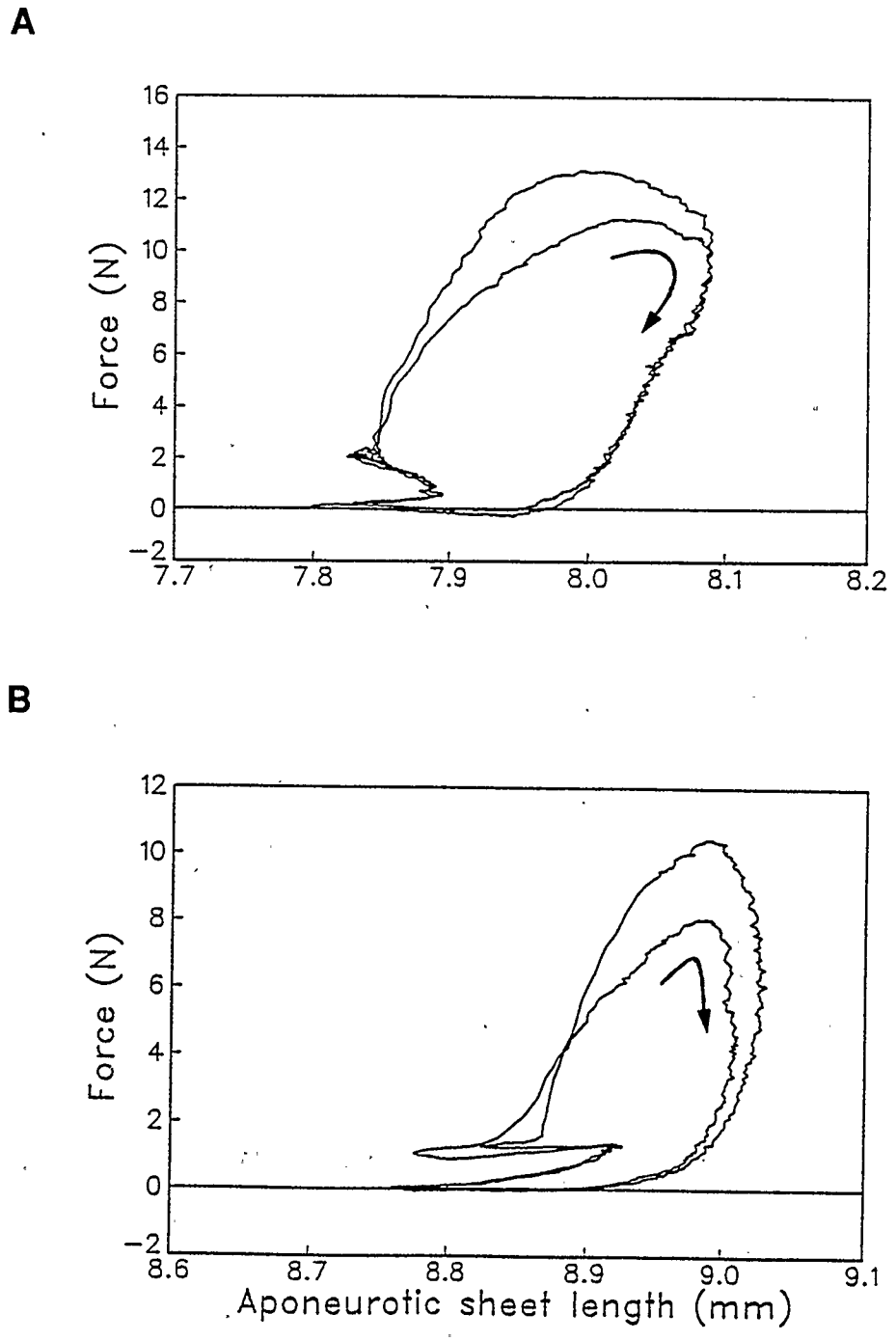

Fig. 4.2. Muscle force vs. aponeurotic sheet length. A. Data from Fig. 4.1A. B. Data from Fig. 4.1B.

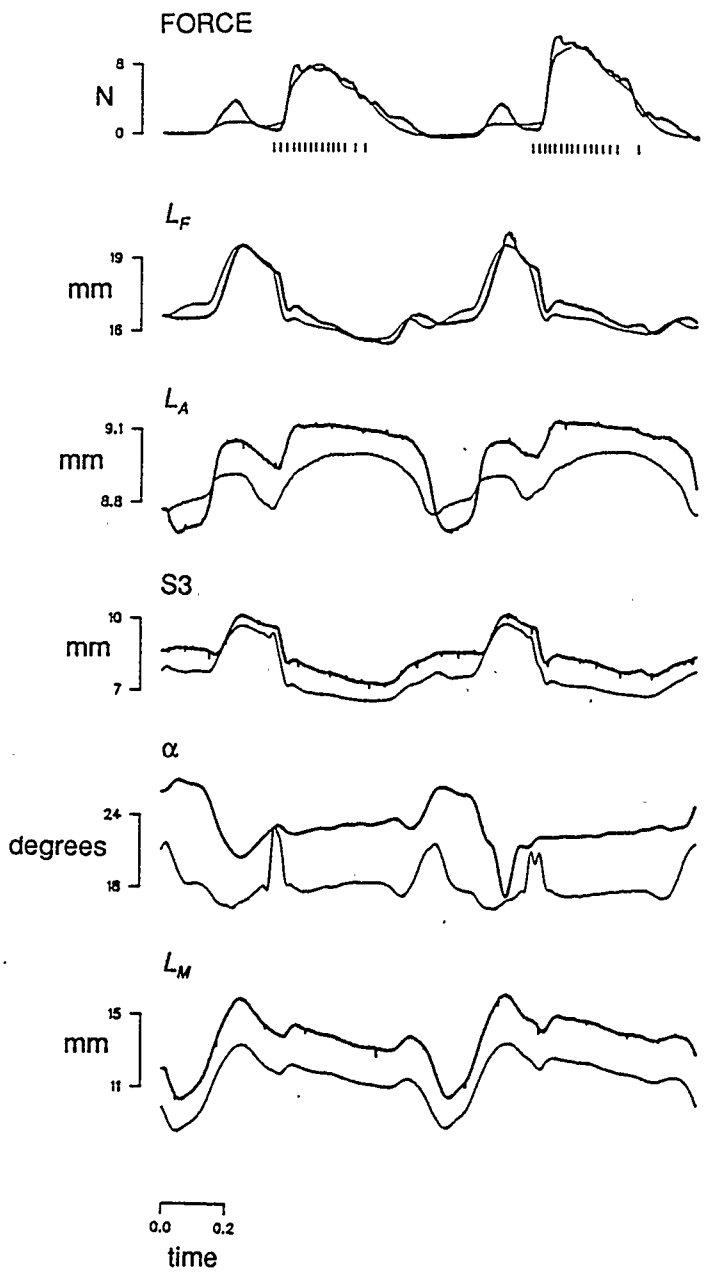

Fig. 4.3. Average acute measurements vs. chronic target signals. The thick traces are the data from the acute experiment. From top to bottom: (1) muscle force, (2) muscle fibre length L_F, (3) aponeurotic sheet length L_A, (4) S3, (5) angle of pinnation α, and (6) muscle length L_M. Also shown are the stimuli used for distributed stimulation. The small irregular peak on top of the maximum in the acute fibre length measurement (second step cycle) is artifactual, and was due to triggering on the wrong wave of the piezoelectric oscillation (see Methods).

six cats implanted with piezoelectric length gauges (see Methods), the acute muscle length signal being shorter than the chronic target in four cats, and longer in one cat (Fig. 4.3). Mismatches in passive force (too much passive force, as in Fig. 4.3) were present in five out of eight cats.

4.3 Muscle length and muscle fibre length in passive and active walking

Fig. 4.4 shows results from passive walking and active walking simulations (data from the same cat as in Fig. 4.1B). In A the forces are shown, in B, muscle length and muscle fibre length (thin and thick traces, respectively), superimposed. During the stance phase, there was non-zero passive force, a consistent finding in all cats. Both muscle fibre length and muscle length changed with activation of the muscle, but the change in fibre length was always substantially larger. The maximum differences for the measurements shown were 0.84 mm (muscle length) and 2.74 mm (muscle fibre length). The mean maximum differences for the six cats implanted with piezoelectric muscle length gauges were 0.46 mm (muscle length) and 3.10 mm (muscle fibre length). Individual values are given in table 4.1.

The changes in muscle length were not due to compliance in the muscle puller, which was very low (0.268 μm/N): the position feedback signals under both passive and active conditions were always indistinguishable, nor to movement of the femur, which was rigidly clamped at the location of the epicondyles, but were due to visible rotation of the calcaneus around the bolts with which it was clamped. This undesirable rotation could not be prevented

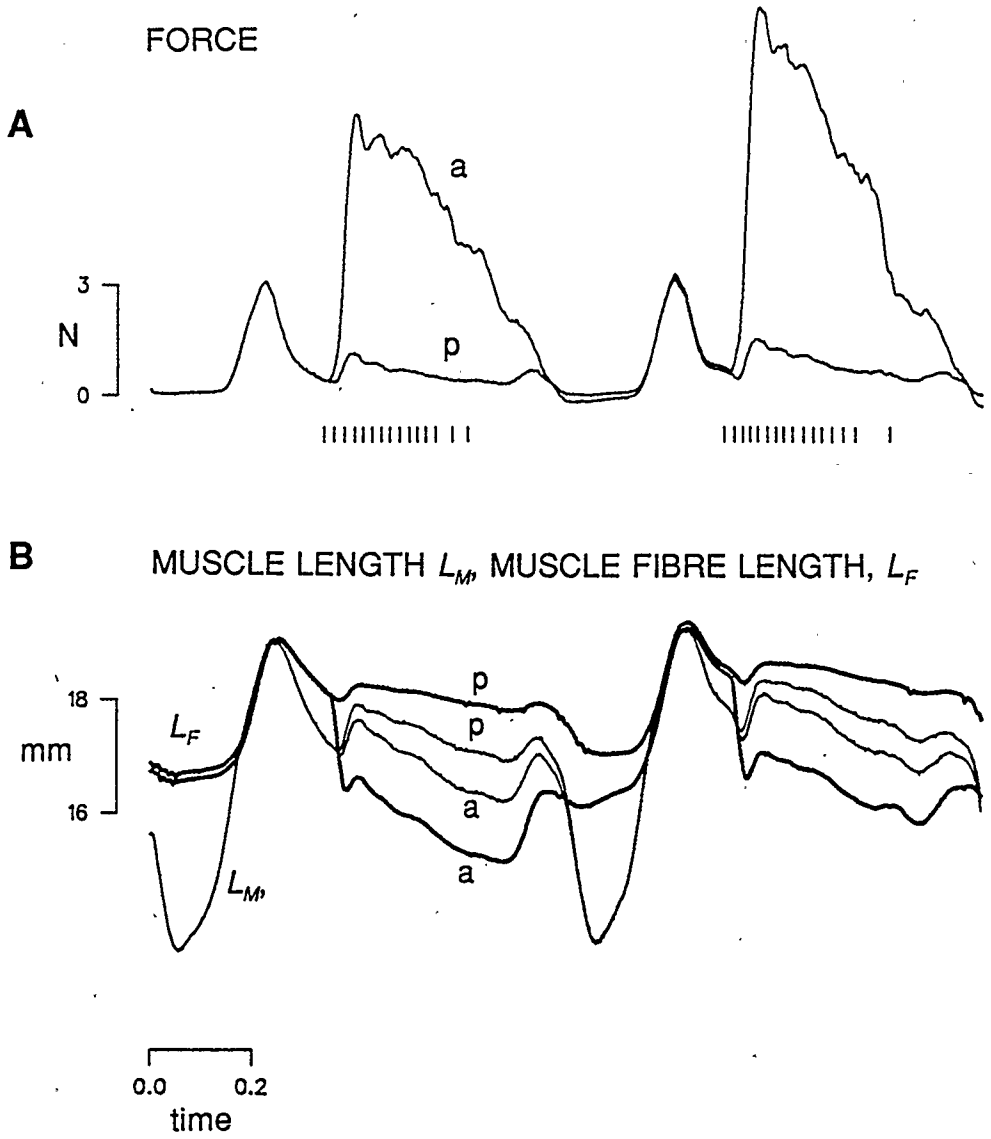

Fig. 4.4. Muscle force (A), and muscle length L_M and muscle fibre length L_F (B) in active and passive walking. The thick traces in B are muscle fibre length. a and p denote active and passive walking, respectively.

since the bolts could not be positioned at the edge of the calcaneus tuber: due to the (roughly) trumpet-like shape of the dorsal part of the calcaneus, they always moved towards the ankle joint when tightened.

As in active muscle, there were also differences between muscle length and muscle fibre length when the muscle was passive: the muscle fibres always lengthened and shortened less than the muscle, as was particularly obvious in the early swing phase, during which, as a result of the absence of active shortening during the stance phase, the discrepancy between muscle and muscle fibre length was always larger than in active muscle. However, unlike in active muscle, changes in muscle and muscle fibre length were always in the same direction; i.e., paradoxical movements, fibre shortening during muscle lengthening or fibre lengthening during muscle shortening, were never seen in passive muscle.

4.4 Tendon compliance

From muscle length and fibre length measurements such as those shown in Fig. 4.4, ΔL_T, the change in tendon length (i.e., external tendons plus aponeurotic sheets; see Methods) was estimated by $\Delta L_T = \Delta L_M - \Delta(L_F\cos\alpha) = (L_{M,a} - L_{M,p}) - (L_{F,a}\cos\alpha_a - L_{F,p}\cos\alpha_p)$, where L_T, L_M, and L_F are tendon length, muscle length and fibre length, respectively, α is the angle of pinnation, and the subscripts a and p denote active and passive, using the simple model of Fig. 4.5A. Results are presented only for the six cats in which muscle length was measured with piezoelectric length gauges. Note that when fibre length is not constant it is meaningless to try to extract from $\Delta(L_F\cos\alpha)$ the change in extramysial

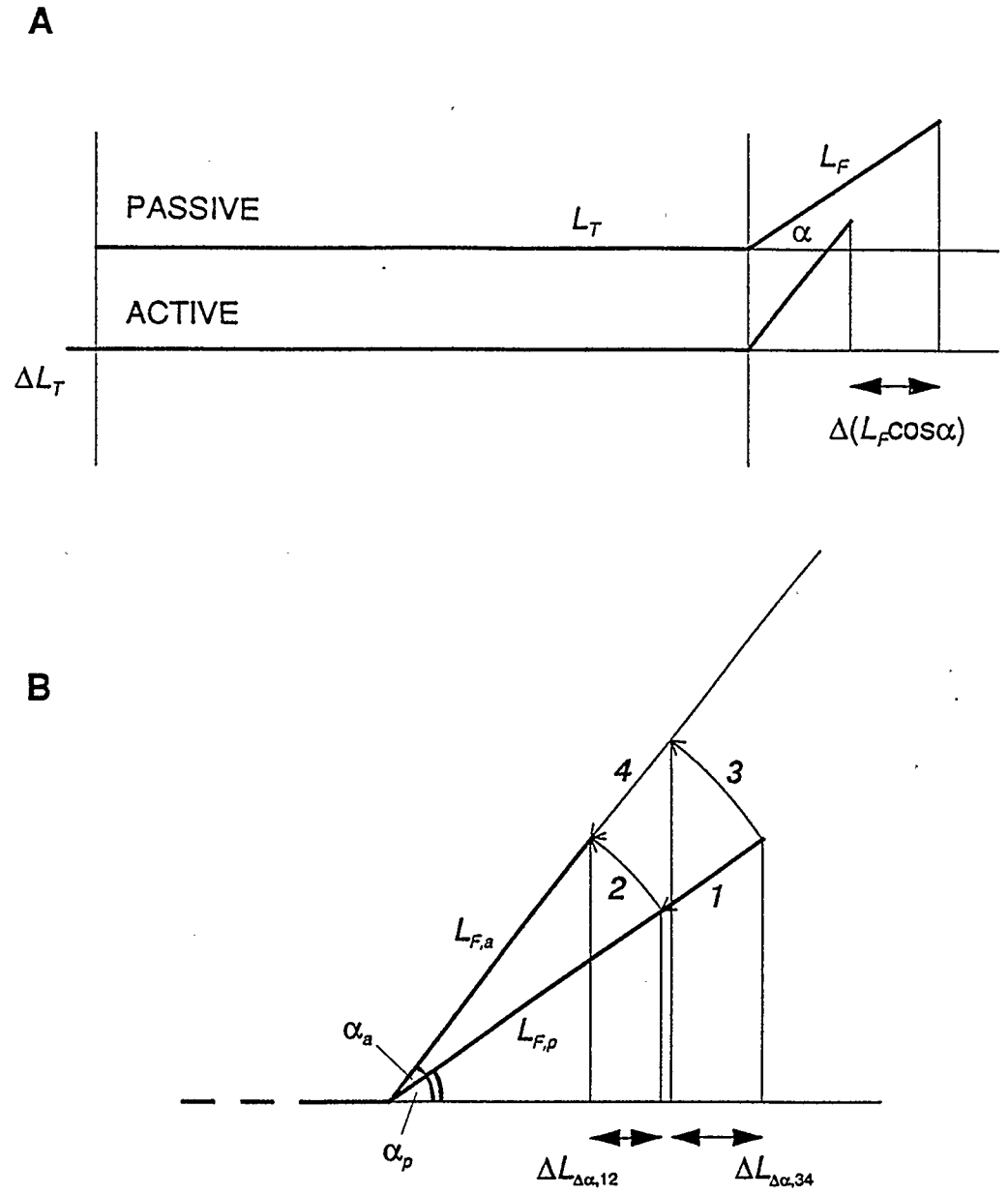

Fig. 4.5. The muscle model used for the calculation of the changes in tendon length during locomotion. The model is schematically depicted in two different states in A: during passive and active walking. L_T, length of the tendinous component of the muscle (lumped); L_F, muscle fibre length; α, angle of pinnation; ΔL_T, the change in the length of the tendinous component; $\Delta(L_F\cos\alpha)$, the change in muscle length due to a change in both fibre length and a change in angle of pinnation. In B the two states of the model are reproduced superimposed at higher magnification. The subscripts *a* and *p* in L_F and α denote active and passive, respectively. The panel illustrates that the contribution of a change in the angle of pinnation to the total extramysial displacement depends on whether the change in fibre length or the change in angle of pinnation is considered first: route 1,2 vs. route 3,4; i.e., $\Delta L_{\Delta\alpha,12}$ vs. $\Delta L_{\Delta\alpha,34}$.

displacement due to a change in angle of pinnation, since the computed change (ΔL_α) depends on whether the change in fibre length or angle of pinnation is considered first: $\Delta L_{\Delta\alpha,12} = L_{F,a}(\cos\alpha_p - \cos\alpha_a) \neq L_{F,p}(\cos\alpha_p - \cos\alpha_a) = \Delta L_{\Delta\alpha,34}$; see Fig. 4.5B.

Fig. 4.6A shows ΔL_M, $\Delta(L_F\cos\alpha)$, and ΔL_T for the measurements shown in Fig. 4.4. (positive axis indicates lengthening). Also shown are the stimuli used for distributed stimulation, and $\Delta F = F_a - F_p$, the difference in force between active and passive walking. The remaining three signals shown are estimates of extramysial displacement computed according to Elek et al. (1990) with three different sets of parameters (see further below). Tendon length and muscle force did not change in phase, as would be expected for a predominantly elastic structure. After an initial more or less proportional increase, the rate of lengthening decreased abruptly, and, although shortly after this change in rate muscle force began to decline, tendon length kept increasing slowly until after the last stimulus. The tendon then shortened slowly back to (almost) its original length, the time course of shortening bearing no obvious relation to the time course of the decline in force. The last 50% or so of the shortening occurred in the absence of force at the tendon. This pattern was observed consistently, also when small ventral root filaments were stimulated in isolation (Paradigm 1), as illustrated in Fig. 4.7A (data from a different cat). In Figs. 4.6B and 4.7B the ΔFs are plotted vs. the corresponding ΔL_Ts. The mean maximum estimated change in tendon length was 2.53 mm. Individual values are listed in table 4.1. In three cats

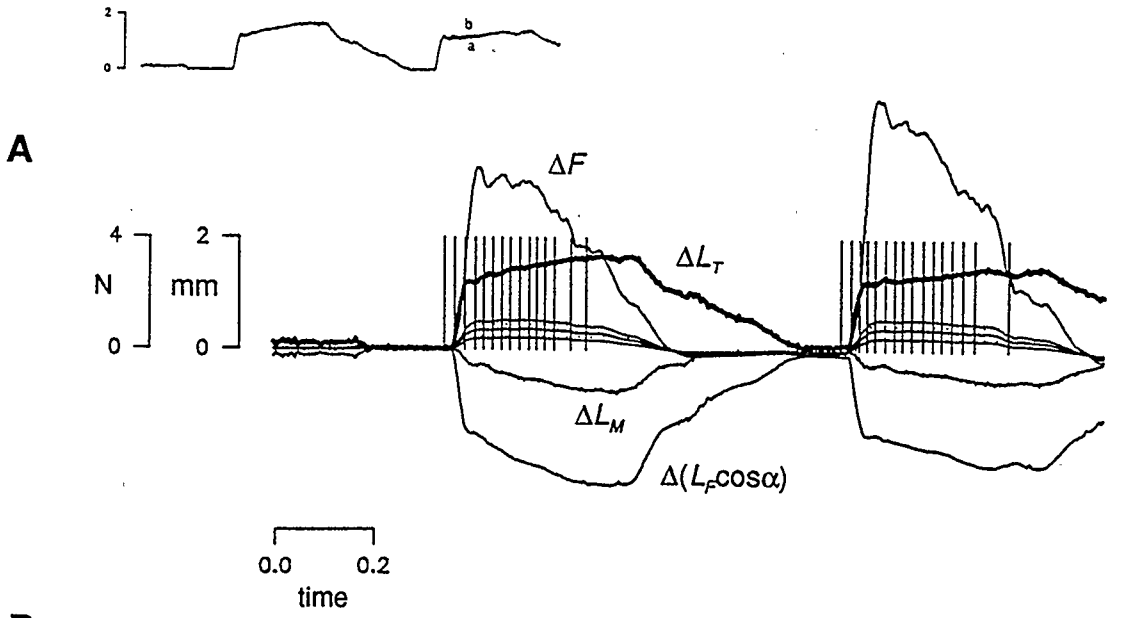

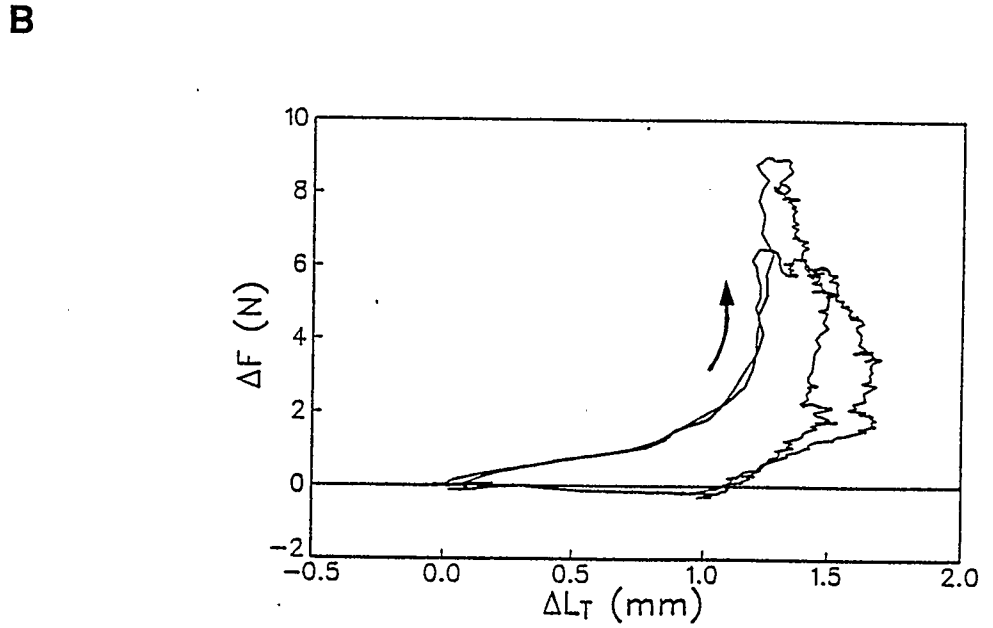

Fig. 4.6. The estimated change in tendon length ΔL_T (A), and active force ΔF vs. the estimated change in tendon length ΔL_T (B). The estimate ΔL_T (thick trace) was derived from the measurements shown in Fig. 4.4. Positive values indicate lengthening. ΔL_M, the change in muscle length; $\Delta(L_F \cos\alpha)$, the change in muscle length due to a change in both fibre length and a change in angle of pinnation. The vertical lines indicate the stimuli used for distributed stimulation. The three unlabelled signals are the changes in tendon length computed with Elek et al.'s equation (1) (Elek et al., 1990; see (4.2) in the text) with a = 2.52, 3.7, and 6.3, and c = 0.46, 0.66, 1.17. The inset compares the estimated change in tendon length as computed with the "true" angle of pinnation α derived from the data (a) and with α=25° (b).

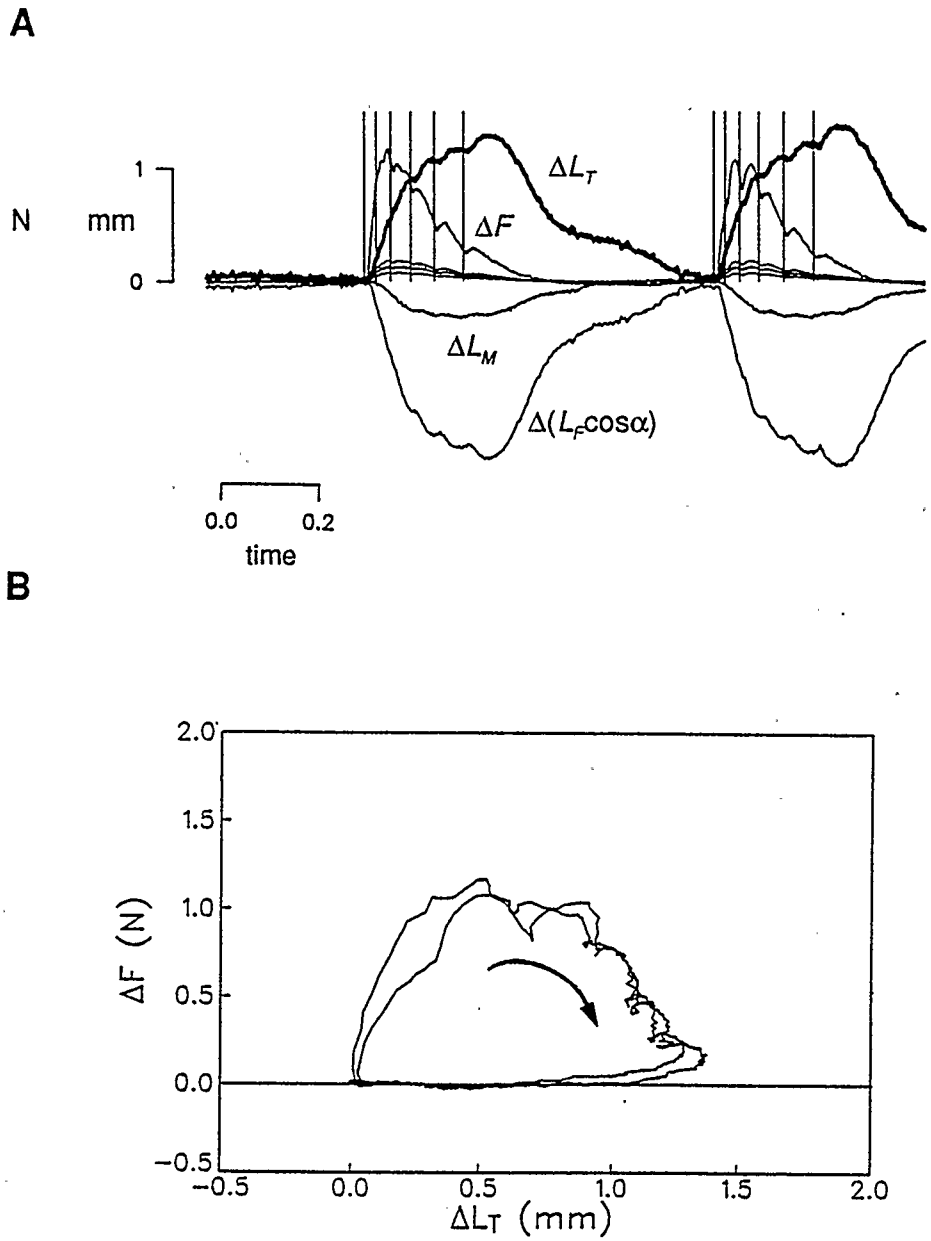

Fig. 4.7. Estimated change in tendon length occurring during simulated walking when only a single small ventral root filament is stimulated. Data format as in Fig. 4.6.

ΔL_F	ΔL_M	ΔL_T	ΔL_A	$L_{A,slack}$	ED_A
2.47	-0.85	3.20	0.50	13.21	59.9
3.70[1]	0.43	3.20[2]	-	-	-
3.39[1]	0.86	2.22[2]	-	-	-
2.68	0.59	2.39[3]	-	-	-
3.51	0.93	2.17	0.30	7.60	92.0
2.86	0.76	1.98	0.16	8.67	47.2

Table 4.1. Summary of measurements made on signals derived from data recorded during simulated walking. ΔL_F, ΔL_M, ΔL_T, and ΔL_A, maximum difference in muscle fibre length, muscle length, length of the tendinous component of the muscle, and length of the aponeurotic sheet in active walking and passive walking. $L_{A,slack}$, slack length of the aponeurotic sheet, defined as the minimum length attained during the phase of rapid muscle shortening in late stance/early swing. The last column, ED_A, lists (in percent) the amount of extramysial displacement (ΔL_T) accounted for by length changes in the aponeurotic sheet. These percentages were computed with $ED_A = 100 \times (\Delta L_A \times 50.6/L_{A,slack})/\Delta L_T$, where 50.6 mm is the slack length of the entire aponeurotic sheet (based on Poliacu Prosé, 1985). [1]Based on raw signals. [2]Computed with α=25°. [3]Computed with α=30°.

the aponeurotic sheet length signal in the acute experiments was of insufficient quality to compute corrected fibre length and angle of pinnation signals (see Methods). In those cases $\Delta(L_F\cos\alpha)$ was computed with α=25° or α=30° (the value used was the one which was closest to the angle of pinnation in the stance phase in the chronic recordings). In one of the three other cats the change in tendon length was computed both with the angle of pinnation as derived from the measurements and with α=25°. The difference was found to be very small; see the inset in Fig. 4.6A.

The ΔL_Ts were not measured directly, but were *derived* from muscle length and muscle fibre length measurements. By contrast, the aponeurotic sheet length signals, L_A, provided a *measurement* of the change in length of the tendon, albeit

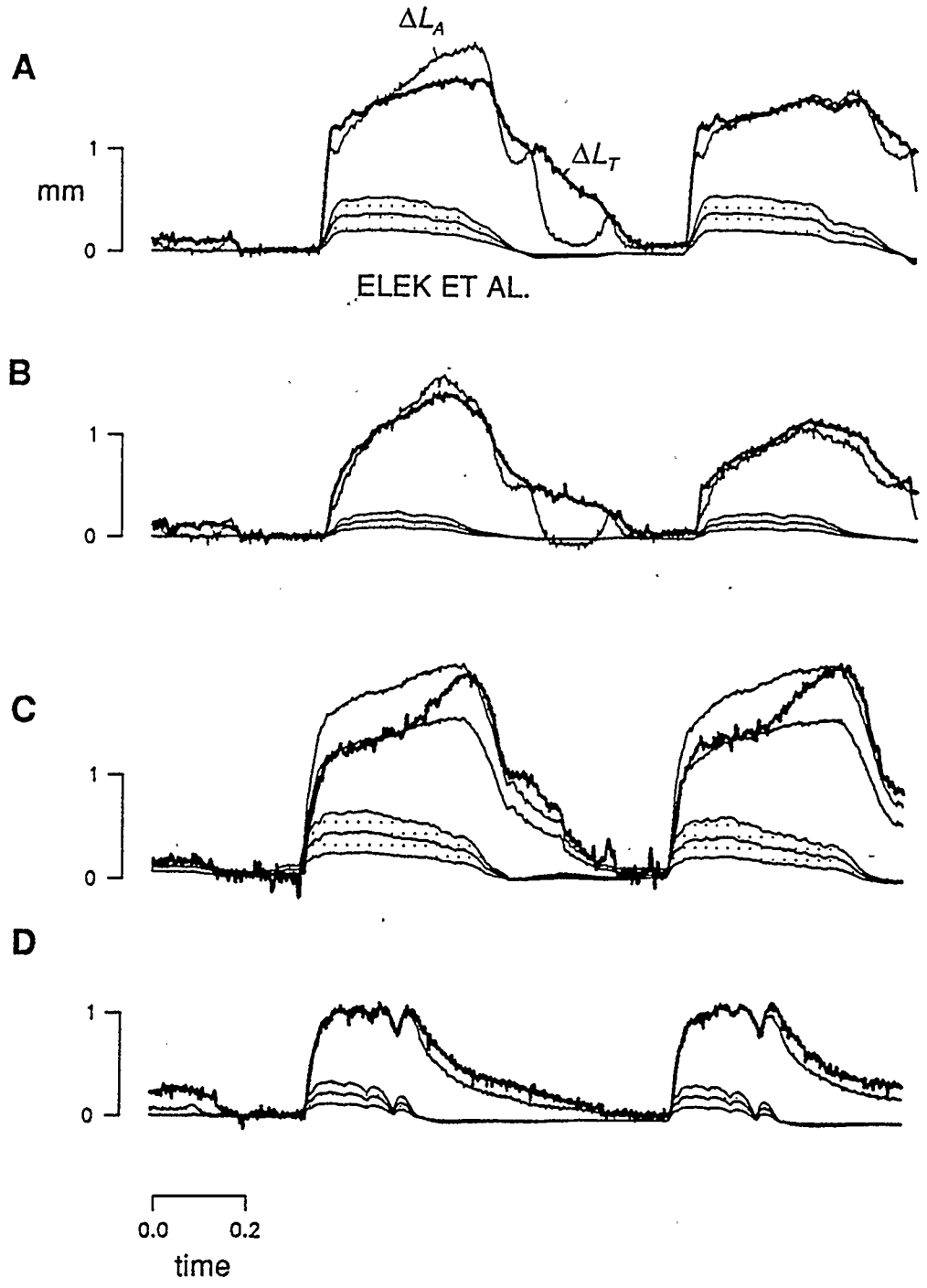

Fig. 4.8. Estimated change in tendon length ΔL_T vs. change in aponeurotic sheet length ΔL_A vs. estimated change in tendon length computed with Elek et al.'s equation (1) (Elek et al., 1990; see (4.2) in the text). The thick trace is ΔL_T. The change in aponeurotic sheet length ΔL_A was scaled to match ΔL_T (in C, two differently scaled versions of ΔL_A are shown). A and C. Distributed stimulation (i.e., active walking). B and D. Stimulation of a single ventral root filament. A and B, and C and D, data from different cats.

of only a fraction of the total length. Fig. 4.8 compares some ΔL_Ts with scaled versions of the corresponding ΔL_As ($\Delta L_A = L_{A,d} - L_{A,p}$). With only one exception (Fig. 4.8A and B; data from the same cat as in Fig. 4.1B) the correspondence was quite good; i.e., the measurements exhibited the same features as the estimates. The discrepancy in the data of Fig. 4.8A and B occurred during the rapid muscle shortening in the early swing phase.

The mean absolute change in aponeurotic sheet length was 0.32 mm (three cats; see table 4.1). The mean maximum change, defined as the difference between the largest length reached during active walking and the slack length, taken to be the minimum length attained during the phase of rapid muscle shortening in early swing, was 0.6 mm. Expressed as a fraction of the slack length these values translate to 3.25% and 6.1%, respectively. Using the ratio of the length of the entire aponeurotic sheet (50.6 mm; Poliacu Prosé, 1985)[2] to the slack length of the measured segment, the ΔL_As could be upscaled to estimate the length change in the entire aponeurotic sheet. These calculations showed that the change in the aponeurotic sheet accounted on average for 66.4% of the estimated change in the length of the entire tendon (range 47.2-92.0%; see table 4.1).

The three smaller signals in Figs. 4.6A, 4.7A, and in each panel of Fig. 4.8, are estimates of the change in tendon length computed using equation (1) of Elek et al. (1990):

---

[2] Since the experiments were not designed with the tendon-compliance controversy in mind (see Introduction), measurements of the dimensions of the aponeurotic sheets were not made.

$$\Delta L_T = \frac{1}{a} \ln \left[\frac{(aF_2 + b)}{(aF_1 + b)} \right], \tag{4.1}$$

which with $F_2 = \Delta F$, $F_1 = 0$, and $c = a/b$ reduces to

$$\Delta L_T = \frac{1}{a} \ln (c\Delta F + 1). \tag{4.2}$$

The values used for a and b were those found by Elek et al. to explain 80% of their data points: a = 3.6, and b = 5.4 (middle curve; Elek et al.'s best fit), and 0.7 and 1.75 times these values (lower and upper curves, respectively). Obviously, the data reported here differed substantially from the estimates derived using Elek et al.'s values for tendon stiffness, not only in amplitude but also in time course.

4.5 Muscle viscosity

The time course of change in tendon length, in particular the increase in length with decreasing force and the slow decline in the absence of tendon force, could not be explained in terms of a purely or predominantly elastic structure, and suggested the presence of substantial viscosity in the muscle, tendon or both. The nature of this viscosity was investigated qualitatively by comparing the length responses of two of the three simple linear mechanical models commonly used in the analysis of viscoelastic materials, the Maxwell, Voigt, and Kelvin elements (Fung, 1981), to triangular force inputs resembling the forces generated in the acute experiments. The Maxwell element consists of a spring in series with a dashpot, the Voigt element consists of a spring in parallel with a dashpot, and the Kelvin element consists of a Maxwell element in parallel with a spring. The

Maxwell element was not studied since it does not give rise to slowly decaying length responses and does not return to its original length when the input force vanishes (its viscosity is "unrecoverable").

Fig 4.9A and B schematically show the *creep* and *relaxation functions* of the Voigt and Kelvin elements. The *creep function* is the length response of the element to a unit force step. The *relaxation function* is the force response to a unit length step (see Fung, 1981). The creep function of the Kelvin element exhibits the basic desired features: (1) an initial increase in length that is proportional to the applied force, (2) slow lengthening, and (3) a slow return to the original length. The creep function of the Voigt element lacks the initial proportional increase in length. The relaxation function of the Kelvin element is characterised by *stress relaxation*, which is known to occur in the medial gastrocnemius muscle of the cat (Heckman et al.; see also Fig. 5.2). The Voigt element, on the other hand, does not relax under constant strain, and, since its dashpot cannot change length instantaneously, its force response at the onset of the unit length step is infinite (a unit impulse function).

The Voigt element

The Voigt element is governed by the differential equation

$$\dot{x} + \frac{x}{\tau_\sigma} = \frac{1}{\eta} F, \tag{4.3}$$

where x is the length of the element, F the imposed force, $\tau_\sigma = \eta/\mu$ the relaxation time for constant stress (Fung, 1981), and η and μ the viscosity of the dashpot and

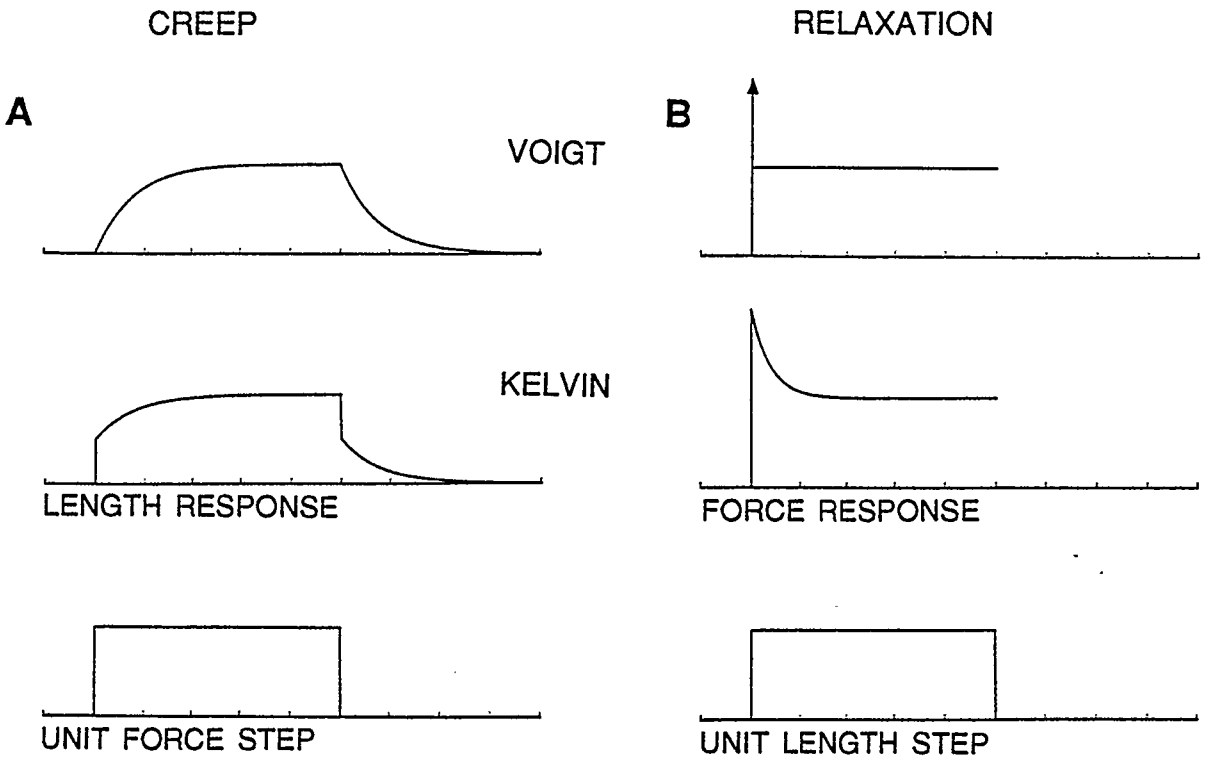

Fig. 4.9. The creep and relaxation functions (left and right, respectively) of the Voigt and the Kelvin model. The creep function is the length response to a unit force step input; the relaxation function is the force response to a unit length step input. The inputs are shown at the bottom.

the stiffness of the spring, respectively. From this equation it is easy to see that for very small τ_σ the behaviour of the Voigt element becomes spring-like. I.e., a fast length response proportional to the input force followed by a slower non-proportional increase in length results if τ_σ is initially small and then quickly increases. Since the relaxation time depends on the viscosity η and the stiffness μ, it can only increase if these parameters vary with time; in particular, the relaxation time increases if either the viscosity η increases, the stiffness μ decreases, or both η increases and μ decreases. Length responses similar to those derived from the data could not be obtained without at least a tenfold decrease in stiffness or increase in viscosity.

The Kelvin element

The governing differential equation is

$$\dot{x} + \frac{x}{\tau_\sigma} = \frac{1}{\mu_P \tau_\sigma}(\tau_\varepsilon \dot{F} + F), \tag{4.4}$$

where $\tau_\sigma = \eta(1/\mu_P + 1/\mu_S)$ is the relaxation time for constant stress (as above), with μ_P and μ_S the stiffness of the parallel and series spring, respectively, and $\tau_\varepsilon = \eta/\mu_S$ the relaxation time for constant strain. In the steady state (all derivatives equal to zero) the solution is $x = F/\mu_P$. When the input is a unit step increase in force (applied at $t = 0$) immediately followed by a linear decline, $F = (1 - ct)U(t)$ with $U(t)$, the unit step function, the initial condition is $x(0) = 1/(\mu_P + \mu_S)$, and the steady state solution is $(1 - ct)/\mu_P$. Of particular interest was whether or not the Kelvin element could lengthen in response to this input. It can be shown that it

can, but whether or not it does so, depends in a complex way on the parameters of the model (in this respect, the Kelvin element differs from the Voigt element, which responds to *any* positive force input with an increase in length). Specifically, the condition for an *increase* in length with *declining* force is

$$\tau_\sigma \frac{\mu_P}{\mu_S} = \frac{\eta}{\mu_S}\left(1 + \frac{\mu_P}{\mu_S}\right) < \frac{1}{c}. \qquad (4.5)$$

A number of responses for different values of the parameters are illustrated in Fig. 4.10. This figure shows that lengthening occurs if (1) the current length of the element is smaller than the steady state length, and (2) the time constant τ_σ with which the element responds is not too large. The initial difference between current and steady state length depends on the ratio $\mu_P/(\mu_P + \mu_S)$ (or μ_P/μ_S). How large the time constant can be in turn depends on this distance.

Of the three responses shown in Fig. 4.10B, responses b and c most closely resembled those derived from the data. Comparison of Fig. 4.10 and Figs. 4.6A, 4.7A and 4.8, however, shows that they differed from them in two respects: (1) the rate at which the length changed during lengthening continually *decreased*, whereas in the data the rate of length change was nearly constant or even increased, and (2) the decay to the original length was slower (especially in c). Both features result if the time constant τ_σ decreases with "activation," as shown in Fig. 4.10C. The time constant τ_σ decreases if either the viscosity η decreases, the stiffness μ_P and/or μ_S increase, or both η decreases and μ_P and/or μ_S increase. The simplest situation is the one in which either the viscosity η and/or the stiffness

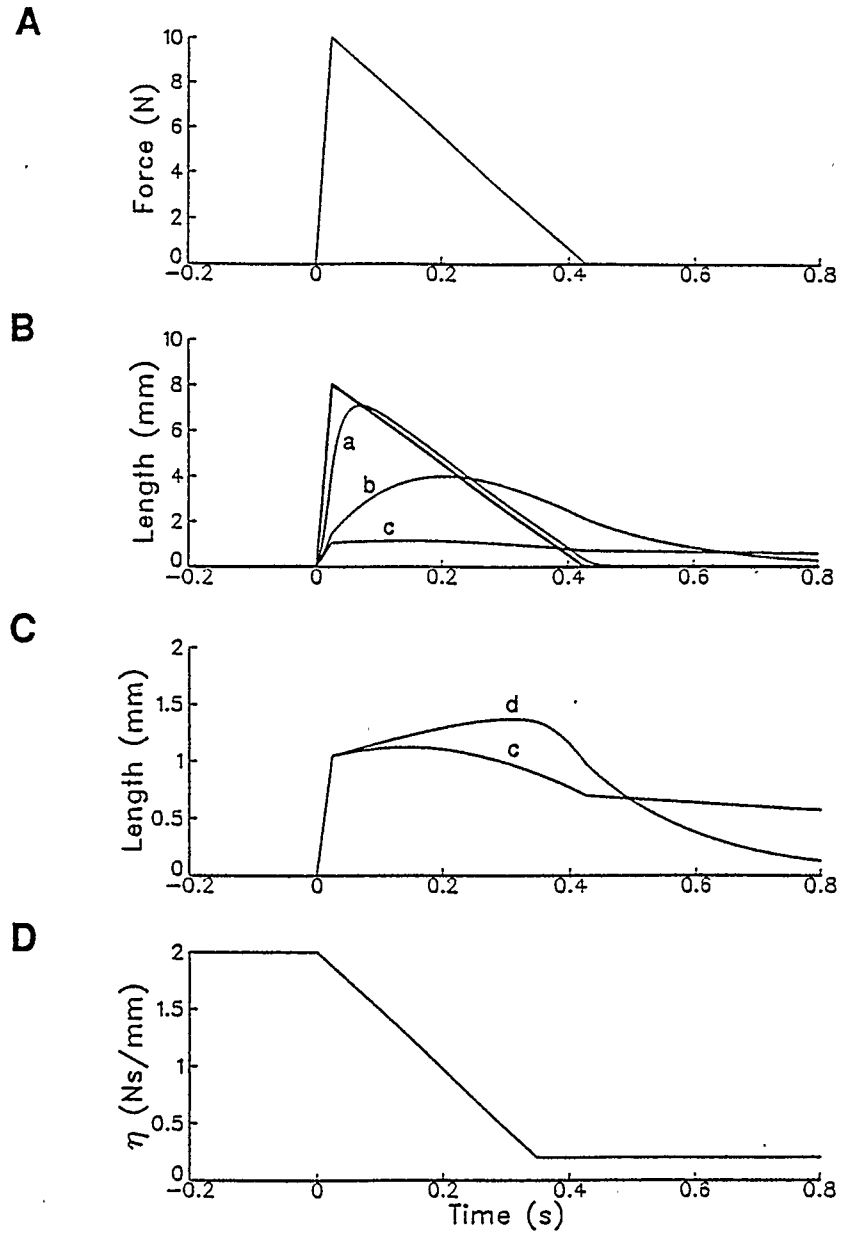

Fig. 4.10. Length responses of the Kelvin model. A. The input force F (F = 0, t < 0; F = 400t, 0 ≤ t < 0.025; F = 10 - 25(t - 0.025), 0.025 ≤ t < 0.425; F = 0, t ≥ 0.425), chosen to mimic the active force generated in the step cycle. The stiffness μ_p and μ_s were chosen to yield an initial displacement of 1 mm (μ_p = 1.25 N/mm, μ_s = 8.75 N/mm). The viscosity η was the free parameter. B. Thick trace: steady state length response. Thin traces: length responses for different values of η: 0.02 Ns/mm (a), 0.2 Ns/mm (b), and 2.0 Ns/mm (c). C. c as in B, but reproduced with larger gain; d: length response of the thixotropic Kelvin model with viscosity η as in D.

of the series spring μ_s change, since a change in the stiffness of the parallel spring μ_p also entails a change in the steady state solution.

4.6 An accidental observation

In one series of runs of simulated walking the muscle puller was turned off by accident after the fourth run (in those runs the muscle puller remained at the initial position, as shown by the position feedback signals). Fig. 4.11A compares the force and (raw) fibre length measurements made in the runs with muscle puller on and off (Paradigm 4). Also shown is the rate of change of fibre length (computed from the corrected average fibre length signals) and the normalized force-length curve (inset). The force generated during reproduction of muscle length was much larger and less smooth, and also rose much more steeply than the force generated in the runs with the muscle puller at constant length. The shortening velocity of the muscle fibres at the onset of active force generation was larger when muscle length was reproduced than when it was not. For comparison, Fig. 4.11B shows the force response of a partially activated distributed thixotropic Kelvin model to the same triangular input as in Fig. 4.10A for two different initial viscosities. The simulated responses are qualitatively similar to the experimental responses. The distributed thixotropic Kelvin model is further discussed in Discussion.

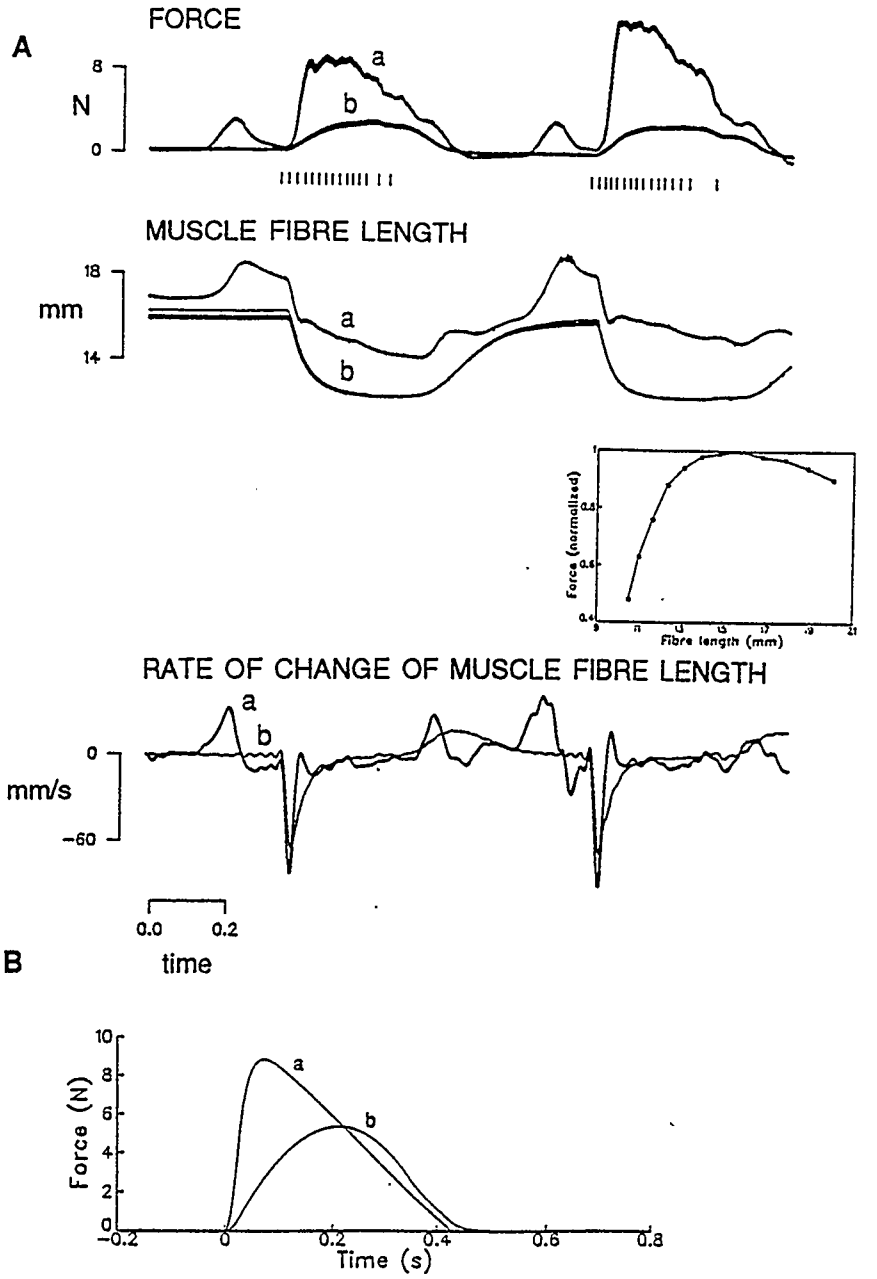

Fig. 4.11. Muscle force and fibre length measurements obtained during active walking with the muscle puller on and off (A), and force responses of the distributed thixotropic Kelvin model to partial activation (B). In the first and second panel of A all measurements are shown superimposed. a, muscle puller on, b muscle puller off. Inset: force-fibre length curve. The third panel in A shows the derivative of the averaged and corrected fibre length signals obtained with the muscle puller on (a, thick trace) and off (b, thin trace). The force responses in B were computed with different initial viscosities: 2.0 Ns/mm in a and 0.2 Ns/mm in b. In both a and b, the viscosity decreased linearly by a factor of 10 during activation, as in Fig. 4.10D. Since all responses were computed at initial length $x = 0$, and *elastic* opposing forces were assumed not to exist, the differential equation solved was $\dot{F} + \mu/n\eta F = \mu/n\eta F_a$, which describes a system consisting of a spring with stiffness μ (μ = 10 N/mm) in series with a parallel arrangement of a contractile element generating a force F_a and n dashpots with viscosity η.

4.7 Decomposition of single motor unit forces?

As indicated in the Introduction, both simulated walking and muscle fibre-*quasi*-isometric data were difficult to measure because of variability in the background force. Only for a small number of filaments then were forces obtained under all of the following four different conditions: (1) passive walking, (2) active walking, (3) muscle-isometric, and (4) muscle fibre-*quasi*-isometric. Rather than forming the beginning of a database for studying length and other dependencies, these measurements exhibited unexpected complexity, as illustrated in Fig. 4.12. For the measurements shown one could argue that the difference between the muscle-isometric and muscle fibre-*quasi*-isometric forces, which occurred mainly during the initial phase of muscle fibre shortening, was a consequence of force-velocity dependence, but this would not explain why the passive and active walking forces rose much more quickly than the isometric measurements, even though the muscle fibres shortened more and faster. Stimulation began when muscle fibre length was about 17.5 mm, which, as shown in Fig. 4.11 (data from the same cat), was on the descending limb of the force-fibre length curve. The force at this length was larger than 95% of the isometric maximum. Moreover, since for non-tetanic stimulation of whole muscle or motor units the maxima of the force-length curves occur at muscle lengths beyond the optimum length for tetanic stimulation (see Historical Background), the explanation is not length dependence. More factors than just length and velocity dependence seemed to be at work. On the basis of the available data, those factors could not be identified. Decomposing the

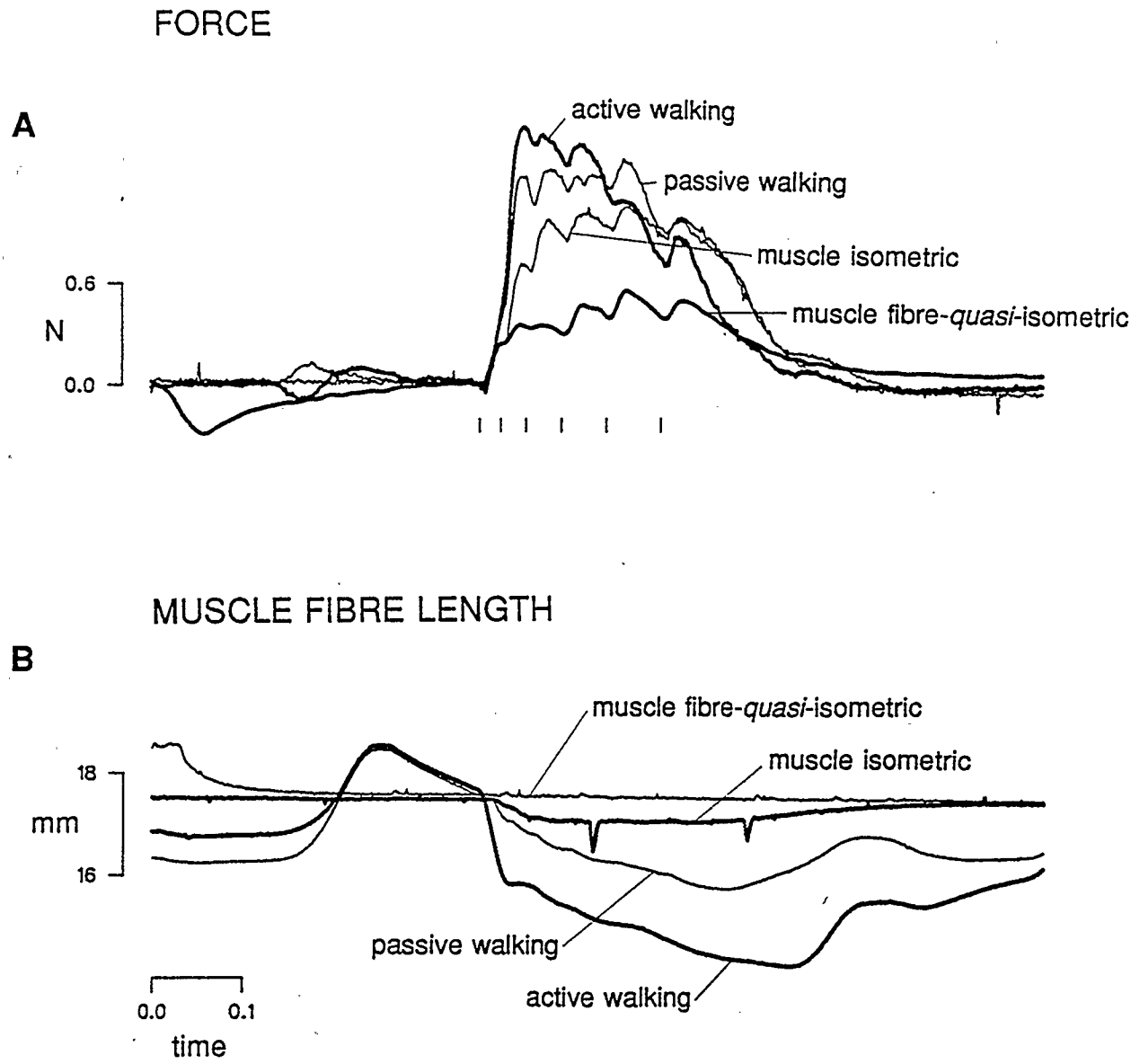

Fig. 4.12. Average multi-unit filament force (A) and muscle fibre length (B) obtained under the following conditions: active walking, passive walking, muscle-isometric, and muscle fibre-*quasi*-isometric.

measured forces then was considered meaningless at this stage; such an analysis would require further, more refined systematic studies, in which for instance fibre length would have to be controlled by other means than background stimulation.

4.8 Motor unit forces during active and passive walking

Multi-unit motor unit forces during simulated walking were obtained from 25 filaments in seven cats. Fig. 4.13 shows representative examples obtained from measurements made under both active and passive walking conditions. In A average measurements are shown (paradigms 1-4), in B individual "passive" and "active" differences, i.e., P1 minus P2 and P3 minus P4, respectively (see Methods). The data in B illustrate two points: (1) within measurement noise the measurements were reproducible, and (2) the active estimates often were initially negative (38 out of 50 step cycles). It has been argued that motor units might contribute negatively to muscle force as a result of interactions with other motor units (Demiéville and Partridge, 1980). However, it has as yet to be shown directly that this does indeed occur in muscle. It seemed more likely that the initial negativity was due to potentiation of the background force in paradigm 4 due to activation in the preceding paradigm 3 (see Methods), since it always began before the filament was stimulated. Simple analytical considerations

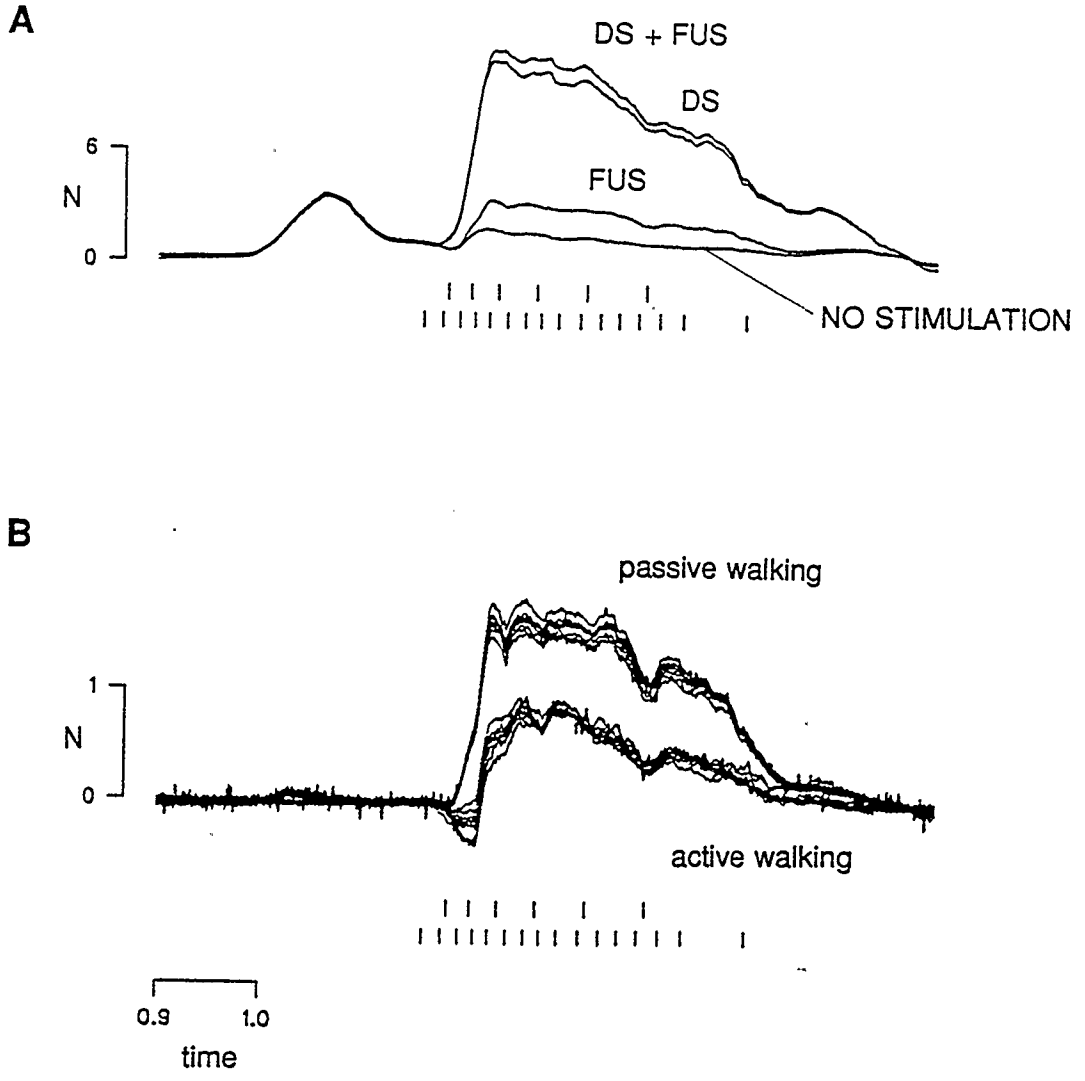

Fig. 4.13. Average muscle force in the four different simulated walking conditions P1 through P4 (A), and differences between active walking forces P3 and P4, and passive walking forces P1 and P2 (B). DS and FUS in A denote Distributed Stimulation and stimulation of the Filament Under Study, respectively. Active walking in B is (DS + FUS) - DS (all differences superimposed); passive walking in B is FUS - NO STIMULATION (*id.*). Also shown are the stimulation patterns used for distributed stimulation of the ventral root filaments and stimulation of the filament under study. Often the active walking forces were initially negative.

showed that the data did not offer an exact way of correcting for this effect.[3] Consequently, the following approach was taken. The change in force from one run to the next *within* both paradigms 3 and 4 was assumed to have the same time course as the potentiation *across* paradigms 3 and 4. A positive estimate of the effect of potentiation was obtained by subtracting all force measurements within both paradigms from the measurement with the largest amplitude and averaging the differences. The averaged difference was scaled to match the initial negative force in the active estimates. For convenience, this matching was done with the average inverted. The scaled average was digitally low-pass filtered (cut-off frequency 25 Hz) and summed with the raw estimates to obtain corrected estimates. The procedure is illustrated in Fig. 4.14.

The corrections applied to the data did not fundamentally change the basic result (see below). However, the very fact that correction was required and was inexact nevertheless cast some doubt on the reliability of all the multi-filament

---

[3] Let $b(t)$ be the background force generated in P3, and $x(t)$ the force generated by the filament under study, for simplicity assumed not to change from one run to the next. Due to the various factors that affect force, $b(t)$ will vary from one run to the next by an amount $n_{3i}(t)$, $i = 2, 3,..., N$ in paradigm 3 and $n_{4i}(t)$, $i = 1, 2, 3,..., N$ in paradigm 4:

P3	P4
$m_{31}(t) = b(t) + x(t)$	$m_{41}(t) = b(t) + n_{41}(t)$
$m_{32}(t) = b(t) + n_{32}(t) + x(t)$	$m_{42}(t) = b(t) + n_{42}(t)$
$m_{33}(t) = b(t) + n_{33}(t) + x(t)$	$m_{43}(t) = b(t) + n_{43}(t)$
⋮	⋮
$m_{3N}(t) = b(t) + n_{3N}(t) + x(t)$	$m_{4N}(t) = b(t) + n_{4N}(t)$,

where $m_{3i}(t)$ and $m_{4i}(t)$, $i = 1, 2,..., N$, denote the measured signals. Averaging and subtracting yields $x(t) + 1/N \sum_{i=2}^{N} n_{3i} - 1/N \sum_{i=1}^{N} n_{4i}$ as the estimate of $x(t)$, which is in error by $1/N \sum_{i=2}^{N} n_{3i} - 1/N \sum_{i=1}^{N} n_{4i}$. The second term can be easily computed from $\sum_{i=2}^{N} n_{3i} = \sum_{i=2}^{N} (m_{3i} - m_{31})$, but the third term cannot be found (N equations, N+1 unknowns).

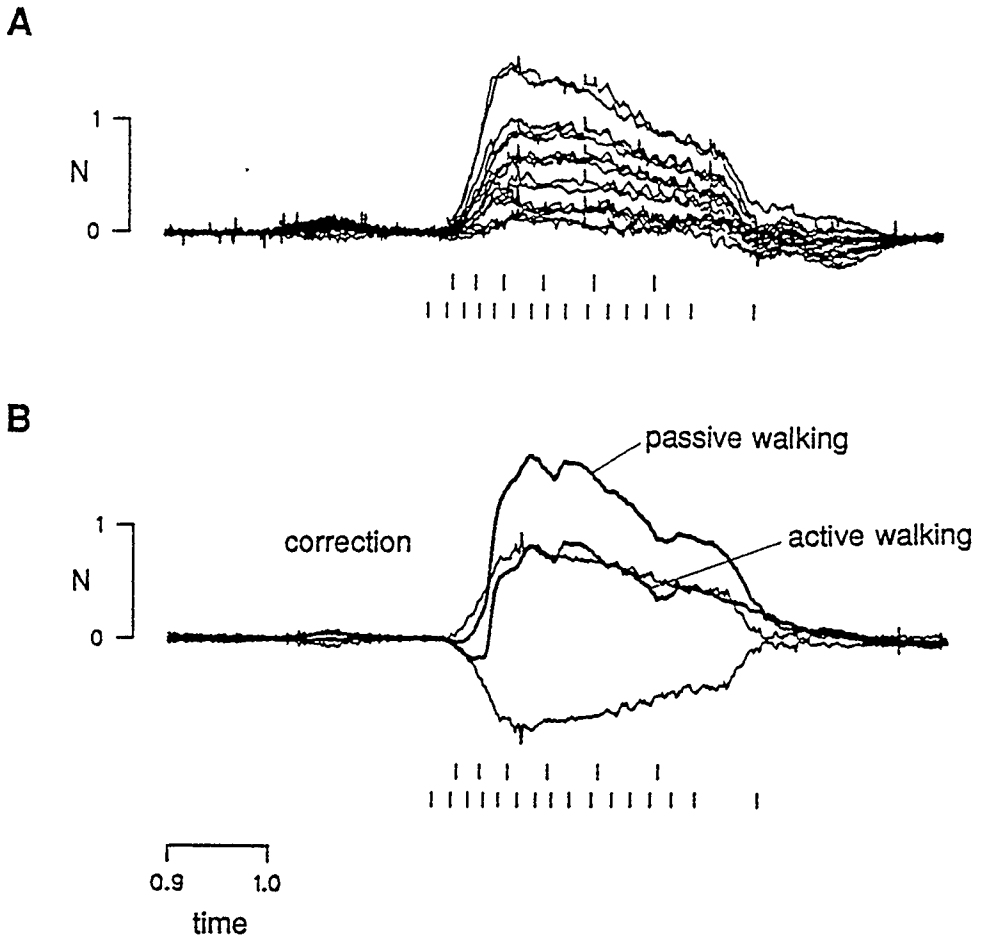

Fig. 4.14. The method of correction of the initial negativity in the estimates of active walking filament forces. A. Differences within both paradigm 3 and 4 between the force measurement with the largest amplitude and the remaining measurements (same data as in Fig. 4.13). B. The averaged differences (thin traces; normal and inverted) were scaled to match the initial negativity in the raw active walking force estimate. The corrected estimate is the sum of the raw estimate and the appropriately scaled and digitally low-pass filtered (cut-off frequency 25 Hz) estimate of the potentiation effect.

force data. Furthermore, the uncertainty associated with the correction procedure made quantification at this stage pointless. Consequently, the results described below are rather anecdotal.

When active and passive estimates were compared, the striking observation was that there was considerable variability, not only in amplitude, but also in time course: some passive and active estimates were virtually identical, some active estimates were smaller than the corresponding passive estimates, and still others were partly greater, partly smaller, despite comparable conditions in terms of fibre length and velocity. Figs. 4.15A through C illustrate this variability with three examples. The insets show the EMG responses to single stimuli delivered to the filament under study, measured at four different locations in the muscle (PR, PIN, DIN and DI; see Methods). As the EMGs indicated, the type of force response did not appear to be correlated with the location of the motor units in the muscle.

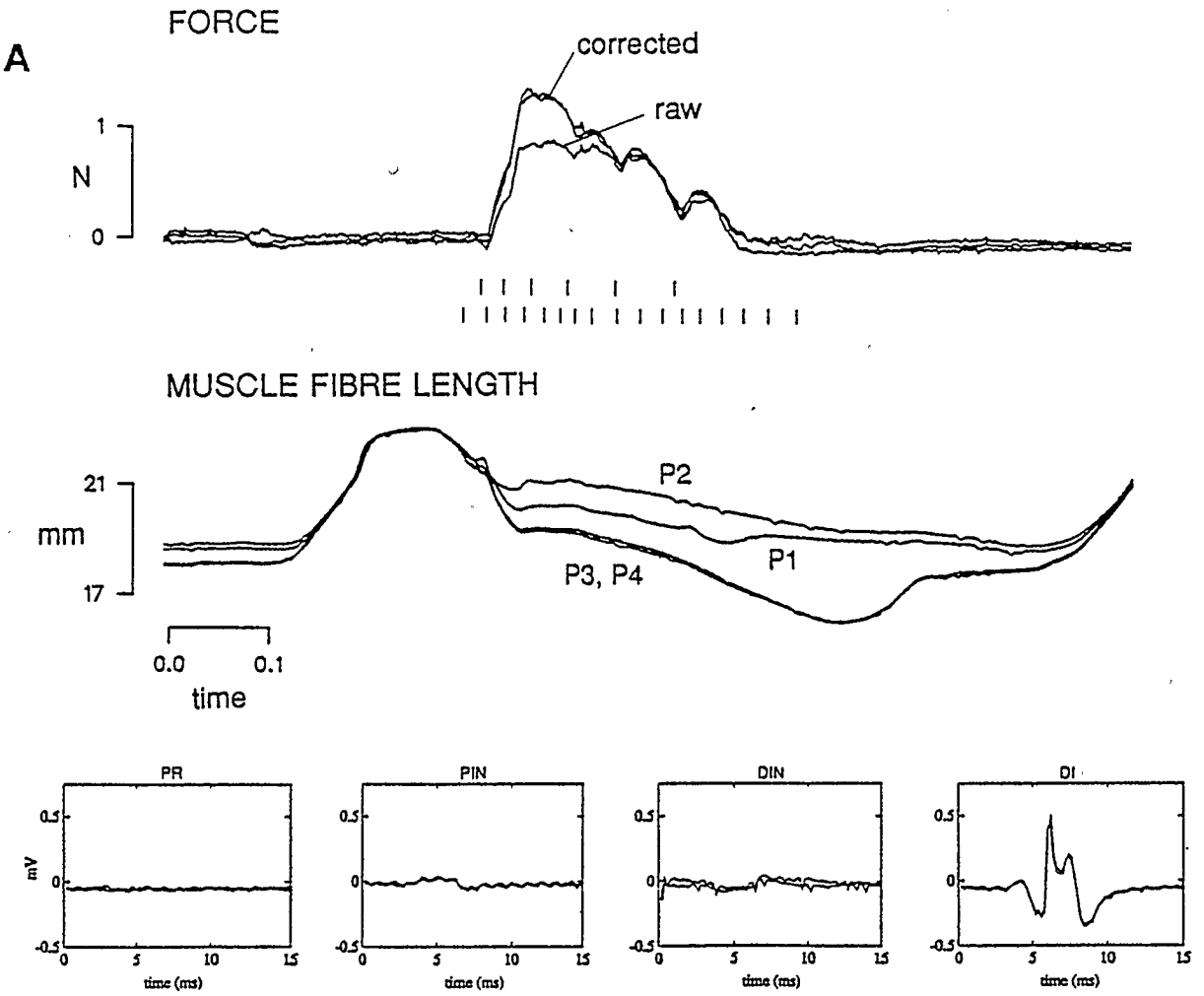

Fig. 4.15. Three examples of raw and corrected active walking and passive walking filament force estimates and corresponding fibre length signals. In A the active and passive walking forces are virtually identical; in B the two estimates are initially very similar (first and second component twitch), but then diverge; in C the third and fourth component twitches are essentially identical. The insets show the EMG responses to single stimuli delivered to the filament under study (PR, PRoximal; DIN, Distal INtermediate; PIN, Proximal INtermediate; DI, DIstal).

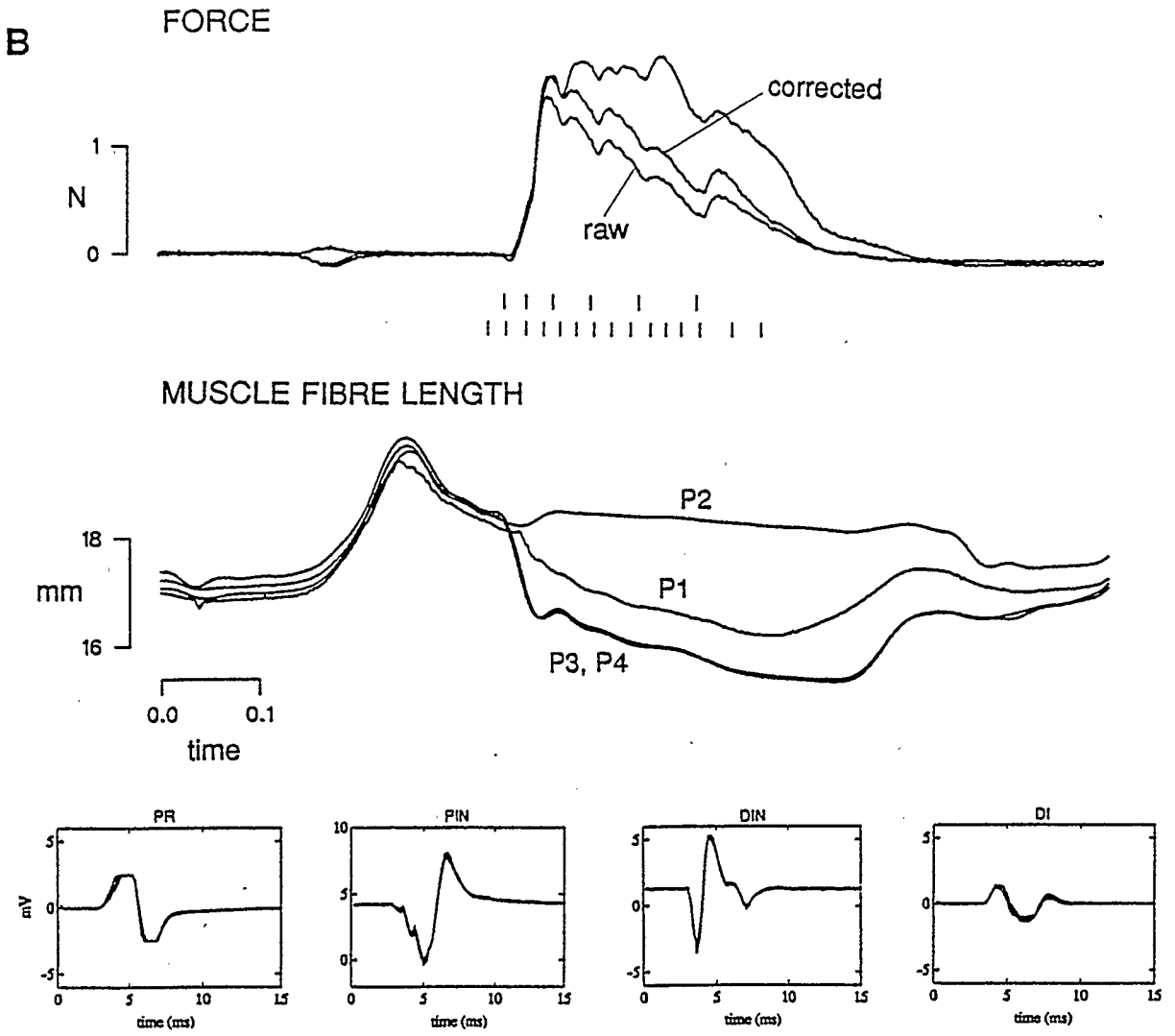

Fig. 4.15. Continued.

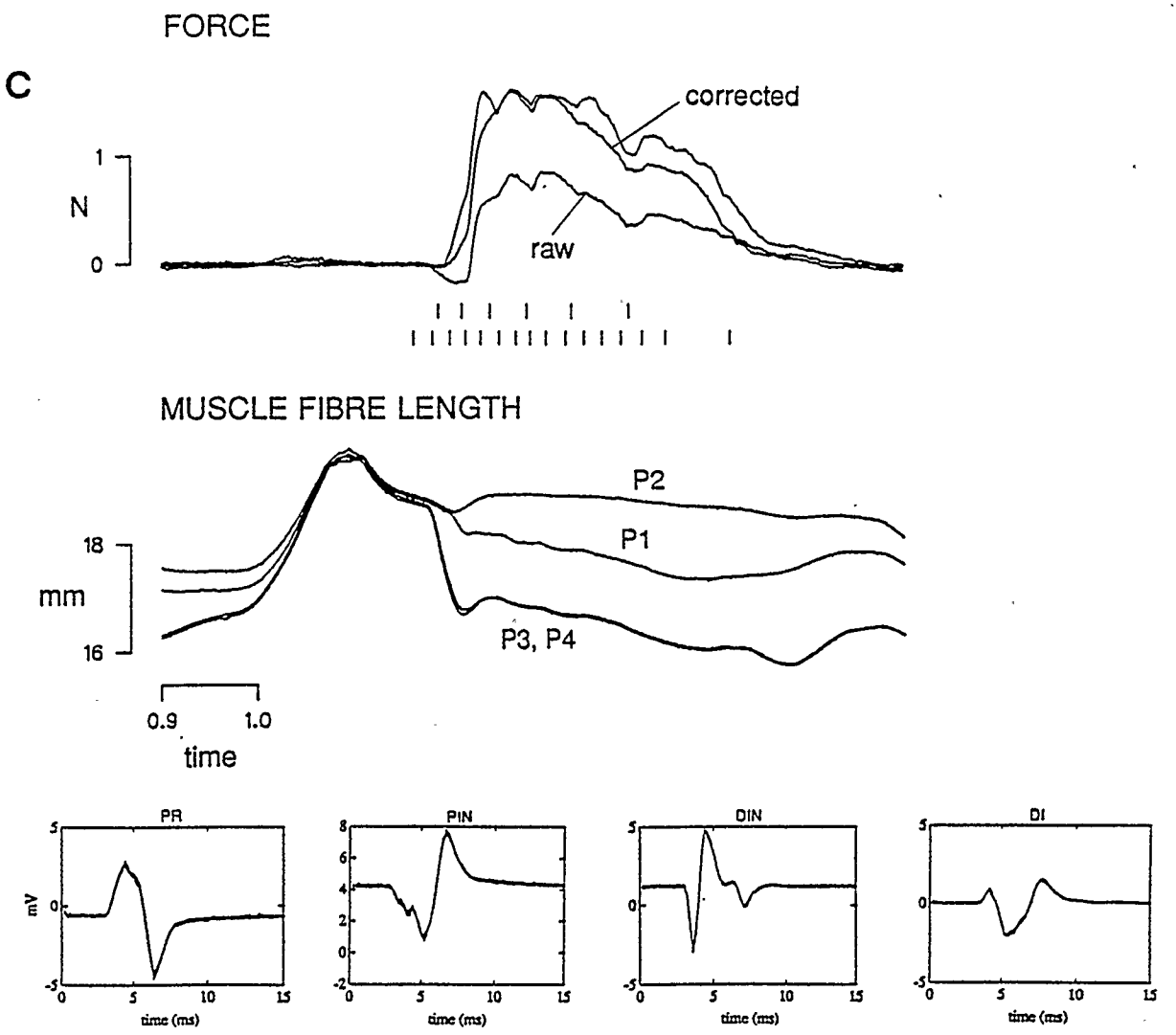

Fig. 4.15. Continued.

Chapter 5.

DISCUSSION

It might turn out that theory will show that a particular process, or implementation of a process, gives a very advantageous performance, even though the experimentalists can, as yet, see no sign of it.
Francis H.C. Crick and Chisato Asanuma, 1986.

5.1 Chronic recordings

The origin-to-insertion length and the length of the muscle fibres of the cat medial gastrocnemius changed in different ways during treadmill locomotion. Differences between muscle length and muscle fibre length have been reported before for this muscle by Griffiths and Hoffer (1987) and Hoffer et al. (1989). The differences described here are very similar to those observed by Hoffer et al. (see their Figure 2B). In Griffiths and Hoffer's data muscle length and muscle fibre length are out of phase during passive lengthening in the late swing phase, muscle fibre length lagging muscle length. This phase difference was never observed in the present experiments.

During swing the length of the aponeurotic sheet changed in more or less the same way as the origin-to-insertion length of the muscle in five out of eight cats. In three cats the length changes in the swing phase were paradoxical: the aponeurotic sheet shortened during the passive lengthening of the muscle. Why

this was so was unclear. Also unclear was why these paradoxical patterns of length change switched to the more "typical" pattern in the acute simulations.

The pattern of change of the angle of pinnation was consistent from step cycle to step cycle within the same cat, but varied a great deal between cats. The reason for this variability was not obvious. The various length measurements from which the angle of pinnation was derived were made with pairs of piezoelectric crystals (see Methods, Figs. 3.1 and 3.4). Systematic errors could have been caused by misalignments of the crystals in the sagittal plane. However, since the patterns changed from rather variable in the chronic recordings to a more "typical" pattern in the acute experiments (an inverse relationship to muscle length in the swing phase, and approximately constant in the stance phase) the observed variability was not due solely to artifact.

5.2 Acute simulations of locomotion

The primary purpose of the simulations was to simultaneously match two different target signals: muscle fibre length and muscle force. Good matching was obtained for both signals, but, as the results have shown, this did not, in general, result in good matching of the origin-to-insertion muscle length, the aponeurotic sheet length, S3, and angle of pinnation.

Matching of the maximum in the muscle length signal in the late swing phase and the corresponding maxima in the passive force and muscle fibre length signals could, obviously, not be done independently, since both passive force and fibre length depend on muscle length. Oddly, the observed discrepancies were

often paradoxical: muscle length too short, yet too much passive force and a good match of muscle fibre length. The reasons for this were not clear. A difference in the temperature of the hind leg in the conscious and anaesthetized animal would have resulted in systematically different length measurements. However, the differences would have been rather small if, as assumed, the variation of the velocity of ultrasound in muscle and interstitial tissue was of the order of 2.4 m/s°C (see Methods). To explain a difference of 2 mm on this basis (as for instance in the data of Fig. 4.3) would require a difference in temperature of more than 100°C. It thus seems unlikely that differences in temperature were the sole cause of the observed discrepancies.

The initial gradual increase in active force could not be simulated: initiation of the distributed stimulation immediately after the occurrence of the maximum in the passive force always resulted in too large a force. Since with ventral root stimulation in the acute experiments the number of motor units stimulated was fixed (all the motor units within each filament were recruited simultaneously), this result suggests that the initial gradual rise in force in normal locomotion is due to gradual recruitment of motor units.

5.3 Muscle length and muscle fibre length

At the core of the recent controversy concerning the role of muscle tendon compliance in locomotion (Hoffer et al., 1989; Elek et al., 1990) is the question whether or not fibre length varies in proportion to muscle length during the step cycle. The experiments have shown that, *during the step cycle as a whole,* it does not

do so, neither during treadmill locomotion nor during active or passive walking, but that *during restricted phases* of the step cycle muscle length and muscle fibre length may change in a very similar way.

The data obtained in the chronically instrumented conscious cats and in the anaesthetized animals under active walking conditions were comparable, and essentially identical to those reported by Hoffer et al. (1989) (which is not surprising, since, except for a few improvements in the construction of the piezoelectric crystals, the same technique was used). Muscle length and fibre length changed in opposite directions in the early stance phase (the muscle lengthened and the fibres shortened) and in the early swing phase (the muscle shortened and the fibres lengthened). The lengthening of the fibres in the early swing phase occurred, at least in part, in the absence of measurable force at the tendon. As discussed extensively below, this passive lengthening was interpreted to be a consequence of the viscous properties of the endomysium and possibly also the aponeurotic sheets and tendon. During the passive lengthening in the late swing phase and throughout most of the stance phase muscle length and muscle fibre length changed not only in the same direction, but also often with very similar time courses and amplitudes. This similarity during the stance phase indicates that, despite changes in force, the length of the tendinous component of the muscle remained more or less constant.

Except in the early swing phase, during which the muscle, but not the muscle fibres, shortened appreciably, the time course of change in fibre length in

passive muscle was rather similar to the time course of change in muscle length. Both the absence of force during the rapid muscle shortening and the absence of concomitant fibre shortening indicate that during this phase the external part of the tendon shortened below slack length.

5.4 Do spindles signal muscle length or muscle fibre length?

This question has been addressed before by Hoffer et al. (1989 and in press), in the most recent communication, on the basis of a more extensive set of chronic data than the one presented here (fibre lengths measured in different locations of the muscle, and also during downhill and uphill walking). The data described here, however, extend Hoffer et al.'s since measurements of muscle fibre length changes were also made in passive muscle during "normal locomotion." In both publications Hoffer et al. answered the question in favour of the muscle fibres, on the basis of (1) the overall discrepancies between muscle length and muscle fibre length and (2) the presence of a "paradoxical, large burst near the end of stance" (Hoffer et al., in press) in the firing patterns of triceps surae Ia spindle afferents (see Fig. 3 of Prochazka et al., 1989). These large bursts were thought to be caused by the fibre lengthening occurring in "centro-distal" fibres in this phase of the step cycle. Fibres in the distal part of the muscle do lengthen during the passive shortening of the muscle that occurs in this phase, and may even exhibit a local maximum (Fig. 1C of Hoffer et al., in press; see also Fig. 4.4), and they may thus cause the spindle afferents to fire even though muscle length decreases and goes through a minimum. However, Prochazka et al.'s data (1989) show that

spindle firing thereafter often declines, even though muscle length, after going through the minimum, increases. It is unclear why this is so, since muscle fibre length has been consistently found to further increase, in parallel with muscle length, during this passive lengthening (Hoffer et al., 1989 and in press; see also Figs. 4.1 and 4.4).

Prochazka et al.'s data (1989) were obtained in chronically instrumented, conscious cats walking on a treadmill. Under those conditions the response of the spindle afferents is not only determined by the length changes experienced by the muscle spindle but also by its fusimotor drive (possibly tonic stimulation from static γ-motoneurones, as the simulation results of Prochazka et al. (1985) indicate). Elek et al.'s work (1990) seems to suggest that Ia spindle afferents signal muscle length (albeit with considerable phase advance) during simulations of the step cycle in the deeply anaesthetized cat, in the absence of fusimotor drive. Two observations, however, indicate that Ia spindle firing (in Elek et al.'s data) was more related to muscle fibre than to muscle length. First, the bursts measured during passive lengthening under active walking conditions were phase advanced by about 25 ms on those measured under passive walking conditions. Elek et al. observed:

> In active trials, kinking [of the external tendon] was reduced; the residue of muscle contraction carried over from the previous cycle was apparently sufficient to take up some of the slack. Thus ... in active trials more of the length variation may have been transmitted, and so relengthening would have been 'seen' slightly earlier.

This fine observation is borne out by the measurements of fibre length reported here: the muscle fibres were always substantially shorter in active walking than in passive walking, and remained so for a while even in the absence of active force, since they regained their "passive" lengths only slowly. Consequently, relengthening occurred earlier in active trials than in passive ones. (Observations of a similar nature have recently been made by Griffiths (1991): after tetanic stimulation of the cat medial gastrocnemius muscle, the muscle fibres regained their initial length only *after* the force had relaxed.) Second, in the stance phase, the main difference between the spindle firing patterns recorded in active and passive trials occurred during the rapid development of active force: in active trials the spindles remained silent longer or fired at lower frequencies. This can be explained by "paradoxical" fibre movement: in active walking the muscle fibres shorten rapidly during force development whereas in passive walking the fibres continue to change in parallel with muscle length.

5.5 Tendon compliance

The main results were that (1) the tendinous component of the muscle did not change its length in phase with the muscle force, as would be expected for a predominantly elastic structure (Elliott, 1965; Abrahams, 1967; Viidik, 1973; Butler et al., 1978; Bennett et al., 1986), and (2) the estimated length changes had much greater amplitude than can be expected on the basis of published values for the stiffness of the cat medial gastrocnemius muscle (Walsmley and Proske, 1981; Elek et al., 1990; Griffiths, 1991).

Both results differed substantially from what one could reasonably expect based on data in the literature. The first question that needs to be addressed then is whether or not the observations were grossly in error. Two possible sources of error come to mind: (1) errors due to the sonomicrometric measurement technique, and (2) errors due to the assumptions made in the analysis.

The errors associated with piezoelectric length measurements—muscle length, fibre length, aponeurotic sheet length, and S3—were discussed at length in Methods. For the muscle length measurements the error range was found to be -1.0 to 3.5%. The actual errors were probably smaller, since this range was a conservative worst case estimate. Similarly, the errors in the three local length measurements were probably smaller than 1%. The large differences between the fibre length measurements made in active and passive walking and the large changes in the length of the tendinous component derived from these and the muscle length measurements thus cannot be explained solely on the basis of these relatively small measurement errors.

It should be stressed that the model illustrated in Fig. 4.5A is a *structural* model of a single muscle fibre (or a small set of neighbouring muscle fibres) in the medial gastrocnemius muscle, and that it does not make *functional* assumptions about the viscoelastic properties of the tendon and the muscle fibre. On physical grounds it is clear that when both muscle length and muscle fibre length change (in different ways), the difference (taking into account pinnation) *must* be due to a change in the length of the structure in series with the muscle

fibre, i.e., the tendon. The model does not specify, however, *how* this length change occurs (stretch, buckling due to shortening below slack length, etc.), nor, for that matter, that the length change be homogeneous. I.e., the observations by Hoffer and colleagues that the patterns of change of length of the muscle fibres and the aponeurotic sheet are not identical in different parts of the muscle[1] (Caputi et al., 1989; Hoffer et al., in press) do not invalidate the analysis in any way, but merely imply that for muscle fibres in different parts of the muscle the length change of the in-series tendon is not identical.

The model could be criticized though on the ground that it did not take into account bulging of the muscle belly with activation and the concomitant changes in the length of the aponeurotic sheets due to curving. However, the straight lines in the figure are deceiving in this respect, since the actual muscle lengths used in the model equations, because of the very nature of the measurement technique—length gauge on top of the muscle belly—did include the effects of muscle bulging.

The relation between tendon length and muscle force was complex: after the initial more or less proportional stretch the tendon remained at its current length or kept lengthening even though the force decreased, and it returned to slack length only slowly and in the absence of force. The fact that the aponeurotic sheet length measurements exhibited the same features strongly suggested that

---

[1] Except for slightly different behaviour during the phase of rapid muscle shortening at the end of stance and differences in amplitude, the patterns are very similar; see, e.g., Fig. 1C in Hoffer et al. (in press).

they were genuine and not the result of artifact. The slow relaxation in the absence of force was taken to be due to the presence of substantial viscosity in the muscle. This is discussed in detail below.

The mean maximum change in the length of the tendon due to activation was 2.53 mm. This value is much larger than those that can be derived from compliance or stiffness values published previously for the cat medial gastrocnemius, assuming a change in force of 9 N (following Elek et al., 1990): 0.54 mm (Walsmley and Proske, 1981; compliance: 0.06 mm/N), 0.9 mm (Elek et al., 1990; stiffness $k = 3.6F + 5.4$), and 0.45 mm (Griffiths, 1991; compliance 0.05 mm/N). These discrepancies cannot be explained on the basis of viscosity alone: viscosity affects the time course of change but not the magnitude. Nor were they due to changes in the angle of pinnation. Any contribution to the change in tendon length due to changes in pinnation were taken into account by using the simple model of Fig. 4.5A (see also the equation for ΔL_T). I.e., the estimated changes must be accounted for by the aponeurotic sheets and external tendons. No measurements were made of the length of the external tendon. Excised tendons studied *in vitro* undergo permanent deformation when strain exceeds 2-4% (Elliott, 1965; Abrahams, 1967; Butler et al., 1978). Under physiological conditions tendon is assumed not to be stretched beyond this limit. There is no reason to believe that the mechanical properties of the tendon of the cat medial gastrocnemius muscle are substantially different from those of other tendons (Bennett et al., 1986). Using Abraham's stress-strain curve for human Achilles

tendon (Abrahams, 1967; his Fig. 5) and 38.4 mm and 3.62 cm^2 for the slack length of the external tendon and the cross-sectional area of the cat medial gastrocmemius, respectively (Poliacu Prosé, 1985), the strain for a change in force of 9 N is about 0.35%, or 0.13 mm. This calculation indicates that the major part of the length change occurred in the aponeurotic sheet. The estimated length change in the aponeurotic sheet accounted on average for only 66.4% (range: 47.2-92.0) of the total estimated length change. This estimate, however, is likely to be an underestimate since it was derived from measurements made on the distal part of the ventral aponeurotic sheet close to the external tendon/aponeurotic sheet transition; i.e., at a point at which the cross-section of the aponeurotic sheet, and presumably also its stiffness, is larger than in the remaining, more proximal part. That the aponeurotic sheet is less stiff than the external tendon is further hinted at by the large fractional changes (up to 6.1%) seen with low muscle forces (less than 20% of the maximum isometric force).

Walsmley and Proske (1981) obtained their stiffness data using Morgan's α-method (Morgan, 1977). This method is based on the assumption that the stiffness of the tendon is constant, which is true only for the linear region of the stress-strain curve. Proske and Morgan (1987) suggested that muscles work in this region if the forces exceed 20-25% of the maximal isometric force (16-20 N for the cat medial gastrocnemius muscle). Walsmley and Proske's stiffness value thus may overestimate the stiffness of the muscle in the locomotor working range (about 0-15 N for walking at a moderate speed).

Elek et al. (1990) used a variant of Rack and Westbury's spindle null method (Rack and Westbury, 1984) to estimate extramysial displacement. The difference between their results and mine are not easy to explain. Given the magnitude of the forces used in their experiments (up to 25 N) and the consistency of the fibre length patterns in my experiments, it seems unlikely that the changes in fibre length in Elek et al.'s experiments were systematically smaller than in mine. Consistent with my data is that the main difference between spindle afferent firing patterns recorded in active and passive trials occurred during the phase of rapid force development, which may be explained by the rapid shortening of the muscle fibres in this phase in active trials. Yet only small adjustments to muscle length were necessary to match active and passive trial spindle firing patterns (0.6-1.1 mm, corresponding to 0.4-0.7 mm inferred extramysial displacement). The explanation is unlikely to be found in fusimotor contamination, since great care was taken to separate γ-motoneurones affecting the spindle under study from the filaments used for distributed stimulation. In the absence of fusimotor stimulation the spindles studied by Elek et al. fired only a few spikes in the stance phase, where the patterns were to be matched. With tonic fusimotor stimulation the spindle responses tended to be quite noisy. Perhaps the spindle null method lacks sufficient sensitivity to allow differences in fibre length to be resolved accurately.

Griffiths (1990) arrived at his figure by dividing tetanic forces by the maximum change in fibre length, measured simultaneously. Absolute values for

the measured forces were not given. Computing back from the average stiffness value yields tetanic forces of about 130-140 N, which are much higher than those reported by other authors (e.g., Walsmley et al., 1978: 75 N; Poliacu Prosé, 1985: 80 N). The reason for this difference is not clear, but it suggests that Griffiths stiffness value may be an overestimate. Also, stiffness increases with force (references for tendon given above; Rack and Westbury, 1984; Proske and Morgan, 1987; Elek et al., 1990), and the extramysial displacement derived from an average value for the total range of force underestimates the actual extramysial displacement in the low force range.

5.6 Mechanical models of viscoelasticity

In order to keep analysis by comparison with model responses as simple as possible only the simplest mechanical analogues of viscoelasticity were investigated. The primary purpose was to gain basic insight into the mechanism(s) that might underlie the observed behaviour, not to construct sophisticated muscle models.

Both the Voigt and the Kelvin models could reproduce the observed changes in tendon length, but the responses of the Kelvin element bore by far the closest resemblance to the experimental data. On two other, more compelling grounds, the Kelvin element, equipped with a movement dependent viscosity (see below), referred to as the "thixotropic Kelvin element," seemed to be the model more likely to provide a possibly correct explanation for the data: (1) on the basis of physico-chemical theory muscle is much more likely to be thixotropic than

dilatant (explained further below), and (2) other experimental results could be explained, at least qualitatively, on the common basis of the thixotropic Kelvin element: (a) mechanical history dependent potentiation of single motor unit forces, (b) the shape of single motor unit force-velocity curves, (c) the time course of the force responses of passive muscle to ramp and hold stretches, and (d) the accidental observation reported in Results.

The springs and/or dashpots of both the Voigt and Kelvin models had to be time-varying (more specifically, movement dependent): the Voigt model required a decrease in stiffness and/or an increase in viscosity, the Kelvin model required the converse, an increase in stiffness and/or a decrease in viscosity. Assuming decreasing stiffness of tendinous tissue with increasing force (Voigt model) or increasing stiffness with decreasing force (Kelvin model) would be contrary to everything that has been published on the mechanical properties of tendons or collagenous tissue (see, e.g., Elliott, 1965; Viidik, 1973; Bennett et al., 1986). On physico-chemical grounds an increase in viscosity as a result of movement (Voigt model) also is unlikely to occur in muscle. The viscosity of many disperse systems is known to be a function of shear rate (Jirgensons and Straumanis, 1962; Hiemenz, 1986). An increase in viscosity with increasing shear rate is called dilatancy or shear thickening, a decrease in viscosity with increasing shear rate is called thixotropy or shear thinning (see also footnote 2 on p. 6 of the Introduction). Dilatancy occurs in disperse systems in which the particles are symmetrical and non-flocculated (Hiemenz, 1986), whereas thixotropy occurs in

disperse systems in which randomly oriented linear (asymmetric) particles align themselves with the flow lines when under shear (Jirgensson and Staumanis, 1962), or in which long asymmetrical particles form networks (flocs) that are disrupted to varying degrees when shear forces are applied and reform when left standing (Jirgensons and Straumanis, 1962; Hiemenz, 1986). Given the abundance of long macromolecules and fibrils in tendon, aponeuroses, muscle fibres, and the extracellular matrix (ECM) of muscle and tendon (see below), thixotropy is more likely to occur in muscle then dilatancy.

Heckman et al. found that motor unit forces are potentiated by prior passive lengthening or shortening of the muscle: twitches elicited 0.1 s after a 2 mm ramp-and-hold stretch or release at 10 mm/s were up to 6 times greater than twitches elicited 10 s after the end of the movement. The amount of potentiation varied inversely with twitch amplitude. If each muscle fibre is thought of as a contractile element in series with a thixotropic Kelvin element, then the muscle consists of a great number of series arrangements of contractile and Kelvin elements in parallel (Fig. 5.1). If not all contractile elements are activated simultaneously, then the active elements push on the inactive ones, which because of the viscosity generate a negative, i.e., *opposing* force. The amplitude of this opposing force depends on (1) the relative number of active elements, and (2) the apparent viscosity of the dashpots. The mechanism underlying the observed potentiation would then be as follows. The apparent viscosity of the dashpots decreases as a result of the shear experienced during the ramp stretch or release.

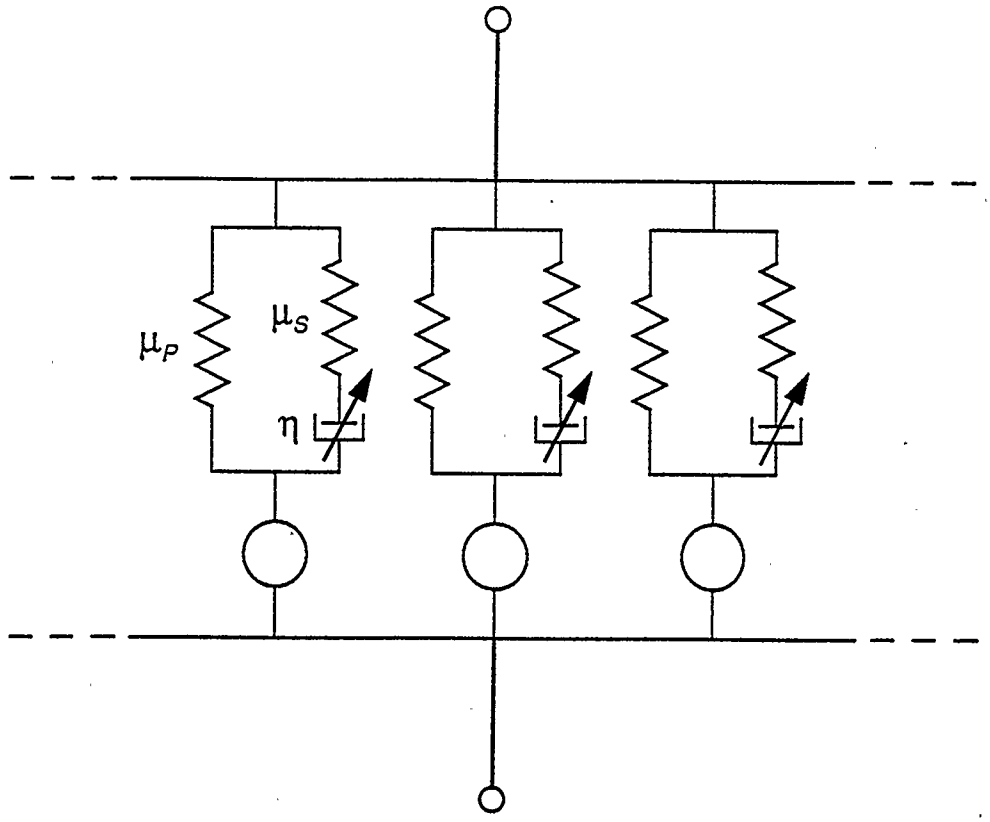

Fig. 5.1. The distributed thixotropic Kelvin model. The contractile elements are represented by the circles.

At the end of the ramp change in muscle length, when conditions are stationary, it slowly increases again. Since the apparent viscosity of the dashpots 0.1 s after the end of the ramp stretch or release is smaller than it is 10 s after the end of the movement, the opposing forces are smaller, and, consequently, the measured twitch forces are "potentiated." This hypothesis also explains why, in the experiments of Heckman et al., potentiation was found to depend on twitch amplitude, i.e., on the number of active muscle fibres, and why the whole muscle twitch did not potentiate (no opposing force).

In the same paper Heckman et al. studied the velocity dependence of single motor unit forces. The passive muscle was stretched and released at various constant speeds and single motor units were stimulated during the movement when a predetermined fixed muscle length was reached. Motor unit forces were found to be larger than those measured under steady state isometric conditions, for both lengthening and shortening (except at the fastest shortening speeds). Since the muscle had already been stretched or shortened at the time of stimulation, this result can be explained on the basis of the same mechanism as the one outlined above for movement dependent potentiation.

Unlike the force responses of isolated tendon to stretch, which, in the physiological range, consist of a "toe region" in which force rises exponentially with stretch, and a linear region, in which force increases in proportion to stretch (Elliott, 1965; Viidik, 1973; Bennett et al., 1986), the force responses of passive muscle follow more complicated trajectories. In the cat medial gastrocnemius

these trajectories typically consist of an initial rapid increase that ends rather abruptly (except when the stretch is imposed at short muscle lengths), followed by a much slower increase, as shown in Fig. 5.2A (modified from Heckman et al.). Fig. 5.2B illustrates how this behaviour can be explained on the basis of thixotropy: the transient force response is initially large, but as the apparent viscosity decreases quickly as a result of the stretch, it becomes abruptly smaller.

Since during normal locomotion the medial gastrocnemius muscle is only partially activated and since active force generation is preceded by fast passive stretch, the question arises to what extent, if any, the active force is shaped by thixotropic effects and variable opposing forces. The accidental observation reported in Results shows that active force in the acute simulations was very different if it was not preceded by passive stretch as it is during normal locomotion: there was a large difference in both amplitude and rate of rise. The difference in amplitude is difficult to explain in terms of length and velocity dependence (see the force-length curve in Fig. 4.11A; the shortening velocity was greater when force generation was preceded by stretch), and the difference in rate of rise is inconsistent with the finding of Stephens et al. (1985) and Heckman et al. that force generation by motor units becomes slower with increasing length, not faster. The model responses illustrated in Fig. 4.11B, however, show that both features result if it is assumed that the apparent viscosity at the onset of force generation is different in both cases, being lower when stimulation is preceded by passive stretch.

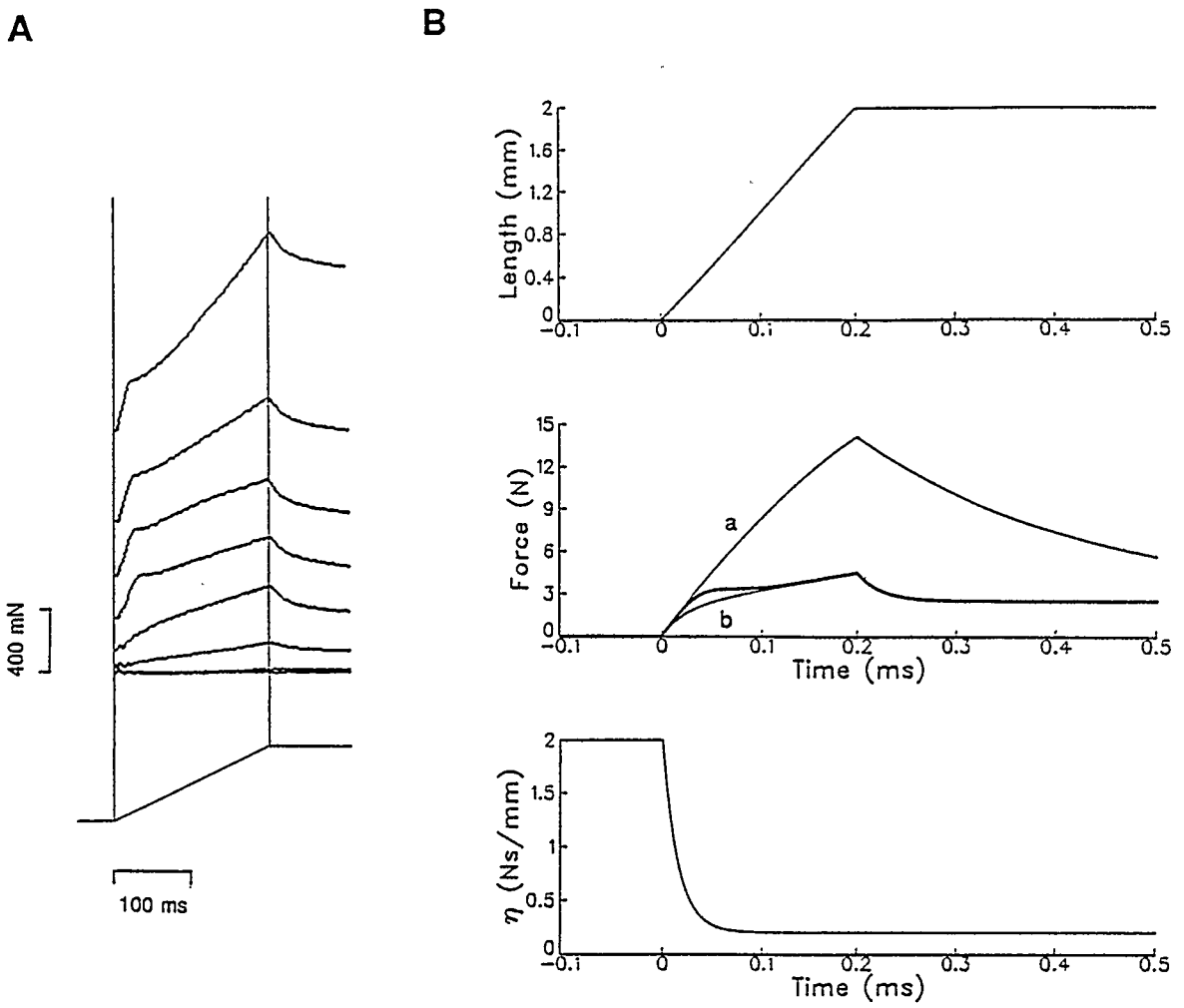

Fig. 5.2. Force responses of the cat medial gastrocnemius muscle to 2 mm ramp-and-hold stretches at 10 mm/s initiated at increasing muscle lengths (modified from Heckman et al.) (A), and force responses of the Kelvin model (B). The stiffness μ_p and μ_s were 1.25 and 8.75 N/mm, as in Fig 4.10. The length input (2 mm ramp-and-hold stretch at 10 mm /s) is shown at the top. Middle panel: force responses for different constant values of the viscosity η: 2.0 Ns/mm (a), 0.2 Ns/mm (b); thick trace: the force response if η decreases exponentially from 2.0 to 0.2 Ns/mm, as shown at the bottom.

Non-linear summation of motor unit forces

As discussed in Historical Background, a number of authors have reported supralinear summation of motor unit forces in various cat hind leg muscles (Emonet-Dénand et al., 1987; Clamann and Schelhorn, 1988; Emonet-Dénand et al., 1990; Powers and Binder, 1991). This supralinear summation was always attibuted to frictional interactions between active and passive muscle fibres. In light of the critique given in Historical Background and the explanation given above for movement dependent potentiation of motor unit forces, however, it seems more natural (at least to me) to explain non-linear motor unit force summation in terms of viscous rather than frictional opposing forces.[2] Since, as indicated above, the magnitude of the opposing force depends on the number of active fibres and the viscosity of the dashpots, this "viscosity hypothesis" also explains why summation of motor unit forces becomes less non-linear as the number of motor unit forces summed increases (Emonet-Dénand et al., 1990), or following imposed movements (Powers and Binder, 1991).

5.7 Is muscle, in casu *the cat's medial gastrocnemius, thixotropic?*

The fact that the same simple model, the thixotropic Kelvin element, can explain a number of different and independent experimental results is appealing, and

[2] The terms viscosity, elasticity, and friction are often used loosely and incorrectly in combinations such as for instance "viscoelastic friction." In the text the terms are used as they are defined in physics, except where "viscosity" refers to the viscosity of a dashpot, in which case it represents the proportionality factor between force and rate of change of length.

suggests that the underlying idea may have a chance of being correct. However, the thixotropic Kelvin element is nothing more than a simple generalization of a simple general model for viscoelasticity, and bears no direct relation to real muscle. The evidence thus needs to be evaluated carefully.

Indicative of and consistent with thixotropy is the fact that the slow lengthening of the tendon persisted until after the last stimulus, i.e., as long as the muscle was "stirred." A 10-fold decrease in viscosity, as required in the simulations, is compatible with data for synovial fluid, which is known to be thixotropic: King (1966) reported a 100-fold decrease in apparent viscosity of synovial fluid from the ankle joint of bullocks and a 500-fold decrease for knee joint synovial fluid.

Movement dependent potentiation of motor unit forces, as revealed by both isometric and isovelocity measurements, could be due to either intracellular mechanisms that increase the active force generated and/or intracellular or extracellular mechanisms that reduce possible opposing forces. Edman (1980) found that passive shortening of single frog semitendinosus and tibialis anterior muscle fibres at 0.45 μm per 200 ms per sarcomere immediately before stimulation had no effect on twitch contraction force, which indicates that the mechanism underlying movement dependent potentiation is to be found in interactions between muscle fibres or muscle fibres and extracellular matrix (0.45 μm per 200 ms per sarcomere translates to approximately one fibre length per second, or approximately twice the velocity used by Heckman et al. for the

isovelocity stretches preceding the isometric measurements (10 mm/s)). Since forces are never "lost" to other fibres and since, as discussed in Introduction, frictional resistance would not result in a loss of transmission of force to the tendon, viscous opposing forces suggest themselves naturally as an alternative explanation. This viscosity likely resides (at least in part) in the endomysium (see below). A shear dependent decrease in the apparent viscosity of the endomysium then provides a plausible explanation for movement dependent single motor unit force potentiation.

The force responses of the passive medial gastrocnemius muscle to ramp and hold stretches bear close resemblance to the force responses of frog and toad passive whole muscle (D.K. Hill, 1968) and frog passive single muscle fibres (Lännergren, 1971) to slow stretch. The initial phase of these passive force responses consists of an almost linear increase in force with increasing length. D.K. Hill attributed this linear force increase to a short-range series elastic component (SREC), which he proposed resides in attached crossbridges. Lännergren (1971) found the Young modulus of the short-range stiffness to be 22.8 N/cm^2 at a sarcomere length of 2.2 μm. Heckman et al. did not study short-range elasticity and did not analyze the passive muscle responses. However, a measurement of the short-range stiffness made on the fourth force record in Fig. 5.2A produced the value 8.56 N/cm, which with 11 cm for muscle length and 3.62 cm^2 for cross-sectional area (Poliacu Prosé, 1985) translates to a Young modulus of 26 N/cm^2. This value agrees rather well with Lännergren's. It seems

unnecessary then to invoke changes in apparent viscosity to explain the passive force trajectories. A number of points need to be made here. First, the mechanism underlying short-range elasticity is not well understood. As indicated above, Lännergren (1971) showed it to be present in single isolated frog muscle fibres, which shows that it is intracellular, but whether or not crossbridges are responsible has not been firmly established. The main difficulty is that the stiffness of the SREC does not decrease with decreasing overlap of the thin and thick filaments, contrary to what would be expected (Lännergren, 1971; Haugen and Sten-Knudsen, 1981). Lännergren studied sarcomere lengths between 2.1 and 2.5 μm only and found the stiffness of the SREC to increase with length in this range. Haugen and Sten-Knudsen (1981) found that the stiffness of the SREC increases with sarcomere length in the range 2.1-3.0 μm, and decreases beyond 3.0 μm to become zero at approximately 3.6 μm. Their analysis, however, was based on the assumptions that the force response of the SREC after the initial linear increase is flat at all sarcomere lengths and that the structures responsible for short-range elasticity are different from those that underlie passive muscle force. Both assumptions may be true but are not necessarily so (Pollack, 1990). Consequently, the dependence of SREC stiffness on sarcomere length beyond 2.5 μm remains uncertain. A rather different explanation for short-range elasticity, although not explicitly stated, was at least implied by Pollack (1990; Chapter 10; see also Chapter 14): short-range elasticity would be due to coil-helix transitions in the tropomyosin molecule, located by Pollack in the connecting filament, in

close association with the thick filament. The passive force response in this theory is the sum of purely elastic forces and forces generated by tropomyosin molecules undergoing a coil-helix transition. Simulations similar to those of Fig. 5.2 showed that the thixotropic Kelvin element could easily produce passive force responses to slow stretch similar to those obtained in single frog iliofibularis muscle fibres by Lännergren (e.g., those in his Fig. 3). While this cannot be taken as evidence for a thixotropic mechanism for short-range elasticity (although it is conceivable that both breakage of crossbridges (disruption of "flocs") and coil-helix transitions (orientation of molecules) would result in a decrease in apparent viscosity), it certainly does illustrate, as does Pollack's theory, that very different mechanisms may produce similar force responses. The point is that it might be misleading to consider the initial short-range "linear" increase in force as indicative of the presence of a short-range elastic element. The initial (almost) linear increase may simply be the initial part of the transient response of the underlying (viscoelastic) system. The force response of for instance the Maxwell element to stretch at constant velocity, which consists of a transient almost linear increase to a steady state force, exemplifies this clearly. Second, the fact that the SREC is present in isolated single muscle fibres does not exclude that extracellular mechanisms may also contribute to the short-range elastic response in whole muscle. Third, if the characteristic time course of the passive force responses of cat medial gastrocnemius is due solely to breakage of crossbridges, then the explanation given above for movement-dependent potentiation of motor unit forces cannot be

valid. Rather, it would have to be sought in the intracellular mechanism underlying short-range elasticity. However, as mentioned above, Edman's data (1980) indicate that breakage of crossbridges does not have any effect on subsequent force generation. Moreover, even if there were evidence to the contrary, it would still be unclear why the potentiating effect would depend on twitch amplitude. In sum, it seems likely that the SREC contributed to the force responses observed by Heckman et al., but unlikely that it was the sole cause. Extracellular mechanisms probably also played a role.

The fact that the differences in active force during simulated walking and "botched" simulated walking could be reproduced qualitatively by a distributed thixotropic Kelvin model cannot be interpreted as *evidence* for this hypothesis. It does show, however, that the observations are *compatible* with the hypothesised mechanism.

If shear thinning does occur in muscle, where exactly would it do so? There are four possibilities, not mutually exclusive: (1) in the muscle fibres, (2) in the endomysium and perimysium, (3) in the aponeurotic sheets and tendons, and (4) in the vascular bed of the muscle.

Intracellular mechanisms were discussed above under short-range elasticity: breakage of attached cross-bridges (D.K. Hill, 1968), and coil-helix transitions in tropomyosin (Pollack, 1990). These mechanisms are not thixotropic *stricto sensu* but may give rise to thixotropy-like effects. Although the molecule has been

hypothesised to be predominantly elastic (Pollack, 1990), it cannot be ruled out that titin may also be responsible in part for the viscoelastic behaviour of muscle.

A pretty good case can be made for the endomysium. First, if the passive muscle is stretched or released (from a length at which passive muscle force is non-zero), or if the muscle contracts, the endomysium is likely to experience high shear forces, particularly so since endomysial connective tissue does not contribute structurally to the tendons (Moore, 1983), unlike muscle fibres which do so by means of their myotendinous junctions. Second, the biochemical composition of the endomysium is compatible with it being thixotropic. Besides the collagens and the non-collagenous glycoproteins (fibronectin, laminin and others), the proteoglycans constitute the third major class of macromolecules present in extracellular matrices (Sanes, 1986). Proteoglycans (for a review, see Heinegård and Paulsson, 1984) consist of glycosaminoglycans and a core protein. Glycosaminoglycans are linear, unbranched polymers of disaccharide monomers. They are attached to the core protein in a configuration resembling a bottle-brush. Different glycosaminoglycans differ by the sugars in the disaccharide units. Of interest here are hyaluronic acid, chondroitin sulphate, heparan sulphate and dermatan sulphate. Five different results need to be mentioned: (1) muscle cells in culture synthesize hyaluronic acid, chondroitin sulphate and heparan sulphate (Mayne and Sanderson, 1985; Sanes, 1986) (the glycosaminoglycan composition of muscle ECM *in vivo* is unknown), (2) synovial fluid is thixotropic and its thixotropy is believed to be due to hyaluronic acid (the largest glycosaminoglycan

known and the only one that, in tissue, may not always be linked to protein), (3) hyaluronic acid interacts with itself to form "extended structure[s, i.e., flocs,] in solution" (Heinegård and Paulsson, 1984), (4) hyaluronic acid also interacts with chondroitin sulphate, and (5) both heparan sulphate and dermatan sulphate interact with themselves, the size of the complexes formed being shear dependent (Heinegård and Paulsson, 1984).

The third possible location is the aponeurotic sheets and tendons, which consist mostly of densely packed collagen fibres and ECM (Fawcett, 1986). If, the collagen fibres are stretched then the ECM is under shear and, just as the ECM between the muscle fibres, may liquefy. Aponeuroses may stretch more than the tendons, as the data suggest, with correspondingly higher shear rates and possibly greater changes in the apparent viscosity of the ECM. External tendon has been studied by many authors, but there seem to have been no reports on thixotropic behaviour. This is perhaps a consequence of the fact that the emphasis has been on tensile strength and energy storage rather than on history dependent changes, which are nevertheless known to occur in tendon. Of particular interest here is the history dependent rightward shift of the stress-strain curves (e.g., Viidik, 1973, Fig. 19, and Bennett et al., 1986, Fig. 2a). Viidik (1973) attributed this shift to plastic, i.e., non-recoverable changes (but in the caption of his Fig. 19 these history-dependent changes are said to be "eliminated with resting periods between the loadings"), but did not discuss possible physico-chemical substrates for these "plastic" changes. Comparison of the length responses of the thixotropic

Kelvin element to loading with Viidik's stress-strain curves (in particular, those in his Fig. 19) indicates that thixotropy may underlie the reversible history dependent changes in tendon properties and that those changes should perhaps be reexamined in this light.

Finally, since blood is known to be thixotropic (Fung, 1981), and since individual muscle fibres are surrounded by a network of capillaries (Jerusalem, 1986), the vascular bed may also contribute to the thixotropic properties of muscle.

Is muscle thixotropic? The working hypothesis is that it is.

One difficulty with the hypothesis is that it requires that during locomotion the viscosity of the muscle, after having decreased as a result of muscle activation in the stance phase, increase again in the swing phase, so that it can go through similar changes in the next step cycle. Powers and Binder's results (Powers and Binder, 1991; see Historical Background) suggest that the viscosity of the endomysium may decrease gradually. It thus seems possible that it can also increase gradually. Whether or not it does so, however, can only be established by further experimentation.

5.8 Motor unit forces during simulated walking

The most important question here is: "Are the data any good?"

There seemed to be no reason to doubt the reliability of the multi-unit filament forces measured during passive walking (paradigm 1). Passive force (paradigm 2) was always quite reproducible. The variability in the data (see

Fig. 4.13) thus was for the most part due to variability in the filament force. In between runs the twitch contraction, and in the last two experiments also the EMGs, evoked by single stimuli delivered to the filament under study were carefully monitored on oscilloscopes. When there were signs that a change in the number of units stimulated could have occurred (as suggested by all-or-none changes in the force and EMG measurements occurring at the stimulus intensity used—due to gradual changes in the threshold of some motor units) data acquisition was discontinued. Also, on comparison of individual digitized force records, such changes were quite obvious (1 filament only; rejected). The variability thus was most likely due to potentiation and fatigue of FR units (and possibly also FF units) present in the filaments rather than to variation in the number of motor units stimulated. Walsmley et al. (1978) by using a simple model of motor unit recruitment deduced for the cat medial gastrocnemius muscle that during walking both type S and type FR units are activated. In light of this result the above explanation begs the question of what role, if any, motor unit force potentiation plays in normal locomotion.

Raw estimates of motor unit forces generated during active walking (paradigms 3 and 4) often exhibited distortions, which were believed to be due to potentiation of the background force. Although it was possible to "correct" the estimates using an intuitively reasonable method, there was no direct evidence that the correction procedure and the results it produced were accurate. Consequently, very few "hard" statements can be made. What does seem safe to

say, on two grounds, is that the variability in the active vs. passive data, i.e., the variability in the estimates of the forces generated by multi-unit ventral root filaments in simulations of the step cycle with and without distributed stimulation of the muscle (see Results),[3] was not artifactual but genuine: (1) active estimates acquired successively in a series of runs always had the same time course (see Fig. 4.13B) and, within noise, also the same amplitude, and (2) it seems unlikely that within an experiment the time course of the potentiation effect differed substantially from one filament to the next, since the background force was always generated using the same ventral root filaments and the same pattern of stimuli.

What is the cause of this variability? The answer is a simple "I do not know (yet)." The fact that different responses were seen despite very similar variations in muscle fibre length and similar EMG responses indicates that it cannot be explained solely on the basis of known properties of force-length and force-velocity dependence, or location of the motor units in the muscle. The explanation may have to be sought in differences in the interactions between motor units due to differences in the relative locations of the muscle fibres of the background motor units and those of the filament under study. Whatever its cause, it suggests that it may not be correct to make inferences about the forces produced by motor units in the normal animal from forces measured in passive muscles.

---

[3] This variability reminds one of the as yet unexplained variability in the responses of spindle afferents in the triceps surae muscles; see Prochazka et al. (1989).

References

Abrahams, M. (1967). Mechanical behavior of tendon *in vitro*. *Med. Biol. Eng.* **5**: 433-443.

Bagust, J., Knott., S., Lewis, D.M., Luck, J.C. and Westerman, R.A. (1973). Isometric contractions of motor units in a fast twitch muscle of the cat. *J. Physiol.* **231**: 87-104.

Bak, M.J. and Loeb, G.E. (1979). A pulsed integrator for EMG analysis. *Electroencephalogr. Clin. Neurophysiol.* **47**: 738-741.

Becker, G.E. (1990). Velocity of sound in various media. In: Lide, D.R. (Ed.), CRC Handbook of Chemistry and Physics, CRC Press, Inc., Boca Raton, Florida, pp. 14-32.

Bennett, M.B., Ker, R.F., Dimery, Nicola, J. and Alexander, R. McN. (1986). mechanical properties of various mammalian tendons. *J. Zool., Lond.* (*A*) **209**: 537-548.

Billington, E.W. and Tate, A. (1981). The Physics of Deformation and Flow. McGraw-Hill, New York, New York.

Butler, D.L., Grood, E.S., Noyes, F.R. and Zernicke, R.F. (1978). Biomechanics of ligaments and tendons. *Exerc. Sport Sci. Rev.* **6**: 125-181.

Caputi, A.A., Hoffer, J.A. and Pose, I.E. (1989). Muscle fiber lengths, pinnation angles and deformation of aponeurotic sheets in the cat medial

gastrocnemius muscle during normal movement. *Soc. Neurosci. Abstr.* **15**: 521.

Caputi, A.A., Hoffer, J.A. and Pose, I.E. (in press). Velocity of ultrasound in active and passive cat medial gastrocnemius muscle. *J. Biomech.*

Clamann, H.P. and Schelhorn, T.B. (1988). Nonlinear force addition of newly recruited motor units in the cat hindlimb. *Muscle & Nerve* **11**: 1079-1089.

Demiéville, H.N. and Partridge, L.D. (1980). Probability of peripheral interaction between motor units and implications for motor control. *Am. J. Physiol.* **238**: R119-R137.

Devasahayam, S.R. (1989). Velocity of shortening of single motor units. Ph.D. Thesis, University of Illinois at Chicago.

Edman, K.A.P. (1980). Depression of mechanical performance by active shortening during twitch and tetanus of vertebrate muscle fibres. *Acta Physiol. Scand.* **109**: 15-26.

Elek, A., Prochazka, A., Hulliger, M. and Vincent, S. (1990). In-series compliance of gastrocnemius muscle in cat step cycle: do spindles signal origin-to-insertion length? *J. Physiol.* **429**: 237-258.

Elliott, D.H. (1965). Structure and function of mammalian tendon. *Biol. Rev.* **40**: 392-421.

Emonet-Dénand, F., Filippi, G.M., Laporte, Y. and Petit, J. (1987). Sommation de tensions tétaniques maximales développées par des unités motrices lentes

ou rapides du muscle long péronier du chat. *C.R. Acad. Sci. Paris* **305**: 417-422.

Emonet-Dénand, F., Laporte, Y. and Proske, U. (1990). Summation of tension in motor units of the soleus muscle of the cat. *Neurosci. Lett.* **116**: 112-117.

Fawcett, D.W. (1986). A Textbook of Histology. W.B. Saunders Company, Philadelphia, 11th ed.

Fried, V., Hameka, H.F. and Bluķis, U. (1977). Physical Chemistry, Macmillan Publishing Co., Inc., New York, New York.

Fung, Y.C. (1981). Biomechanics. Springer Verlag, New York, New York.

Goldman, D.E. and Richards, J.R. (1954). Measurement of high-frequency sound velocity in mammalian soft tissues. *J. Acous. Soc. Am.* **26**: 981-983.

Griffiths, R.I. (1987). Ultrasound transit times gives direct measurement of muscle fiber length in vivo. *J. Neurosci. Meth.* **21**: 159-165.

Griffiths, R.I. (1991). Shortening of muscle fibres during stretch of the active cat medial gastrocnemius muscle: the role of tendon compliance. *J. Physiol.* **436**: 219-236.

Griffiths, R.I. and Hoffer, J.A. (1987). Muscle fibers *shorten* when the whole muscle is being stretched in the "yield" phase of the freely walking cat. *Soc. Neurosci. Abstr.* **13**: 1214.

Hagbarth, K.-E., Hägglund, J.V., Nordin, M. and Wallin, E.U. (1985). Thixotropic behaviour of human finger flexor muscles with accompanying changes in spindle and reflex responses to stretch. *J. Physiol.* **368**: 323-342.

Haugen, P. and Sten-Knudsen, O. (1981). The dependence of the short-range elasticity on sarcomere length in resting isolated muscle fibres. *Acta Physiol. Scand.* **112**: 113-120.

Heckman, C.J., Weytjens, J.L.F. and Loeb. G.E. The effect of velocity and mechanical history on the forces of motor units in the cat medial gastrocnemius muscle. *J. Neurophysiol.*, accepted pending revisions.

Heinegård, D. and Paulsson, M. (1984). Structure and metabolism of proteoglycans. In: Piez, K.A. and Reddi, A.H. (Eds.), Extracellular Matrix Biochemistry, Elsevier, New York New York, Chapt. 8, pp. 277-328.

Hiemenz, P.C. (1986). Principles of Colloid and Surface Chemistry. Marcel Dekker, Inc., New York and Basel, 2nd ed.

Hill, A.V. (1970). First and Last Experiments in Muscle Mechanics. Cambridge University Press, Cambridge.

Hill, D.K. (1968). Tension due to the interaction between the sliding filaments in resting striated muscle. The effect of stimulation. *J. Physiol.* **199**: 637-684.

Hoffer, J.A. (1990). Techniques to study spinal-cord, peripheral nerve, and muscle activity in freely moving animals. In: Boulton, A.A., Baker, G.B. and Vanderwolf, C.H. (Eds.), Neurophysiological techniques: Applications to Neural Systems, Neuromethods, Vol. 15, The Humana Press Inc., Clifton, New Jersey, pp. 65-145.

Hoffer, J.A., Caputi, A.A., Pose, I.E. and Griffiths, R.I. (1989). Roles of muscle activity and load on the relationship between muscle spindle length and

whole muscle length in the freely walking cat. In: Allum, J.H.J. and Hulliger, M. (Eds.), Afferent Control of Posture and Locomotion, Prog. Brain Res., Vol. 80, Elsevier Science Publishers B.V., Amsterdam, pp. 75-85.

Hoffer, J.A., Caputi, A.A. and Pose, I.E. (in press). Activity of muscle proprioceptors in cat posture and locomotion: relation to EMG, tendon force, and the movement of fibres and aponeurotic segments. In: Muscle Afferents and Spinal Control of Movement, IBRO Symposium Series, Pergamon Press.

Hoffer, J.A., Sugano, N., Loeb, G.E., Marks, W.B., O'Donovan, M.J. and Pratt, C.A. (1987). Cat hindlimb motoneurons during locomotion. II. Normal activity patterns. *J. Neurophysiol.* **57**: 530-553.

Huxley, A.F. (1980). Reflections on muscle. Liverpool University Press, Liverpool.

Jerusalem, F. (1986). The microcirculation of muscle. In: Engel, A.G., and Banker, B.Q. (Eds.), Myology, McGraw-Hill, New York, New York, Vol. 1, Chapt. 11, pp. 343-356.

Jirgensons, B. and Straumanis, M.E. (1962). A Short Textbook of Colloid Chemistry, The MacMillan Company, New York, New York, 2nd ed.

King, R.G. (1966). A rheological measurement of three synovial fluids. *Rheol. Acta.* **5**: 41-44.

Lakie, M., Walsh, E.G. and Wright, G.W. (1984). Resonance at the wrist demonstrated by the use of a torque motor: an instrumental analysis of muscle tone in man. *J. Physiol.* **353**: 265-285.

Lännergren, J. (1971). The effect of low-level activation on the mechanical properties of isolated frog muscle fibres. *J. Gen. Physiol.* **58**: 145-162.

Lewis, D.M., Luck, J.C. and Knott, S. (1972). A comparison of isometric contractions of the whole muscle with those of motor units in a fast-twitch muscle in the cat. *Exp. Neurol.* **37**: 68-85.

Loeb, G.E. and Gans, C. (1986). Electromyography for Experimentalists. The University of Chicago Press, Chicago and London.

Loeb, G.E. and Levine, W.S. (1990). Linking musculoskeletal mechanics to sensorimotor neurophysiology. In: Winters, J.M. and Woo, S. L-Y. (Eds.), Multiple Muscle Systems, Springer-Verlag, New York, New York, Chapt. 10, pp. 165-181.

Loeb, G.E., Walsmley, B. and Duysens, J. (1980). Obtaining proprioceptive information from natural limbs: implantable transducers vs. somatosensory neuron recordings. In: Neuman, M.R., Fleming, D.G., Cheung, P.W. and Ko, W.H. (Eds.), Physical Sensors for Biomedical Applications, CRC Press, Inc., Boca Raton, Florida, pp. 135-149.

Ludwig, G.D. (1950). The velocity of sound through tissue and the acoustic impedance of tissues. *J. Acous. Soc. Am.* **22**: 862-866.

Mayne, R. and Sanderson, R. D. (1985). The extracellular matrix of skeletal muscle. *Collagen Rel. Res.* **5**: 449-468.

McMahon, T.A. (1984). Muscles, Reflexes, and Locomotion. Princeton University Press, Princeton, New Jersey.

Moore, M.J. (1983). The dual connective tissue system of rat soleus muscle. *Muscle & Nerve* **6**: 416-422.

Morgan, D.L. (1977). Separation of active and passive components of short-range stiffness of muscle. *Am. J. Physiol.* **232**: C45-C49.

Petit, J., Filippi, G.M., Emonet-Dénand, F., Hunt, C.C. and Laporte, Y. (1990). Changes in muscle stiffness produced by motor units of different types in peroneus longus muscle of cat. *J. Neurophysiol.* **63**: 190-197.

Poliacu Prosé, L. (1985). De Functionele Stabiliteit van de Knie van de Kat. Ph.D. Thesis, Vrije Universiteit Amsterdam and Vrije Universiteit Brussel.

Pollack, G.H. (1990). Muscles & Molecules. Ebner & Sons Publishers, Seattle, Washington.

Powers, R. K. and Binder, M.D. (1991). Summation of motor unit tensions in the tibialis posterior muscle of the cat under isometric and non-isometric conditions. *J. Neurophysiol.* **66**: 1838-1846.

Prochazka, A. (1984). Chronic techniques for studying neurophysiology of movement in cats. In: Lemon, R. (Ed.), Methods for Neuronal Recording in Conscious Animals, IBRO Handbook Series: Methods in the Neurosciences, Vol. 4, Wiley, Chichester, pp. 113-128.

Prochazka, A., Hulliger, M., Zangger, P. and Appenteng, K. (1985). 'Fusimotor set': new evidence for α-independent control of γ-motoneurones during movement in the awake cat. *Brain Res.* **339**: 136-140.

Prochazka, A., Trend, P., Hulliger, M. and Vincent, S. (1989). Ensemble proprioceptive activity in the cat step cycle: towards a representative look-up chart. In: Allum, J.H.J. and Hulliger, M. (Eds.), Afferent Control of Posture and Locomotion, Prog. Brain Res., Vol. 80, Elsevier Science Publishers B.V., Amsterdam, pp. 61-74.

Prochazka, V.J., Tate, K., Westerman, R.A. and Ziccone, S.P. (1974). Remote monitoring of muscle length and EMG in unrestrained cats. *Electroenceph. clin. Neurophysiol.* **37**: 649-653.

Proske, U. and Morgan, D.L. (1987). Tendon stiffness: methods of measurement and significance for the control of movement. A review. *J. Biomech.* **20**: 75-82.

Rack, P.M.H. and Westbury, D.R. (1984). Elastic properties of the cat soleus tendon and their functional importance. *J. Physiol.* **347**: 479-495.

Ralston, A. and Rabinowitz, Ph. (1978). A first course in numerical analysis. McGraw-Hill, New York, New York, 2nd ed.

Rushmer, R.F., Franklin, D.L. and Ellis, R.M. (1956). Left ventricular dimensions recorded by sonocardiometry. *Circ. Res.* **4**: 684-688.

Sanes, J.R. (1986). The extracellular matrix. In: Engel, A.G., and Banker, B.Q. (Eds.), Myology, McGraw-Hill, New York, New York, Vol. 1, Chapt. 5, pp. 155-175.

Stephens, J.A., Reinking, R.A. and Stuart, D.G. (1975). The motor units of cat medial gastrocnemius: electrical and mechanical properties as a function of muscle length. *J. Morphol.* **146**: 495-512.

Trotter, J. (1990). Interfiber tension transmission in series-fibered muscles of the cat hindlimb. *J. Morphol.* **206**: 351-361.

Viidik, A. (1973). Functional properties of collagenous tissues. *Int. Rev. Connect. Tiss. Res.* **6**: 127-215.

Walmsley, B., Hodgson, J.A. and Burke, R.E. (1978). Forces produced by medial gastrocnemius and soleus muscles during locomotion in freely moving cats. *J. Neurophysiol.* **41**: 1203-1216.

Walsmley, B. and Proske, U. (1981). Comparison of stiffness of soleus and medial gastrocnemius muscles in cats. *J. Neurophysiol.* **46**: 250-259.

Weytjens, J.L.F., Viberg, D.A., Caputi, A.A., Kallesøe, K. and Hoffer, J.A. (submitted). New transducers for measuring muscle length in unrestrained animals. *J. Neurosci. Meth.*

Weytjens, J.L.F. and Loeb, G.E. (1987). An electromyogram-to-force-processor and its testing in cat hindlimb muscles. *Soc. Neurosci. Abstr.* **13:** 1178.

Winters, J.M. (1990). Hill-based muscle models: a systems engineering perspective. In: Winters, J.M. and Woo, S. L-Y. (Eds.), Multiple Muscle Systems, Springer-Verlag, New York, New York, Chapt. 5, pp. 69-93.

Winters, J.M. and Woo, S. L-Y. (1990). Multiple Muscle Systems. Springer-Verlag, New York, New York.

Woledge, R.C., Curtin, N.A. and Homsher, E. (1985). Energetic Aspects of Muscle Contraction. Monographs of The Physiological Society No. 41, Academic Press, London.

Zahalak, G.I. (1990). Modeling muscle mechanics (and energetics). In: Winters, J.M. and Woo, S. L-Y. (Eds.), Multiple Muscle Systems, Springer-Verlag, New York, New York, Chapt. 1, pp. 1-23.